DISCLAIMER:

This document does not meet the
current format guidelines of
the Graduate School at
The University of Texas at Austin.

It has been published for
informational use only.

The Dissertation Committee for Stevan Ashad Samuel Certifies that this is the approved version of the following dissertation:

Exploration of Novel Architectures for Aromatic Electronic Donor-Acceptor Hetero-duplexes

Committee:

Brent L. Iverson, Supervisor

Christopher W. Bielawski

Eric V. Anslyn

Christian P. Whitman

Yan Jessie Zhang

Jonathan L. Sessler

Exploration of Novel Architectures for Aromatic Electronic Donor-Acceptor Hetero-duplexes

by

Stevan Ashad Samuel, B.S.

Dissertation

Presented to the Faculty of the Graduate School of

The University of Texas at Austin

in Partial Fulfillment

of the Requirements

for the Degree of

Doctor of Philosophy

The University of Texas at Austin

December 2011

Dedication

To my family

Acknowledgements

I would first like to thank my P.I. Professor Brent Iverson for his patience, wisdom and the much needed words of encouragement during my matriculation through his research labs. Your drive to continually nurture that passion for science, both within impressionable undergraduate minds as well as seasoned, skeptical graduate students, will be something that I am sure will remain with me throughout the remainder of my scientific career. I would also like to thank members of the Ansyln, Sessler, and Willson labs for their time and effort spent assisting me in navigating the difficult waters of graduate research. Whether it was the last minute loan of a back-ordered chemical, being a sounding board for discussion of an inchoate research idea or simply as a sympathetic ear, you have my gratitude. I would also like to thank the members of the Iverson group, both past and present. Joe Reczek and Valerie Bradford your ability to tolerate my seemingly endless questions was greatly appreciated. Chelsea Martinez thank you for helping to keep me sane in the most trying times, Amy Rhoden Smith, Mike Elmuccio and Garen Holman for taking my money in annual March Madness brackets as well as in reminding me that it was never too early to "plan for my future." My thanks also go to Cameron Peebles and Mike Alvey for always willingly offering advice, good and bad, scientific and otherwise.

Lastly I would like to thank my parents and my annoying kid sister for all their love, support and devotion throughout all my years of education. Their unwavering support and belief in me, has kept me going at times when I was on the verge of giving up myself. I can never truly express how grateful I am for all that you have done for me in enabling me to be where I am today. Thank you.

Exploration of Novel Architectures for Aromatic Electronic Donor-Acceptor Hetero-duplexes

Publication No._____

Stevan Ashad Samuel, Ph.D.

The University of Texas at Austin, 2011

Supervisor: Brent L. Iverson

Research within the Iverson group has been primarily focused around the investigation of aromatic donor-acceptor interactions between an electron-rich 1,5-dialkoyxnaphthalene (DAN) molecule and the electron-deficient 1,4,5,8-naphthalenetetracarboxylic diimide (NDI) species. The complementary electrostatics within this aromatic system is responsible for the powerful associative properties of these two molecules when placed in aqueous environments, leading to highly ordered, discrete face-centered modes of stacking upon complexation. The exploitation of these interactions has lead to the formation of novel molecules, called aedamers, which achieve a variety of directed folded topologies and extended hydrogel networks, oligomers which form distinct intermolecular hetero-duplex assemblies, and unique crystalline materials with novel tunable liquid crystalline properties.

This dissertation describes the use of DAN-NDI aromatic donor-acceptor interactions in the design and construction of new oligomer architectures, with the aim of

driving intermolecular hetero-duplex formation with higher fidelity and increased binding affinities.

Chapter 2 describes efforts towards the design and construction of an amino acid based oliogmer with a highly rigidified molecular framework. A structurally rigidified scaffold would enhance the intermolecular association observed in our aromatic donor-acceptor hetero-duplexes allowing access to highly intricate and well-ordered networks in aqueous environments. Chapter 3 describes the design and synthesis of a novel DNA based architecture with the intention of creating aromatic donor-acceptor nucleoside analogs of the ubiquitous DNA building blocks. Fabrication of this novel subunit would facilitate the modular construction of larger, extended donor-acceptor oligomers enabling the formation of more expansive hetero-duplex assemblies hopefully exhibiting increased binding affinities.

As a whole, these projects seek to probe the specific elements necessary for the selective intermolecular association of DAN-NDI donor-acceptor oligomers. Fine tuning of the non-covalent interactions of this class of molecules can increase the level of control we see in the directed self-assembly of these aromatic hetero-duplexes in aqueous environments. With this in hand, these systems can now potentially be utilized in a variety of applications ranging from surface immobilization techniques, to novel water-soluble polymeric materials and biologically compatible non-natural peptide based artificial proteins.

Table of Contents

LIST OF FIGURES

LIST OF SCHEMES

CHAPTER 1

Self assembly driven by Aromatic Donor Acceptor interactions

1.1 DIRECTED SELF ASSEMBLY THROUGH NON-COVALENT INTERACTIONS

For much of the history of organic chemistry, the focus of research was mainly directed at developing methodologies for the synthesis and construction of novel compounds. Access to these compounds was accomplished predominantly through the formation of covalent bonds. Finding new ways to join individual atoms together served as the driving force in the pursuit of new compounds. However, within the last half century, significant attention has been devoted to exploring the range and utility of non-covalent interactions within the scope of organic chemistry.

Within Nature there is a plethora of natural assemblies that rely on a host of non-covalent interactions in order to maintain structure within highly ordered three-dimensional architectures. These non-covalent interactions range from electrostatic and Van der Waal's interactions, to more complex associations such as hydrogen bonding, metal coordination and aromatic interactions. More importantly, as is seen throughout Nature, form dictates function and as such fully understanding the role of non-covalent interactions in directed molecular assembly has the potential to grant access to materials with unique and highly novel properties.

An elegant example of the utility of non-covalent interactions in directed self-assembly is that of the DNA double helix. This unique molecule, essential to all life on our planet, has the ability to store genetic information by using four very simple building blocks. The structure and consequent function of the double helix itself arises as a result of a combination of non-covalent interactions. Firstly, there is *interstrand* hydrogen bonding contacts made between individual H-bond donors and acceptors of the base pairs

that comprise the scaffold of DNA. These inter-molecular contacts are responsible for the extremely high fidelity of molecular recognition of one strand of DNA for its complementary strand, without which the information storage capabilities of the double helix would not exist. Secondly, there are *intrastrand* aromatic interactions that exist between adjacent base pairs along the same strand of DNA. These non-covalent interactions contribute significantly to the stability of the DNA double helix and its ability to form a well-defined secondary structure.

Yet another similarly impressive example of the importance of non-covalent interactions in the biological world is that of proteins. These intricate and well-ordered supramolecular assemblies rival DNA in terms of structural complexity[1]. Here the exact composition of amino acids within the protein directs its ability to fold and consequently determines the secondary structure of the protein based on hydrogen bonding contacts between individual amino acids. This is of particular importance since the function of a protein is solely dependent of its ability to self-assemble into its active secondary structure, hence non-covalent interactions are responsible for not only the structure but also the activity of protein assemblies.

The biological world is replete with examples of non-covalent interactions, working alone or in tandem, to control highly ordered structures as well as many complex processes. These range from the catalytic activity of enzymes, to the information storage capabilities of the DNA and the extremely high degree of molecular association exhibited by many proteins in term of substrate recognition. With the establishment of the field of supramolecular chemistry along with the advancement of synthetic techniques within organic chemistry, the novel and elaborate assemblies seen in Nature are no longer as seemingly unattainable as they once were. However, in order to synthetically access these

self-assembled structures we must first obtain a firm grasp on the nature of non-covalent interactions and the intricacies involved utilizing them to direct higher order structure.

1.1.1 Hydrogen bonding in self assembly

There has been a tremendous amount of research dedicated to the utilization of hydrogen bonding as a means of directing self-assembly within supramolecular structures. As early as 20 years ago, seminal work by Rebeck and co-workers demonstrated the unique self-assembly of a dimeric "tennis-ball" held together primarily by hydrogen bonds[2]. The utility of hydrogen bonds arise out of their directionality and complementarity[3]. A hydrogen bond donor will exclusively interact with a hydrogen bond acceptor, hence the order and individual sequence of H-bond donors and acceptors within a particular molecule will dictate with which partner the molecule will interact[4]. It is this attribute that enables the information storage properties of the DNA double helix and, as such, makes it an attractive motif in the directed assembly of synthetic materials.

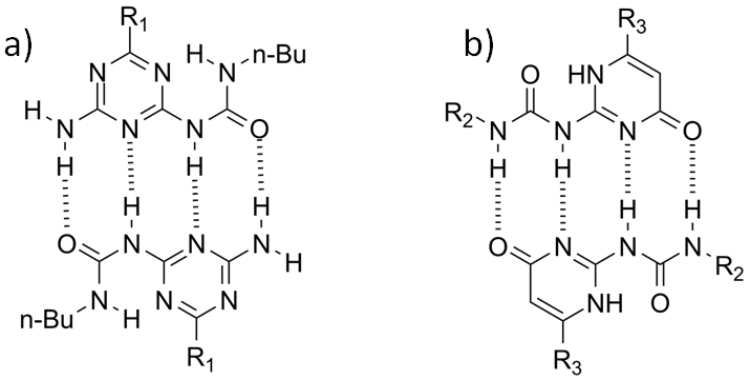

Figure 1.1 Quadruple hydrogen bond donor (D) and acceptor (A) arrays of Meijer and co-workers. a) ADAD hydrogen bonding sequence. b) AADD hydrogen bonding sequence.

Work published by Meijer and co-workers incorporated this design paradigm by using pyridines, triazines and pyrimidines to create complementary hydrogen bonding arrays[5].These quadruple arrays demonstrated respectable dimerization constants in chloroform which could be increased predictably based on the specific combination of H-bond donor (D) and acceptor (A) groups as seen in Figure 1.1.

A natural extension of this work was seen in the construction of novel supramolecular polymers achieved through a combination of two H-bond donor and acceptor arrays within the same molecule[6]. In this case the tunability and programmable nature of hydrogen bonding was used to form polymer assemblies with significant affinities in organic solvents[7]. This tunability and specificity for hydrogen bonding assemblies is also evident in the work of Gong and co-workers where oligoamides consisting of *meta*-substituted aromatic rings connected by glycine residues led to the formation of H-bonded oligomeric duplexes[8]. The authors demonstrated that the introduction of a deliberate mismatch in the H-bond donor and acceptors on individual oligamides led to a predictable decrease in the stability of the assembled duplex. This highlights the utility of hydrogen bonding as a means of imparting highly discriminate molecular recognition properties to well-ordered assemblies.

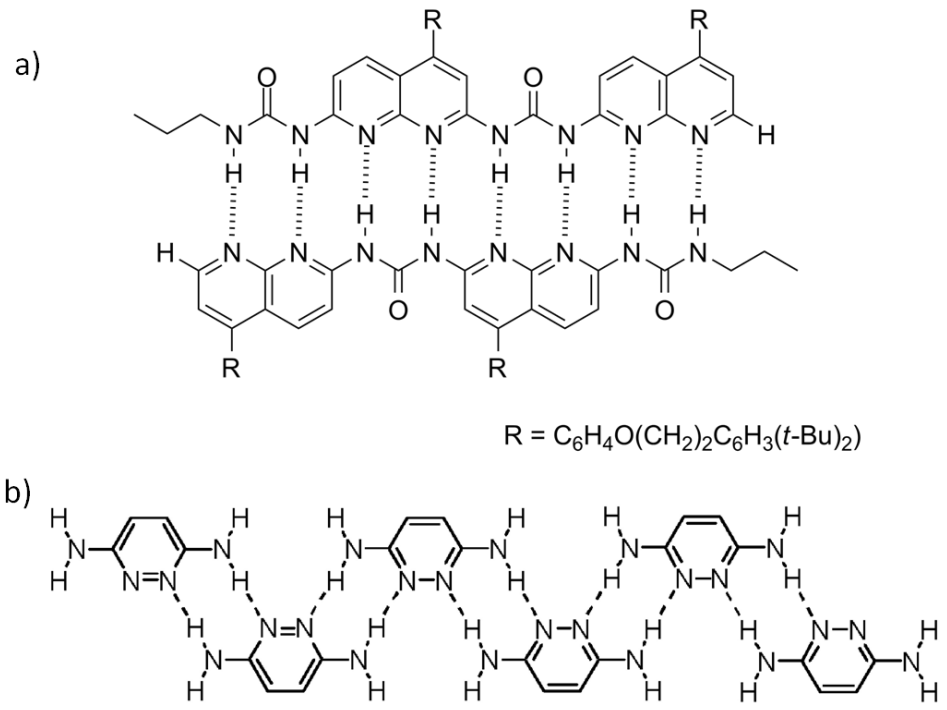

Figure 1.2 a) Hydrogen bonding donor-acceptor array based on ureido-naphthyridine scaffold from Zimmerman et al. b) 3,6 diaminopyrazine Hydrogen bonded duplex of Krische and co-workers.

A driving force within this field has been the construction of assemblies with even higher associative properties as is seen in the work of Zimmerman and co-workers[9]. Here the authors used a ureido-naphthyridine dimer to effect association through a network of eight H-bond donors and acceptors as seen in Figure 1.2. Association measurements were conducted in a mixture of DMSO and deuterated chloroform, however, as the concentration of DMSO increased there was a concomitant decrease in the strength of dimerization. This clearly demonstrated the significance of the effect of solvent polarity on the efficacy of hydrogen bond formation in highly ordered assemblies, due to competition with the polar solvent for hydrogen bonding.

The power of hydrogen bonding in driving self-assembly can also be seen in the work of Krische and co-workers in the construction of duplex forming oligomers based on oligoaminotriazines[10]. Here oligomers consisting of smaller subunits with specific H-bond patterns lead to the formation of oligomeric duplexes with remarkably high affinities in chlorinated solvent. Interestingly, the trimer duplex containing ten intermolecular H-bonds, demonstrated the highest association constants, as when the systems were extended to a possible fourteen H-bonds affinities dropped off significantly. A proposed explanation was that the longer strands exhibited competition between *inter*-molecular hydrogen bond formation and *intra*-molecular association in the formation of self-folded strands. This highlights the fact that in the design of self-assembled supramolecular architectures special attention must be paid to not only the number and directionality of the H-bonding contacts but to the structural nature of the molecular framework used as well.

1.1.2 Metal coordination

The strength of a metal cation coordinated to an organic ligand can approach that of a full covalent bond, making it one of the more powerful tools in the modern synthetic chemist's toolbox. This strongly associative non-covalent interaction has been utilized by itself or in conjunction with other various interactions to drive the ordered assembly of a number of well-defined structures. As early as a half century ago, metal-ligand interactions were exploited to direct molecular recognition as seen in the work of Pedersen and co-workers where crown ethers were used to bind potassium cations[11]. An extension of this work is seen in the research of Lehn[12] and co-workers and Cram *et al* [13], where metal cations were fully sequestered within a polyether cryptate and small molecule amino acids trapped within the binaphthalene systems, respectively. These

seminal works contributed significantly to the progression of supramolecular chemistry as field in its own right and any discussion of metal coordination interactions would be incomplete without their mention.

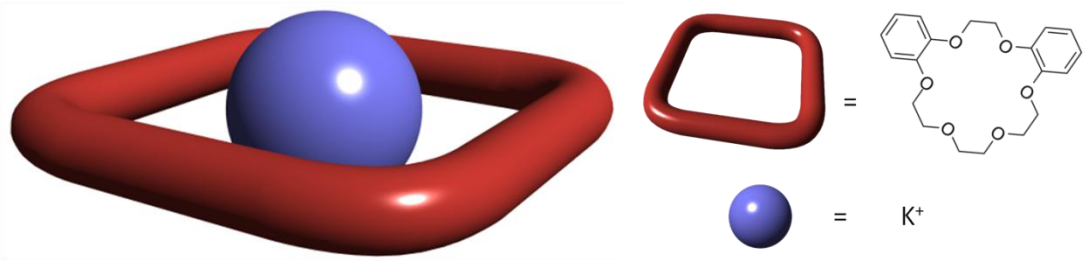

Figure 1.3 Illustration of the cation binding cyclic polyethers of Lehn and co-workers.

Metal-ligand non-covalent interactions can be superior to purely hydrogen bonding interactions in polar environments due to a lack of competition for the metal-ligand association with the polar solvent molecules[14]. This significant advantage has led to the construction of highly intricate metallo-supramolecular assemblies as seen in the work of Fujita and co-workers[15]. In this work the self-assembly of a palladium-ligand metal center $[enPd(II)]^{2+}$ with a bipyridine ligand was observed in a polar alcohol/water mixed solvent system. The self-assembled aggregate led to the formation of a well defined square planar structure with a hydrophobic internal cavity (figure), which the researchers showed capable of binding electron rich species such as 1,3,5-trimethoxybenzene.

This concept of directed assembly using metal-ligand interactions has been exploited by a number of other research groups in the construction of novel two-dimensional and three-dimensional architectures with a host of interesting topologies and material properties. Aggregates ranging from capsules, to cages and even spheres are

seen in the work Raymond and co-workers as well as Stang *et al* [16,17], all utilizing metal-ligand interactions as a means of self-assembly. Würthner and co-workers utilized this non-covalent interaction to form self-assembling coordination polymers consisting of perylene bisimide monomers containing terpyridine subunits which allowed polymerization through metal coordination to Zn^{2+} ions. Expectedly, it was shown that the degree of polymerization was directly dependent on the concentration of metal ions present[18]. These early studies have given rise to an expanding field of research in which three-dimensional polymeric matrices are constructed from metal-organic frameworks (MOFS).Aromatic-aromatic interactions

Significant research has been devoted to the full elucidation of the non-covalent association described under the umbrella of aromatic-aromatic interactions. Early work by Hunter and Sanders laid much of the foundation for understanding the nature of these interactions through empirical observations of porphyrin-porpyhrin interactions[19,20]. This class of non-covalent interactions is dominated by considering the polarization of pi electron clouds and the electrostatic interactions. The Hunter-Sanders model has been used to predict accurately the variety of possible orientations observed between interacting aromatics such as *stacked*, *edge-to-face* and *off-set stacked* (Figure 1.4) assemblies. Furthermore, within aqueous environments, desolvation of these large, non-polar, planar aromatic surfaces lead to an aggregation mode favoring face-centered stacking, a phenomenon known as the hydrophobic effect. The utility of these two non-covalent interactions working in tandem was quickly recognized and a tremendous amount of work has been published where these associative forces have been used to direct not only molecular assembly but *intra*-molecular folding as well.

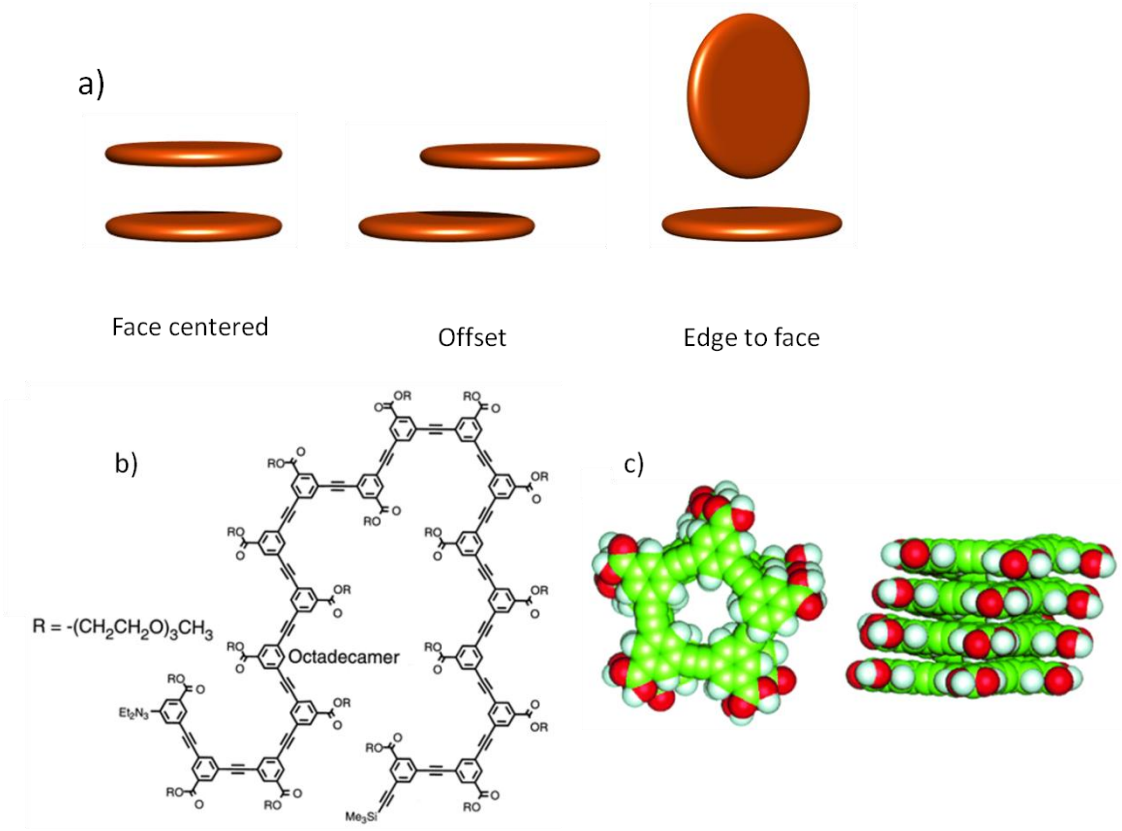

Figure 1.4 a) Graphical representation of the various modes of aromatic interactions. b) Phenylacetylene oligomers of Moore *et al*. c) Computational model of the folded helical oligomer

Some of the earlier work in the field of directed folding of aromatic systems was seen in the research of Moore and co-workers[21,22]. Here *meta*-phenylacetylene oligomers were reported to form stable helical structures in which the topology of the molecule was dictated by solvophobically driven aromatic-aromatic interactions within the non-polar backbone (Figure1.4). Surprisingly, spectroscopic analysis of the oligomers showed that the helical conformation proposed occurred in the more polar acetonitrile solvent whereas less polar solvents such as chloroform led to a denaturing of the assembly. This result lent credence to the ability of the hydrophobic effect to direct folding in supramolecular assemblies. Extension of this paradigm was seen in work done by Brunsveld and co-

workers where the aromatic oligomer used was appended with chiral side chains and placed in a mixture of achiral oligomers. Surprisingly, the oligomers assembled into helices and formed supramolecular helical columns, indicating some sort of cooperative intermolecular assembly in the transfer of chirality from the chiral oligomers to the achiral molecules.

Aromatic folded systems have been designed to more fully take advantage of the solvophobic effect seen in the directed assembly of aromatic oligomers in polar solvents. An example of this was seen in the work of Moore and co-workers where a fully water soluble analog of their *meta*-phenylene ethynylene was developed by incorporating solubilizing hexaethylene glycol side chains[23]. The researchers observed in water/acetonitrile solvent mixtures that the ability of the oligomer to adopt a helical conformation was again directly influenced by the overall polarity of the aqueous environment. The oligomer however did not fully adopt this conformation in 100% water, an observation that the researchers attributed to the absence of acetonitrile necessary to completely solvate the oligomeric aromatic backbone.

Despite the versatility of aromatic-aromatic interactions in mediating self-assembly, a variety of research has been conducted in which this non-covalent interaction is utilized in conjunction with other associative forces to access more well defined supramolecular assemblies. An early example of this was seen in the Lehn group where aromatic oligoamides containing 2,6 diaminopyridine and 2,6 diaminopyridinedicarboxylic acids were shown to interconvert between single and double helix conformations[24,25]. Extensive spectroscopic studies indicated that the double helix was stabilized predominantly by intermolecular hydrogen bonds in addition to favorable aromatic-aromatic interactions[26]. Hunter and co-workers constructed an aromatic system consisting of isophthalic acid and bisaniline derivatives that self-assembled into a well

ordered "zipper-like" structure[27]. The assembly was held together through a combination of edge to face aromatic interactions in addition to intermolecular hydrogen bonds between the amide functionalities on individual strands. However as the polarity of the solvent was increased the association constant for the heterodimers formed decreased. This highlighted the significance of the effect of solvent polarity on the strength of H-bonds and that despite the extensive network of aromatic interactions the stability of the dimers was primarily dependent on hydrogen bonding contacts.

1.2 DONOR ACCEPTOR AROMATIC INTERACTIONS

1.2.1 Donor acceptor aromatic interactions: a deeper look

The term π-stacking has been used quite frequently to describe a variety of aromatic-aromatic interactions that take place within organic chemistry. This term may be somewhat misleading since it can infer an inherent tendency for face-centered stacking of planar aromatics, a phenomenon that is in reality relatively uncommon and very rarely observed. With this in mind it is important to make a distinction between donor-acceptor aromatic interactions and traditional aromatic-aromatic interactions.

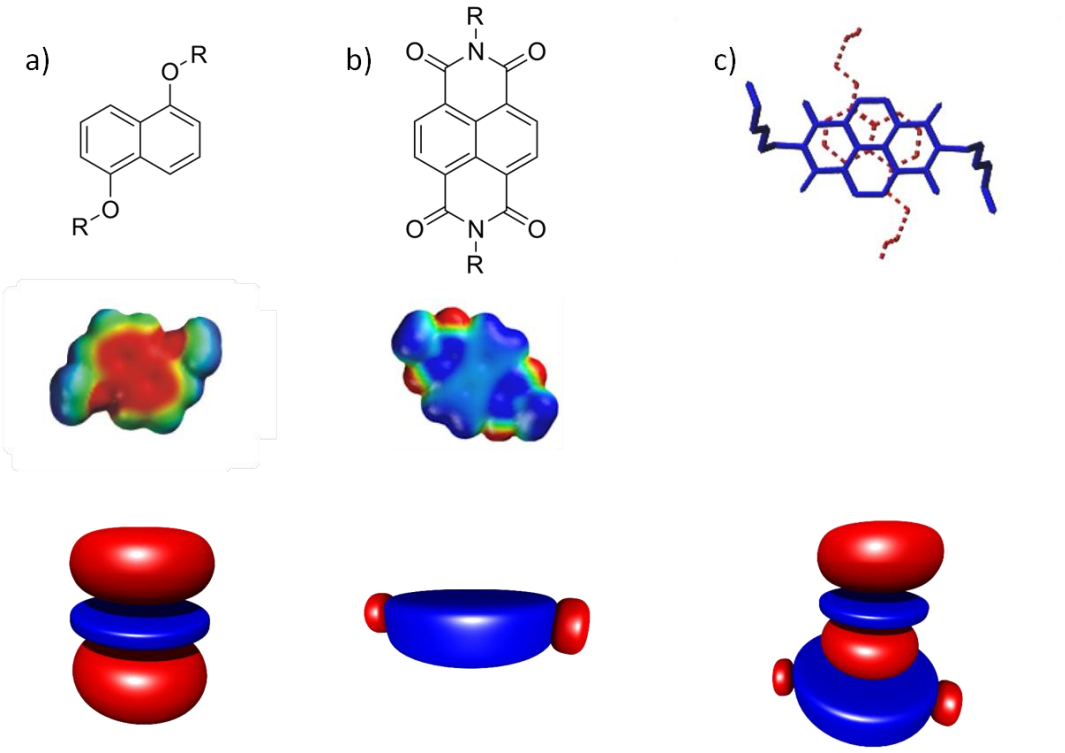

Figure 1.5 a) Electron rich 1,5-dialkoxynaphthalene donor unit (DAN), electrostatic surface potential map of the donor, cartoon representation of the electronic system. b) Electron deficient 1,4,5,8-tetracarboxylic diimide acceptor unit (NDI), electrostatic surface potential map of the acceptor, cartoon representation of the electronic system. c) Crystal structure of the DAN-NDI stacked complex, cartoon representation of the face-centered aggregated system

The canonical view of aromatic-aromatic interactions describes the aggregation of electron dense aromatic surfaces in a host of differing geometries such as T-shaped, herringbone or parallel offset stacking. These modes of aggregation arise as a means of reducing the electrostatic repulsion observed when the π-systems of both aromatic faces come into close proximity of each other. Donor-acceptor aromatic interactions are markedly different from these more traditional interactions. In these types of interactions an electron rich aromatic unit is utilized in which strongly electron donating functional groups contribute significant additional electron density to the π-system of the aromatic

core. This serves to increase the partial negative charge seen above and below the ring. Additionally an electron deficient aromatic unit is also utilized in which electron withdrawing groups remove electron density from the interior π-system hereby increasing the partial positive charge seen above and below the core of the aromatic ring. The complementary electrostatic surfaces of both these molecules facilitate a preferential face-centered stacking geometry of the aromatic cores. This face-centered stacking orientation fully allows the non-polar aromatic surfaces to hide themselves from surrounding polar solvent molecules in aqueous environments, hereby maximizing the hydrophobic effect. Consequently the magnitude of the association of aromatic donor-acceptor systems using this geometry is significantly greater than those observed in more traditional edge-to-face or offset aromatic stacking arrangements.

1.2.2 Donor-acceptor aromatic interactions in molecular assembly

One of the most prominent examples of aromatic donor-acceptor interactions being used to direct molecular assembly is seen in the work of Stoddart and co-workers in the self-assembly of pseudorotaxanes, catenanes and rotaxanes. Early work involved the use of an electron-rich macrocyclic bis-*p*-phenylene[34]crown-10 moiety binding to an electron deficient paraquat dication. Here the psuedorotaxane assembly was held together by a combination of aromatic donor-acceptor interactions between the complementary units and hydrogen bonding interactions[28]. Numerous examples of donor-acceptor templated synthesis of rotaxanes have been published within the last few decades with increasing levels of complexity. Work also published by the Stoddart group, described the design and synthesis of a donor-acceptor based rotaxane in which molecular motion could be controlled in response to environmental stimuli[29,30]. In this elegant example a cyclobis(paraquat-*p*-phenylene) cyclophane ($CBPQT^{4+}$) was used as

the electron deficient receptor to encircle benzidine and biphenol electron-donating functionalities. The difference in the ability of both these electon-rich groups to donate electron density enabled the selective molecular recognition of each by the $CBPQT^{4+}$ acceptor. This molecular "shuttling" of the acceptor was controlled with a very high degree of precision by varying the protonation state of the benzidine unit creating a positively charged cation which repelled the $CBPQT^{4+}$ acceptor biasing it towards selective association with the weaker π-donating biphenol unit as seen in Figure 1.6.

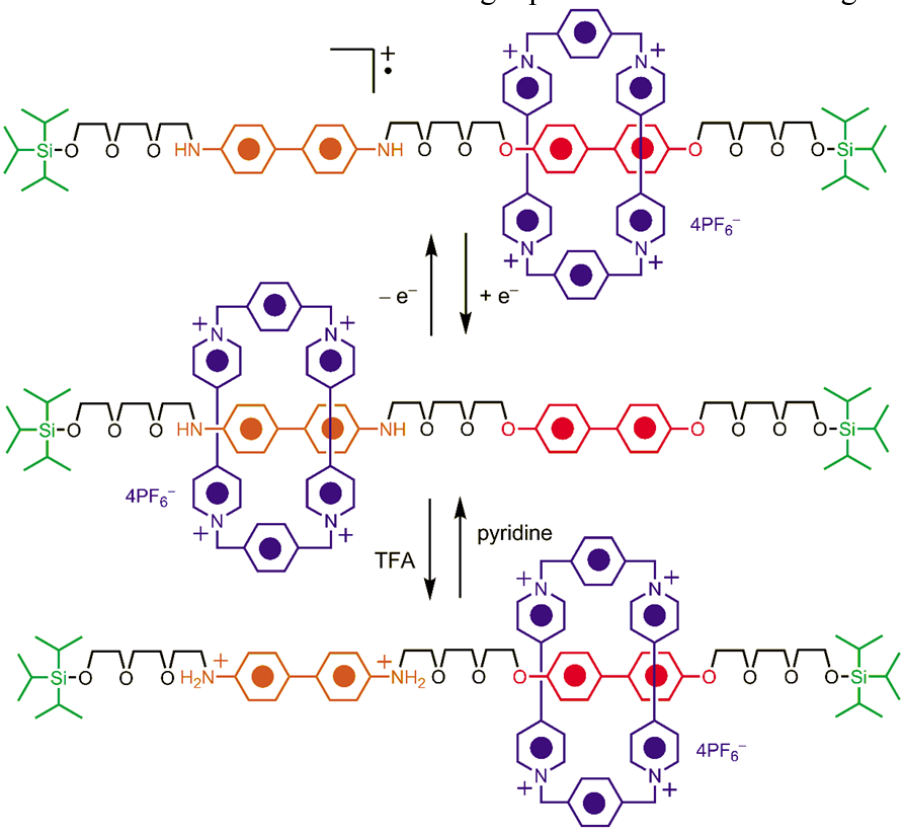

Figure 1.6 Schematic representation of the molecular shuttling of a cyclobis(paraquat-*p*-phenylene) cyclophane ($CBPQT^{4+}$) rotaxane by Stoddart and co-workers

Donor-acceptor directed self-assembly has also been used in the design and synthesis of astonishingly complex catenanes[31,32]. These interlocked supramolecular

structures display a host of unique topologies and material properties through clever use of aromatic donor-acceptor template synthesis. Early examples of this is seen in the work of Stoddart *et al.* where a 1,4-bis(bromomethyl)benzene (BPP34C10) electron-rich unit is used to form a catenane with the electron-deficient $CBPQT^{4+}$ unit[33]. Molecular movement within these catenane systems was also achieved through selective association of the aromatic acceptor with one donor over another in response to external forces. One example involving a three-station catenane demonstrates the ability of the $CBPQT^{4+}$ macrocycle to circumrotate among three electron-rich functional groups within a macrocyclic polyether. Here the oxidation states of each one of the donor functionalities was carefully controlled leading to preferential association of the aromatic acceptor with one of the electron-rich donors at a time. An interesting consequence of this controllable molecular recognition was the generation of three distinct colors, red, blue and green, as a result of the charge transfer interaction of the electron-deficient $CBPQT^{4+}$ molecule with each of the aromatic donors[34]. The mobility and electrochemical switching properties of the three-station catenane was confirmed spectroscopically however, confirmation of the emission of the aforementioned colors proved difficult due to obfuscation of the signal by interference of the absorption bands of two of aromatic donors used.

1.2.3 Donor-Acceptor interactions in directed intramolecular assembly

Research within the Iverson group has been focused predominantly on exploiting the associative properties of aromatic donor-acceptor interactions in aqueous environments. More specifically, the interaction of an electron-rich unit, 1,5 dialkoxynaphthalene (DAN) with an electron-deficient 1,4,5,8-tetracarboxylic diimde (NDI). The complementary electrostatics of the DAN-NDI system enabled them to take full advantage of the solvophobic effect when placed in very polar solvents. Pioneering

work in this area was carried out by Scott Lokey in which alternating units of electron-rich DAN units and electron-poor NDI units were tethered with flexible aspartic acid residues. When this system was placed in water the hydrophobic effect forced the linear oligomers to fold into a well-ordered pleated structure where each aromatic face hid itself by stacking in a face-centered geometry with its nearest neighbor[35].

The topology of this pleated structure was well explored by a host of spectroscopic studies including ^{1}H NMR, UV and visible absorption spectroscopy. Due to the optimal face-centered stacking arrangement of the folded structure in solution there was significant orbital mixing of the donor and acceptors as evidenced by the appearance of a charge transfer band in the visible region. Interestingly enough, this charge transfer band was seen even at elevated temperatures in water, indicating some degree of temperature independence of the ordered assembly's intramolecular association. UV studies also revealed the existence of hypochromism in the folded structure in relation to the individual DAN and NDI monomers further confirming the well-ordered pleated topology of the folded structure. This class of folding molecules called aedamers (*A*romatic *e*lectronic *d*onor-*a*cceptor oligo*mers*) opened the door to significant advances toward directed self-assembly in aqueous environments (Figure 1.7).

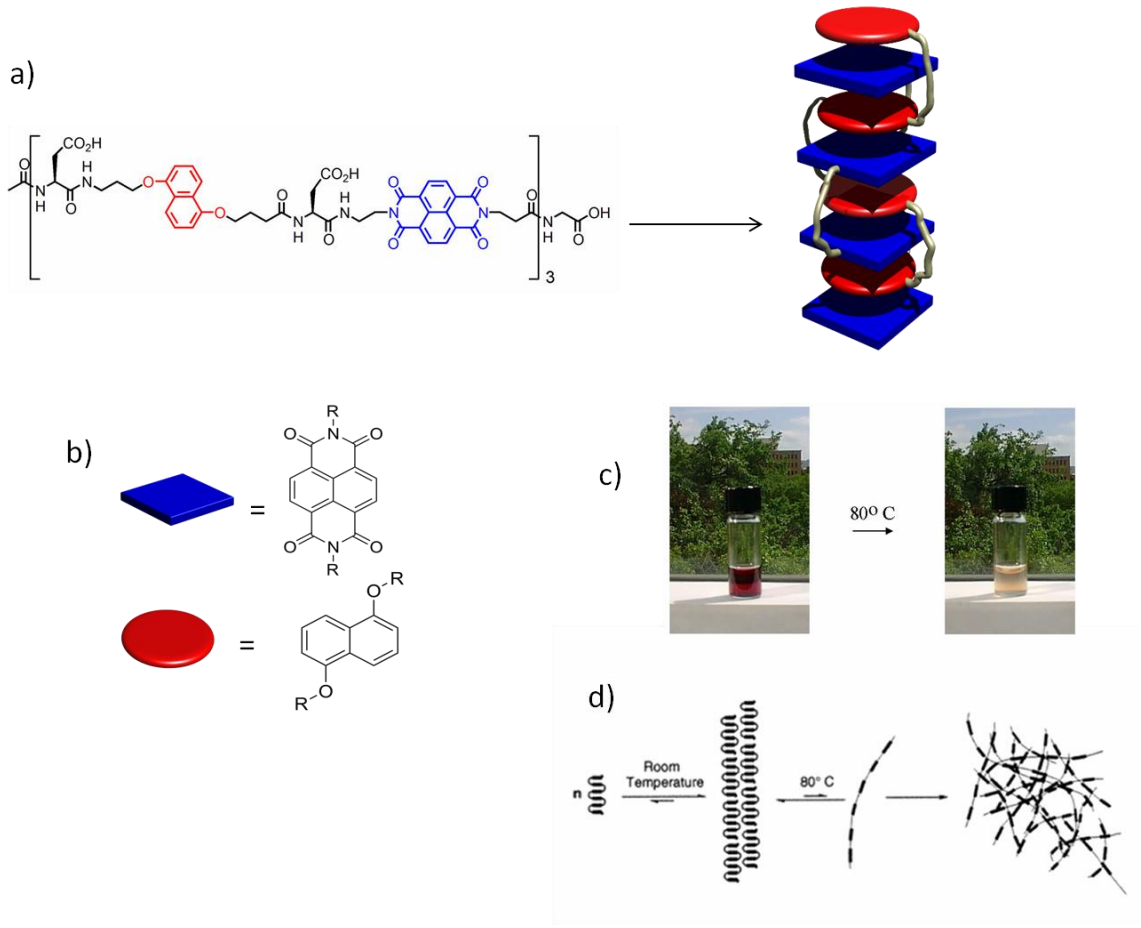

Figure 1.7 a) Structure and cartoon representation of the DAN-NDI aedamer. b) Cartoons of the donor and acceptor monomers. c) Loss of charge transfer band upon heating of amphiphilic aedamer. d) Proposed model of aggregation of the amphiphilic aedamer

With the efficacy of the intramolecular folding proven, the next step was the design and synthesis of an amphiphilic aedamer in which connective aspartate residues on one side of the molecule were replaced by the more hydrophobic leucine. This led to the formation of an aedamer which upon folding formed very highly aggregated networks in water unlike the previous aedamer. Further studies indicated the disappearance of the purple-hued charge transfer band upon heating to 80°C pointing to the disruption of the face-centered stacking as a result of intermolecular aggregation. It was proposed that

unfolding of the pleated structure immediately led to the formation of random tangled aggregates seen in many hydrogels. Most surprisingly it was found that aggregation could be induced more rapidly by seeding the sample with "pre-gelled" material, effectively creating a nucleation-type event that facilitated formation of the intermolecularly associated aggregates.

Further studies into the aggregation of amphiphilic aedamers were conducted in which a series of similar aedamers were constructed wherein the relative hydrophobicity of the molecules was varied by changing the side chains of the amino acids used in connecting the donor and acceptor sub-units. Theses side chains consisted of leucine, norleucine, isoleucine, valine and aspartic acid residues[36]. After conducting UV, SEM and circular dichroism (CD) spectroscopic studies it was found that the subtle differences in the molecular properties of the structurally similar folded aedamers became amplified once the material was heated above 80^{o}C and the material aggregated (Figure 1.8). CD studies also confirmed that the aggregated material existed as a highly ordered aggregate arising from reorganization of the kinetically stable folded aedamer. This irreversible hydrogel formation upon heating was conceptually analogous to the misfolding of proteins in the formation of amyloid fibrils. More importantly, these results alluded to the fact that the associative behavior of amyloids may not be exclusive to proteins but may be a general property of amphiphilic folding molecules in aqueous environments.

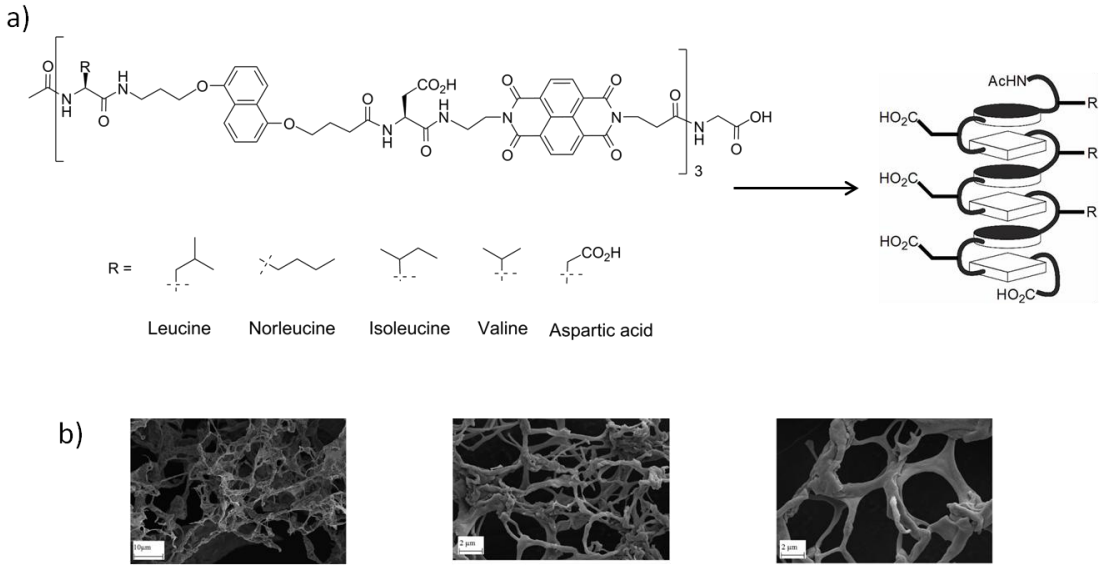

Figure 1.8 a) Chemical structures of the amphiphilic aedamer variants. b) SEM micrographs of the "gelled" aedamer aggregate.

A more detailed investigation of the associative properties of the Iverson group aedamers was carried by Andrew Zych in which the linkers used to connect DAN and NDI dimers were varied in order to determine their effect on the intramolecular association of the dimers[37,38]. ^{1}H NMR 1-D and 2-D studies confirmed the face-centered stacking proposed due to the upfield shift of the aromatic proton signals in response to the ring current effects of the adjacent aromatic moieties. It was found that folding of the dimers was influenced by the degree of flexibility within the amino acid tethers used and more importantly that the mode of association of the pleated structures did not follow a simple two-state model but existed in a variety of different folded confirmations. These conformations despite being different for a given dimer were not random and all shared the key face-centered stacking geometry indicative of the donor-acceptor aromatic stacking.

Up to this point it was known that there were two components to the donor-acceptor interactions seen in the Iverson aedamers, complementary electrostatics in addition to the solvophobic effect. It remained unclear as to which of these components was essential to donor-acceptor stacking hence in order to truly exploit the associative properties of the DAN and NDI aromatic units a greater understanding of the driving force behind this interaction was required. Work by Cubberly was carried out in which the donor and acceptor units were appended with tetraethylene glycol side chains in order to afford solubility of the aromatic cores in a variety of solvents[39,40]. ^{1}H NMR studies were conducted to investigate the binding affinities of the individual donor and acceptor monomers in a variety of deuterated solvents covering a broad range of solvent polarities.

It was shown that the affinity of the donor and acceptor monomers for each other (DAN:NDI) was always slightly preferred to the association of the individual homo-dimers (DAN:DAN),(NDI:NDI) regardless of the solvent used. More interestingly, as the polarity of the solvent changed going from dimethyl sulfoxide to acetonitrile the association constant for the DAN:NDI hetero-dimer was an order of magnitude greater than those observed for the individual homo-dimer associations. This trend indicated the importance of the complementary electrostatics of the hetero-dimer system in facilitating the donor-acceptor interaction. The most important revelation of this study however, was seen when the solvent was switched from methanol to water. Here the association of the DAN:NDI monomers increased by two orders of magnitude, the DAN:DAN and NDI:NDI association increased by one and two orders of magnitude, respectively. This increase in binding affinity in response to increasing solvent polarity was indicative of the hydrophobic effect as the driving force behind the interaction of the donor and acceptor aromatic units as seen in Figure 1.9.

a)

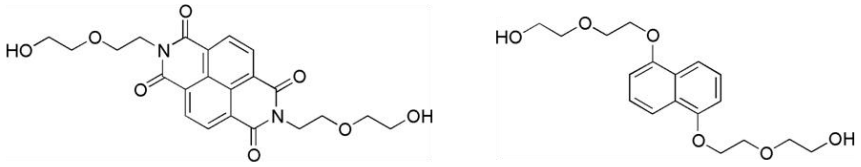

b)

Solvent	K_a (M^{-1}) DAN:DAN	K_a (M^{-1}) NDI:NDI	K_a (M^{-1}) DAN:NDI
$CDCl_3$	-	-	2
DMSO-*d6*	1	2	3
CD_3CN	1	3	11
CD_3OD	1	8	30
D_2O	20	245	2045

c)

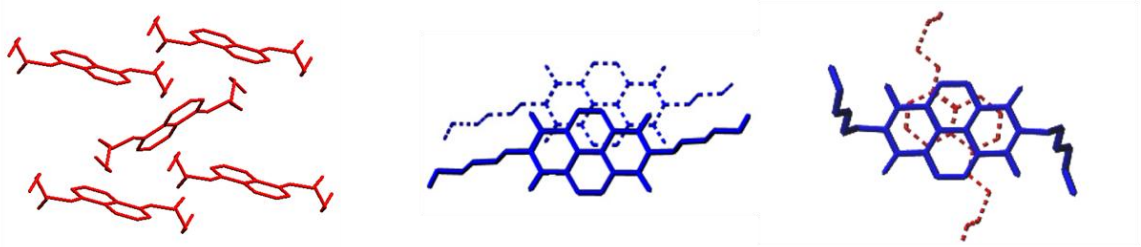

Figure 1.9 a) Structure of the DAN and NDI monomers used in solvent polarity investigation of the DAN-NDI interaction. b) Association constants of a DAN-NDI complexes in a variety of solvent. c) Crystal structures of the DAN-DAN interaction, NDI-NDI interaction and DAN-NDI interactions respectively.

The hetero-dimer association of the DAN:NDI monomers was only one order of magnitude greater than that of the NDI:NDI association. This indicated that solvation of the homo-dimer complex was very similar to that of the hetero-dimer aggregate in highly polar solvents. This was explained by the crystal structures of the monomers obtained in which the packing order of each of the monomers was clearly defined. The DAN:DAN monomer stacked in an edge-to-face or herringbone manner and provided the largest aromatic surface area remaining to be solvated. The DAN:NDI monomers stacked in the

expected face-centered geometry characteristic of the donor-acceptor interaction, providing the smallest surface area remaining to be solvated hence displaying the highest association constants, i.e. greatest hydrophobic effect. The association NDI:NDI homo-dimer was observed as a face-to-face offset stacking arrangement validating its moderate association affinity.

There have been reports of other systems utilizing aromatic donor-acceptor interactions in directing the folding of larger molecules albeit in polar organic solvent. Examples of these are seen in the work of Zhao and co-workers where an ornithine based peptide foldamer was functionalized with pyromellitic diimide (PDI) and DAN donor and acceptors. The resulting oligomer folded into a "zipper-like" complex when placed in polar organic solvents and exhibited the diagnostic spectroscopic signals associated with aromatic donor-acceptor stacking[41]. Similarly work from the Ghosh group has explored the formation of a well-folded polymer based on PDI and DAN aromatic subunits connected by polyethylene oxide linkers. Despite only being soluble in organic solvents it was shown that the degree of folding of the polymer could be increased by the addition of alkali metal ions. These ions bound to the polyethylene oxide linkers influencing the degree of turn seen within the polymer backbone further facilitating folding[42-44].

1.2.4 Donor-acceptor interactions in directed intermolecular assembly

Having demonstrated the utility of aromatic donor-acceptor interactions in directing *intra*-molecular folding, the focus within the Iverson group shifted to the use of these interactions in directing *inter*-molecular assembly. Work by Greg Gabriel investigated this prospect by constructing individual oligomers of NDI and DAN units connected by aspartic acid residues. These oligomers assembled into discrete heteroduplexes in water demonstrating a remarkably high affinity for one another. The

strength of the association was investigated using isothermal titration calorimetry (ITC) in conjunction with ^{1}H NMR spectroscopy and gel electrophoresis[45] (Figure 1.10).

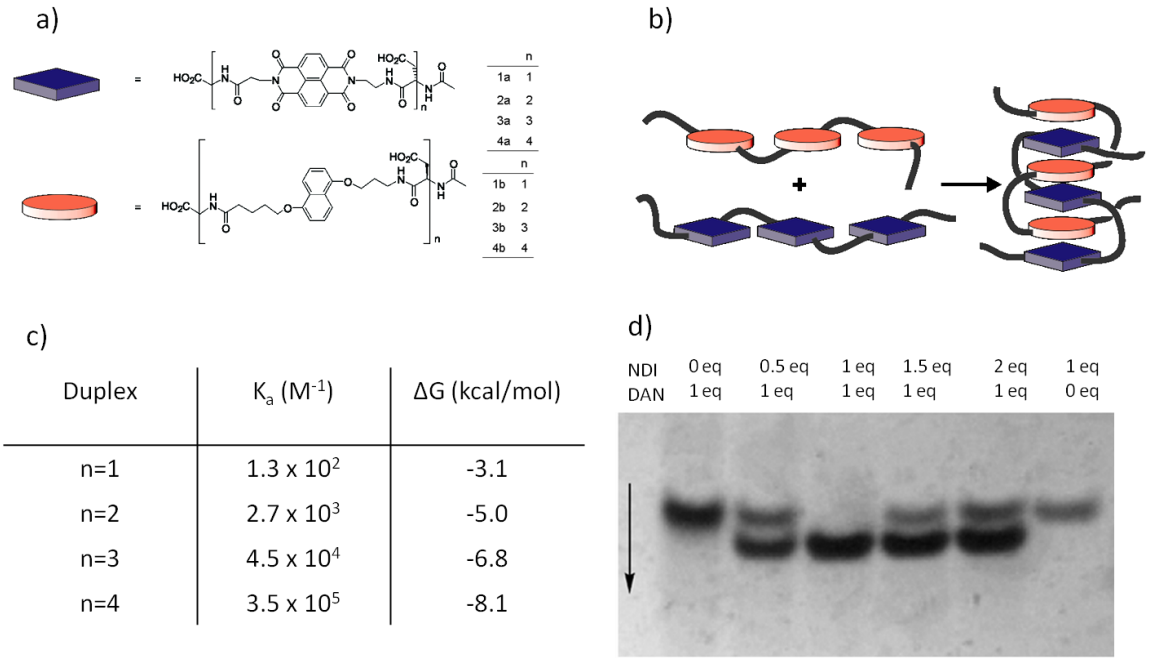

Figure 1.10 a) Chemical structures of the individual DAN and NDI oligomers. b) Cartoon representation of the association of the DAN and NDI oligomers to form the heteroduplex. c) Association constants and Gibbs free energies of binding of various heteroduplexes. d) Polyacrylamide Gel Electrophoresis (PAGE) titration of the heteroduplexes indicating specificity upon duplex formation.

Interestingly, it was found that as the length of the oligomers increased, so too did the binding affinities of the heteroduplexes formed. Going from the monomer to the tetramer the binding affinities increased by roughly one order of magnitude with the addition of each successive donor and acceptor subunit. The change in the Gibbs free energy (ΔΔG) observed upon complexation was -1.9, -1.8 and -1.3 kcal/mol going from the monomer to dimer, dimer to trimer and finally trimer to tetramer. It is important to note that although the strength of the intermolecular association appears to be additive,

there seemed to be an apparent decrease in the binding affinities as the oligmers themselves become larger. This decrease in binding affinity was attributed to charge repulsion between the individual donor and acceptor strands upon complexation, bringing more negatively charged aspartic acid residues in close proximity of each other with each additional DAN and NDI subunit. It was also proposed that the intra-molecular aggregation of the acceptor oligomers prior to complexation may have also been responsible for this loss in binding affinity since no significant change in association was seen when the larger pentameric and hexameric systems were investigated.

The fidelity of the donor-acceptor heteroduplexes formed was probed via titration experiments run using a polyacrylamide gel (PAGE). These gels separate compounds on the basis of charge density and it was hoped that the tetrameric heteroduplex would be bound tightly enough to migrate differently on a PAGE gel as opposed to the individual donor and acceptor oligomers. This turned out to be an accurate prediction as it was shown that a 1:1 mixture of the DAN and NDI oligomers yielded a single discrete complex that migrated further down the gel than the individual oligomers regardless of concentration. The addition of an excess of either oligomer in a non-equimolar mixture still yielded the formation of the discrete duplex with the excess oligomer after complexation travelling less far down the gel than the assembled duplex. This exclusion served only to highlight the remarkably high degree of discrimination and molecular recognition present in these donor-acceptor oligomers, underscoring the power of aromatic donor-acceptor interactions in driving self-assembly.

1.2.5 Donor-acceptor interactions in materials

With aromatic donor-acceptor interactions in DAN and NDI oligomers being rigorously investigated, the focus within the Iverson group turned towards the

development of independent water-soluble polymer analogs. This was done with the hope of creating highly ordered assembled macrostructures, fully exploiting the powerful associative properties of the DAN-NDI system, potentially leading to new materials with novel and interesting properties. Early work in this area was done by Joeseph Reczek in which DAN and NDI polymers were constructed by functionalization of polyethylene-alt-maleic anhydride. These polymers were soluble in aqueous environments at a relatively high pH due to the number of negative charges associated with the individual polymer strands. As was evidenced in the investigation of the aedamer complexes, this polymeric system demonstrated markedly different behavior between the individual donor and acceptor strands and a mixture of the two in both the solution and bulk phases.

Remarkably, the interaction of the DAN and NDI units within these mixtures were easily characterized by the appearance of the charge transfer band[46]. Thin films of the individual donor and acceptor strands, as well as mixtures of the two, were analyzed via Atomic Force Microscopy and it was found that each of the three displayed significantly different topologies. The NDI containing strands formed very smooth thin films unlike the DAN containing strands which formed very small aggregated micelles. Mixtures of the two strands formed highly interconnected macrostructures indicative of a highly integrated polymeric network as seen in Figure 1.11.

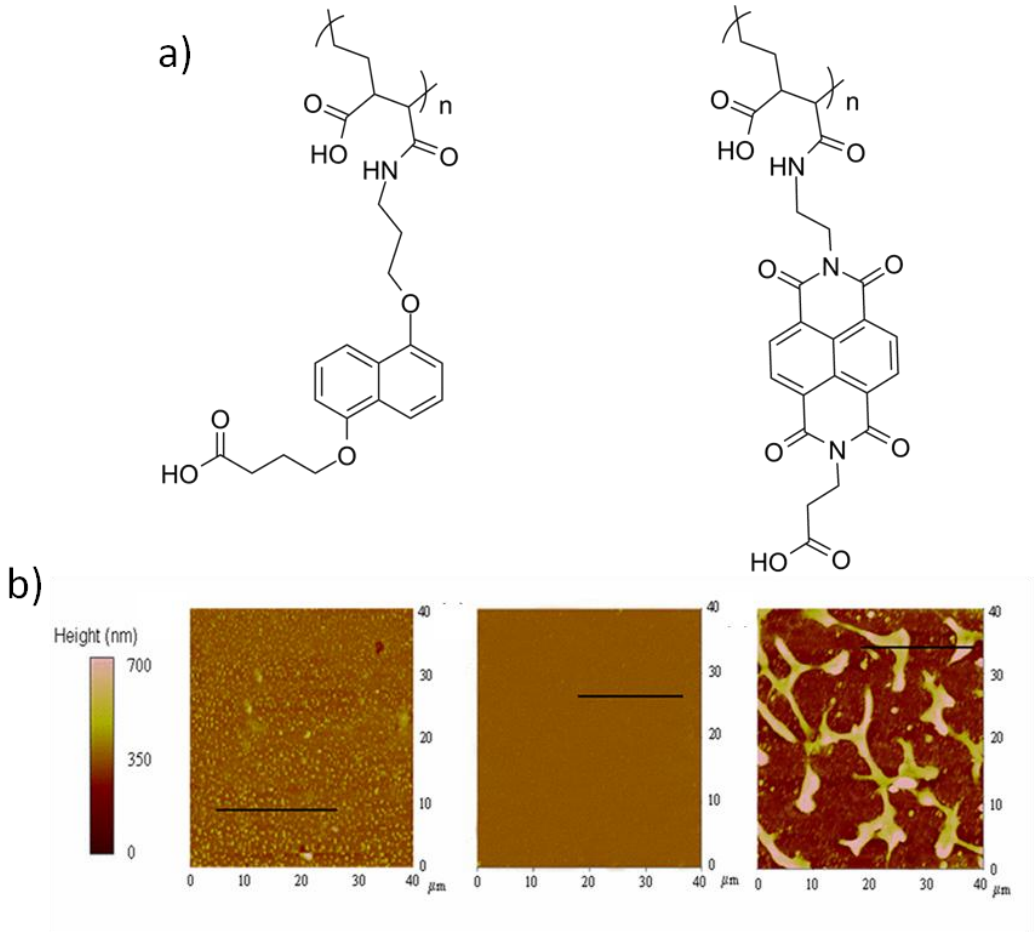

Figure 1.11 Chemical structures of the DAN and NDI functionalized polymers. b) Atomic Force Microscopy (AFM) micrographs of the DAN polymer, NDI polymer and a mixture of the DAN and NDI polymers respectively (from right to left).

Significant effort was also directed towards understanding the bulk material properties of the DAN and NDI aromatic donor-acceptor association in the solid phase[46,47]. A library of donor and acceptor monomers were synthesized, in which variations in the length, steric bulk and chirality of the side chains utilized were introduced. Heating neat mixtures of these donor and acceptor molecules lead to the formation of mesophases that demonstrated remarkable stability over a wide range of temperatures ranging from 25°C to 110°C. More importantly, observation of the charge-

transfer band in the mesophase of the mixtures pointed to the formation of extended columnar assemblies of alternating donor and acceptor monomers arranged in a face-centered orientation. Two very intriguing results came out of these preliminary studies. Firstly, there appeared to be a correlation of the melting/clearing point of the NDI monomers within the mixture of donor and acceptor components. Secondly, the crystallization points of the mixtures also correlated to the melting point of the DAN component. This behavior was attributed to the difference in the rotational freedom of the side chains associated with the individual DAN and NDI monomers in the mesophase. Since the side chains on the DAN monomers had significantly more mobility than those of the NDI units, the crystallization point of the mixture was ascribed to the restriction of motion of the DAN side chains (Figure 1.12).

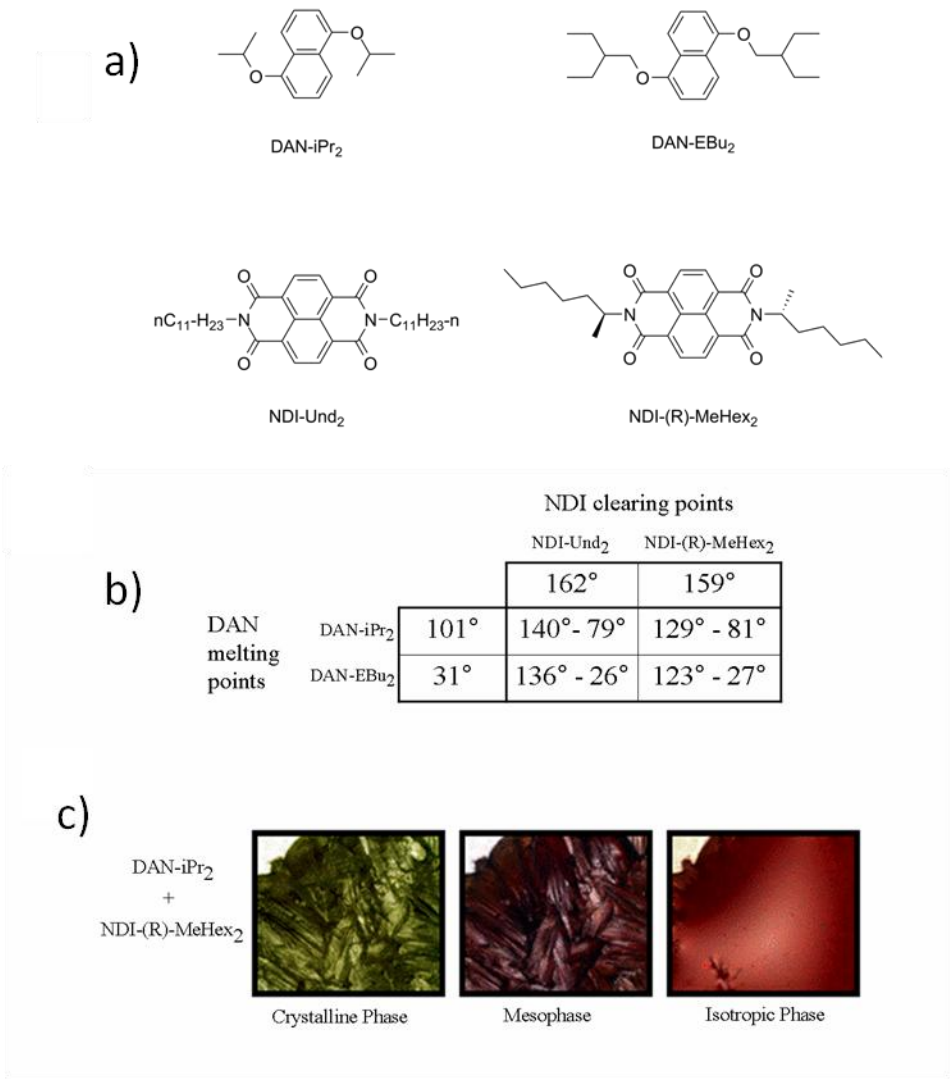

Figure 1.12 a) Chemical structures of the DAN and NDI monomers used in the mesophase formation studies. b) Clearing points (left) and crystallization points (right) of the DAN-NDI mixtures in comparison to the melting points of the individual DAN monomers and clearing points of individual NDI monomers used in the mixture. c) Colors of the DAN-iPr$_2$ and NDI-(R)-MeHex$_2$ in the crystalline phase (60^{o}C), mesophase (110^{o}C) and isotropic phase (160^{o}C).

Work done by Paul Alvey provided a more detailed look at the unique thermochromic behavior of solid-state mixtures of these donor-acceptor crystalline materials[48]. In an effort to determine the origin of the dramatic color change observed

upon crystallization from the mesophase, equimolar mixtures of DAN-NDI variants were studied via UV-Vis spectroscopy and Differential Scanning Calorimetry (DSC). The side chains of both the donor and acceptor monomers were systematically altered and the resultant crystalline mixtures probed. Interestingly it was found that in the mesophase, the donor-acceptor interactions between the DAN and NDI monomers dictated the packing structure of the mixture when the individual side chains maintained some degree of mobility, evidenced by the characteristic deep red color, indicative of a face-centered mode of stacking.

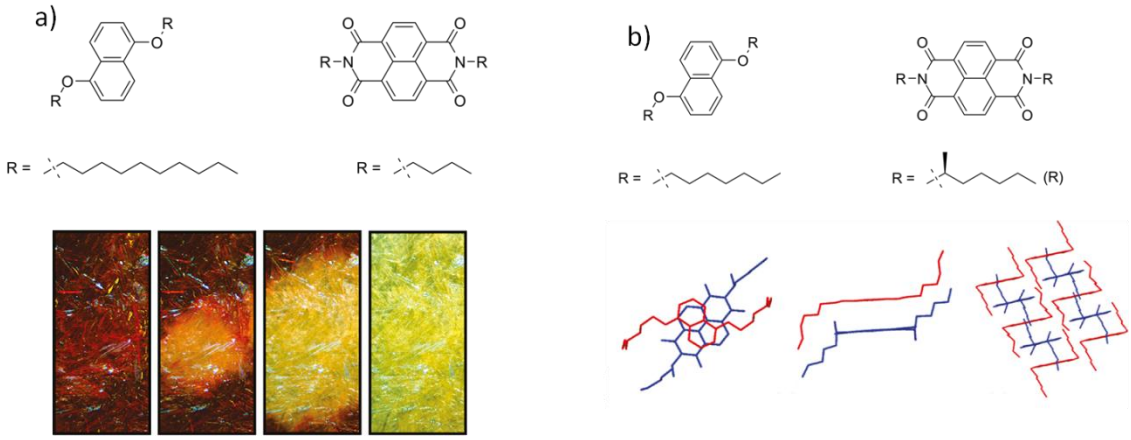

Figure 1.13 a) Chemical structure of the DAN and NDI monomers used in the thermochromic studies of side chain effect on donor-acceptor interactions in the bulk phase (top), Dramatic loss of the deep red color of the charge transfer band upon cooling from the mesophase to the crystalline phase (below left to right). b) Chemical structure of the DAN monomer and chiral NDI monomer (top) and the crystal structures of the packing observed in the crystalline state (below).

However, upon crystallization, steric interactions between the now less mobile side chains, appeared to be the dominant force driving molecular orientation, disrupting the ordered stacking of the aromatic cores resulting the dramatic disappearance of the

charge transfer band absorbance. This study demonstrated the ease with which the mesophases of these bulk phase liquid crystalline donor-acceptor systems could be tuned, as well as the precision with which the thermochromic behavior of the mixtures could be controlled.

Chapter 2

2 Linker Morphology and Aedamer Hetero-Duplex Formation.

2.1 CHAPTER SUMMARY

Introduction

Within the last decade there has been increasing interest in the field of directed self-assembly of supramolecular structures, more specifically with regard to discrete duplex formation. Synthetic duplex assemblies hold tremendous potential for developing materials with novel mechanical properties, information storage capabilities and new surface immobilization techniques. As previously reported this lab has developed a series of donor and acceptor oligomers that form unique hetero-duplexes in aqueous environments[45]. The work of this chapter seeks to extend this design paradigm by constructing a new oligomer scaffold that can more fully exploit the associative properties of these donor-acceptor molecules.

Goals

The goal of this project is to incorporate some measure of rigidity within the donor and acceptor oligomers by redesigning the linker architecture used to tether the DAN and NDI units. It is hoped that the decreased flexibility will lead to a degree of pre-organization which may possibly circumvent the entropic penalty associated with the formation of the donor-acceptor hetero-duplex.

Approach

Self association of the NDI acceptor units was attributed to the inherent flexibility of the aspartic acid residues used to tether the units together. This freedom allowed acceptor units within the same oligomer to interact with one another leading to the formation of the homo-duplex. Disruption of this unfavorable interaction prior to hetero-

duplex formation with the complementary donor (DAN) oligomer was hypothesized to be the reason for the loss of binding affinity that was observed as the length of the donor and acceptor chains increased. In order to address this problem the individual oligomers were redesigned to incorporate rigidity in to linker framework. Molecular modeling was used to determine the structural requirements of the linkers needed to allow the pre-organization of the individual donor and acceptor oligomers prior to complexation while maintaining the face-centered orientation necessary for the optimal donor-acceptor interaction.

Results

The work in this chapter describes the efforts made toward the synthesis of a novel linker architecture for use in the hetero-duplex forming donor and acceptor oligomers. Computational studies did give significant insight into the design and structural parameters necessary for a rigidified linker, however efforts to access this novel scaffold were defeated by a combination of low coupling efficiencies and the synthetically demanding approach taken towards construction of the rigidified scaffold.

2.2 BACKGROUND : DUPLEX SELF-ASSEMBLY

There are many examples of biological materials that form highly ordered structures within an aqueous environment. Proteins and other supramolecular assemblies contain highly ordered secondary and tertiary structures that are engineered towards a very specific purpose. In many instances multiple non-covalent interactions such as hydrogen bonding contacts, hydrophobic as well as electrostatic interactions are primarily responsible for maintaining the integrity of these higher order structures. The composition of the linear precursors to these ordered aggregates dictate the structure, and consequently the function of these complex biomolecules. (Figure 2.1)

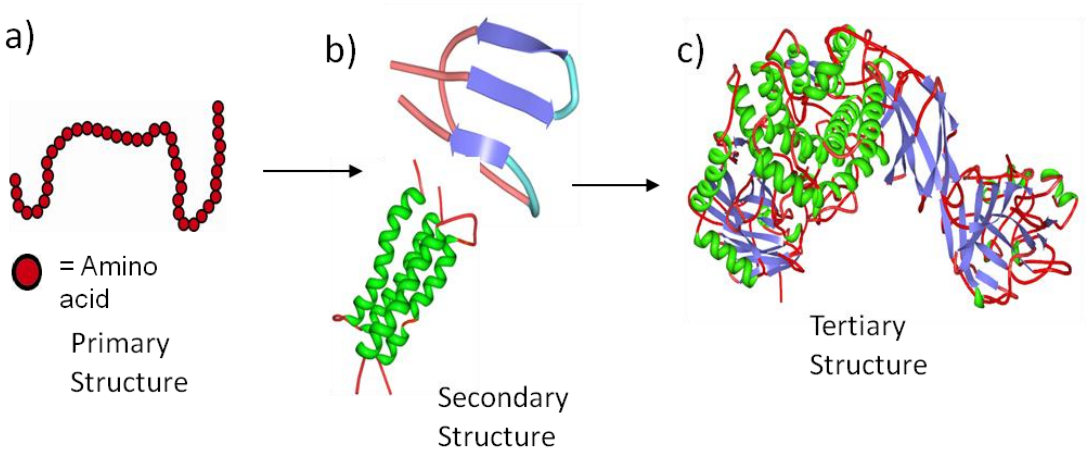

Figure 2.1 Primary amino acid sequence controls the structure and consequent function of large protein assemblies. a) Illustration of amino acid chain. b) Crystal structures of 4-α-helix bundles[49,50] and a designed mini protein with β-sheets[51], c) Crystal structure of Glucodextranase from *A. Globiformis* I42[52].

It quickly becomes evident that in order to design well ordered self-assembled complexes that particular attention must be paid to the primary structure of the individual component chains that aggregate to form these assemblies. With this in mind, there has been an increasing trend towards a "ground-up" approach in the design and synthesis of novel self-assembling frameworks. Within the last decade there have been a number of groups which have exploited this design paradigm to construct novel protein assemblies in which very unique complexes were formed[53,54] as well as assemblies specifically engineered for the emerging field of nanobiotechnology[55].

The ordered assembly of discrete complexes consisting of two artificial molecular chains has recently been generating significant interest. The archetypal duplex, the DNA double helix, has demonstrated such remarkable capability in molecular recognition, duplex stability and modularity of the individual nucleic acid oligomers, that it has become the "holy grail" of synthetic duplex forming strategies. The ability to construct

artificial duplexes holds significant promise in the fields of information storage, molecular recognition, directed self-assembly and surface immobilization.

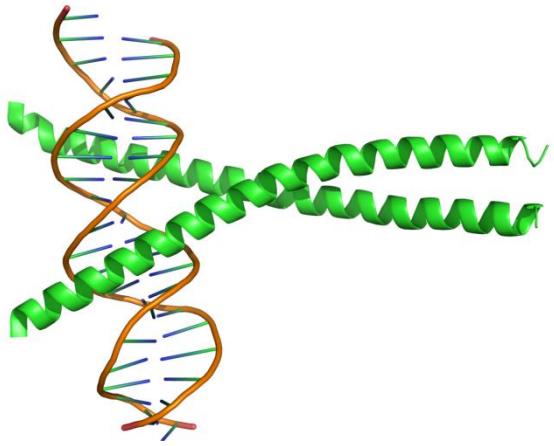

Figure 2.2 Crystal structure of C/EBP alpha leucine zipper bound to DNA.[56]

A classic, well- researched example of formation of a bi-molecular duplex from separate molecular strands is that of the leucine zipper. This assembly consists of two α-helical peptides, each containing roughly 30 amino acid residues, in which a leucine amino acid serves as a repeat unit every 7th position within the chain. Due to the hydrophobic nature of the leucine subunit, residues in adjacent peptides preferentially interact with one another in order to avoid the less favorable interaction with the surrounding polar water molecules. This results in a strongly associative interaction between both α-helices leading to the formation of a Y-shaped "tweezer-like" duplex as seen in Figure 2.2.[57] Self-assembly of the complex here clearly demonstrates the importance of chain composition in determining the 3-dimensional structure and consequently the function of complex supramolecular frameworks.

One of the most predominant non-covalent interactions utilized by Nature to direct structural assembly is that of hydrogen-bonding, and as such many research groups

have focused their attention of developing synthetic duplexes which make use of this associative property. Some interesting examples can be seen in the work done by Zimmermann *et al.,* in which linear monomers consisting of complementary hydrogen bond donors and acceptors were used to form linear ladder-type duplexes in organic solvent[58]. Several other groups have also pursued this design motif as well resulting in very highly ordered linear H-bonded duplexes with remarkably high association constants[59,60].

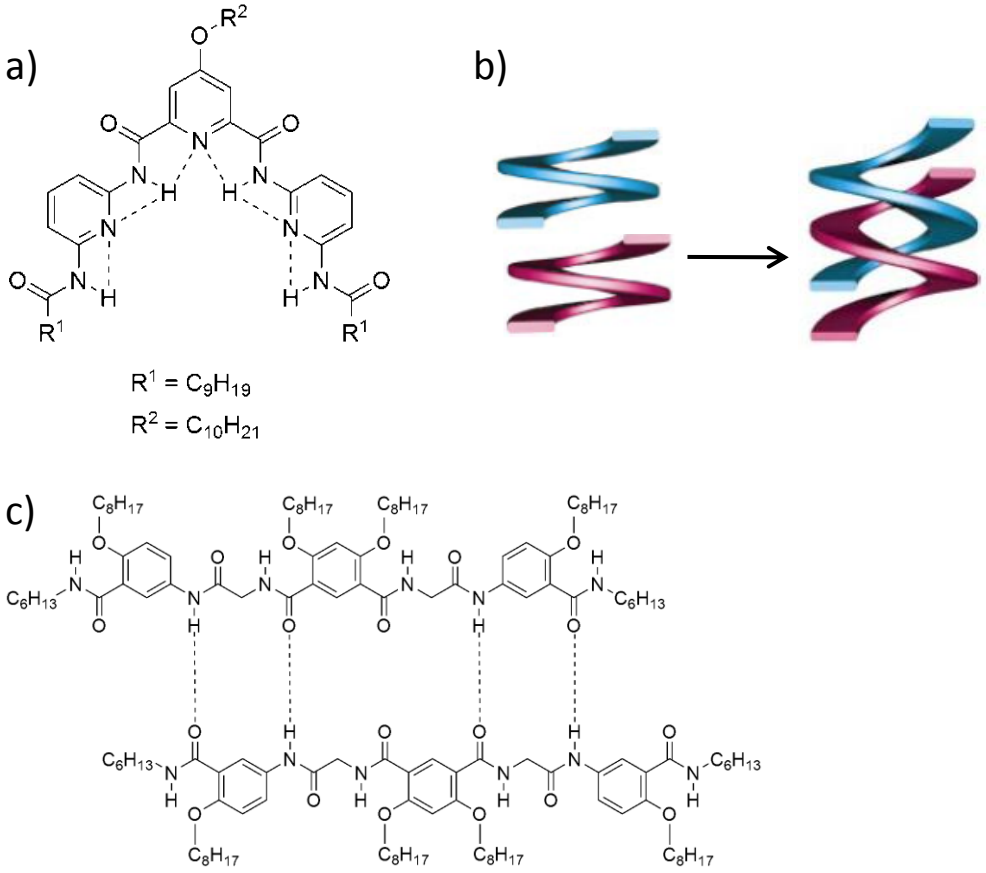

Figure 2.3 a) Hydrogen bonding responsible for helicity in folding oligo-pyridinecarboxamides, b) Illustration of the association of individual pyridyl oligomers to form duplex dimer[25]. c) H-bonded linear tapes[58].

Hydrogen bonded duplex formation has been extended beyond that of the linear duplex and into the realm of helical duplexes which more closely mimic that of the DNA double helix. One such example of this class of directed folding is that of the aromatic oligoamides used by Lehn and Huc[24,25]. Here a combination of hydrogen bonding and aromatic interactions are used to assemble the supramolecular complex. The helicity of individual strands are conferred through H-bonding contacts and duplex dimerization is facilitated by aromatic stacking interactions as shown in Figure 2.3. A unique variation of this theme is seen where the authors utilize hydrogen bonds in conjunction with metal ligand chelation to achieve dimerization of helical molecular strands[61].

One of the primary drawbacks of the hydrogen bonding motif is their relatively limited strength in highly polar solvents and as such significant research has gone into developing orthogonal strategies for duplex formation. One such approach is seen in the work of Coll and co-workers where metal-ligand interactions were used to drive duplex and triplex assemblies[62]. Interesting work has also been done to address the problem of directionality in metal-ligand helicate duplex forming systems, where creative use of ion pairing electrostatics lead to discrete molecular recognition[63,64] as seen in Figure 2.4.

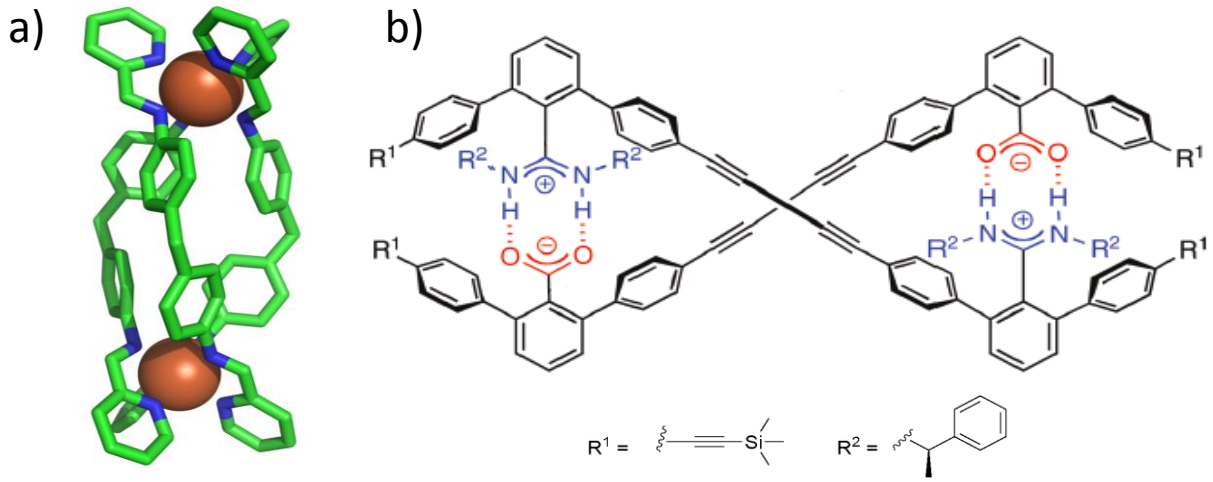

Figure 2.4 a) Bis-pyridylimine/Iron(II) trimeric complex[62]. b) m-terphenyl ion pair stabilized duplex[64]

Another orthogonal design motif that has been explored recently has been that of aromatic interactions. This associative property has been utilized by different research groups to drive the assembly of higher order molecular structures albeit using different modes of interaction (face centered, offset or edge-to-face). One of the earliest examples in the literature is seen in the work of Bisson and co-workers where isophthalic and bisaniline derivatives were used to form amide oligomers which assembled into stable zipper like duplexes held together by a combination of hydrogen bonding and edge-to-face π stacking interactions[65] as seen in Figure 2.5. Work from the Zhou lab also demonstrated the ability of donor-acceptor interactions to drive duplex assembly. In this case an electron deficient pyromellitic diimide and electron rich di-alkoxy naphthalene were used to introduce a measure of electrostatic complementarity in the individual oligomers leading to a face-centered stacking mode upon duplex formation[66] shown in Figure 2.5.

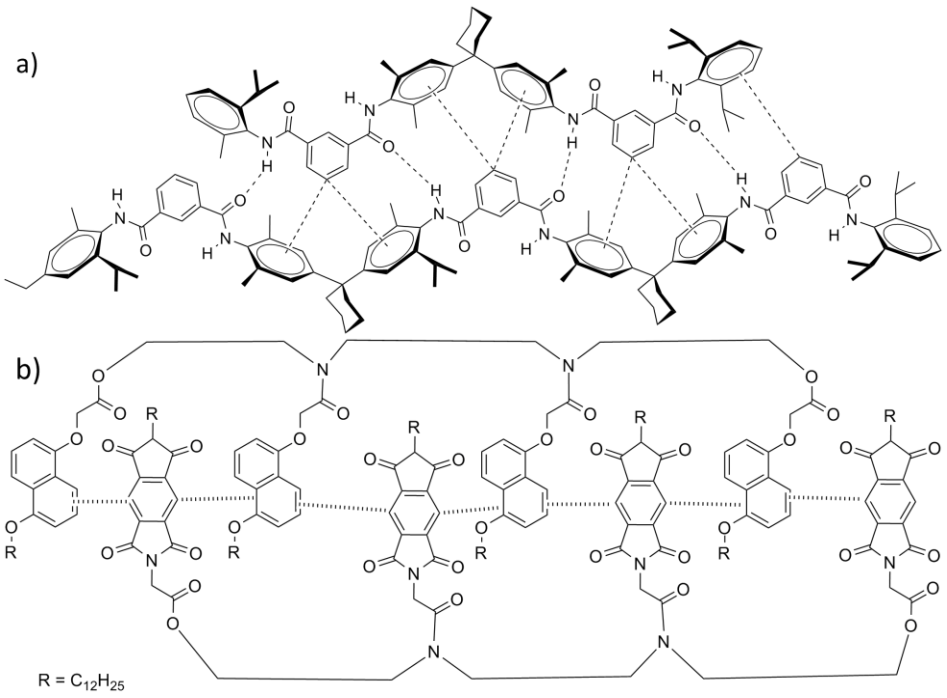

Figure 2.5 a) Molecular zippers held together by hydrogen bonding and edge-to-face aromatic interactions. b) Proposed orientation of donor-acceptor duplex utilizing donor-acceptor aromatic interactions.

This work though similar to the earlier published aromatic donor acceptor work from this lab, differed from the Iverson aedamer duplexes in two very distinct ways. Firstly, the electron deficient aromatic acceptor used was the pyromellitic diimide versus the naphthalene tetracarboxylic diimide from the Iverson lab, secondly the donor and acceptor units in their system was appended to the backbone of the oligomer as opposed to being fully integrated in to the oligomer as was seen in the seminal work from this lab[45].

The systems discussed previously in this section have all been designed for organic solvents, clearly due to the predominantly hydrocarbon based nature of these designs. Early work from this lab detailed the unique ability of our donor-acceptor duplex assemblies to have remarkably high affinities for one another in aqueous environments[39].

Creative exploitation of this powerful associative property has lead to the construction of large water soluble assemblies where we have shown not only the ability to control *intra* molecular association and directed folding topologies, but also ability to drive *inter* molecular association as well *vide infra* Figure 2.6. Oligomers consisting of the DAN and NDI units connected through aspartic acid residues we used to form intertwined supramolecular structures that were readily characterized by the appearance of a charge transfer band indicative of the donor-acceptor interaction. The novel pleated structures seen upon hetero-duplex formation demonstrated remarkably high association constants in aqueous environments where the driving force for molecular assembly was attributed primarily to the hydrophobic effect.

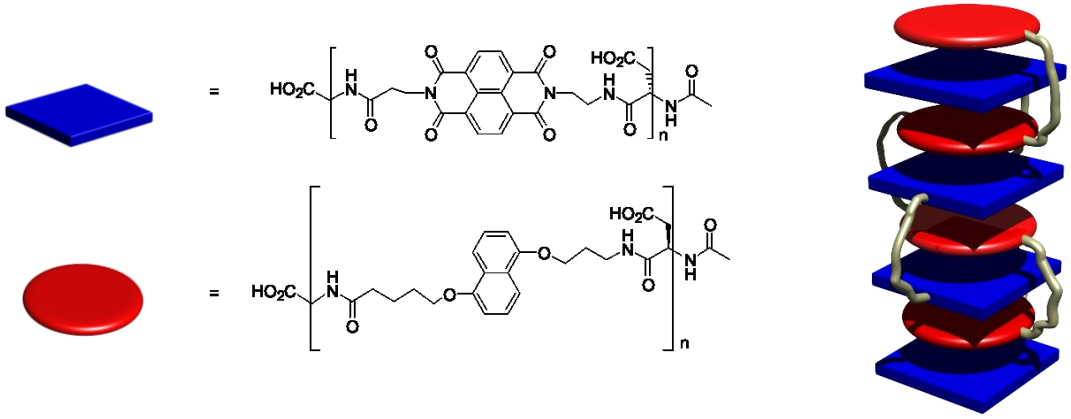

Figure 2.6 Cartoon representation of the pleated hetero-duplex formed using aspartic acid linkers.[45]

2.3 RESULTS AND DISCUSSION

2.3.1 Computational Studies

The loss of binding affinity seen as the donor and acceptor oligomers increased in length was attributed to the intra molecular "self-stacking" of the NDI acceptors with themselves prior to complexation with the donor strand. The inherent flexibility of the

aspartic acid residues used to tether the individual monomer units enabled the electron deficient NDI units to stack with each other in an offset manner. The disruption of this self association and subsequent reorganization into the conformation necessary for binding to the donor strand was seen as the entropic penalty associated with duplex formation. Pre-organization of the donor and acceptor monomers prior to duplex formation was seen as a potential solution to this problem and with this in mind the pursuit of a more rigidified linker was initiated.

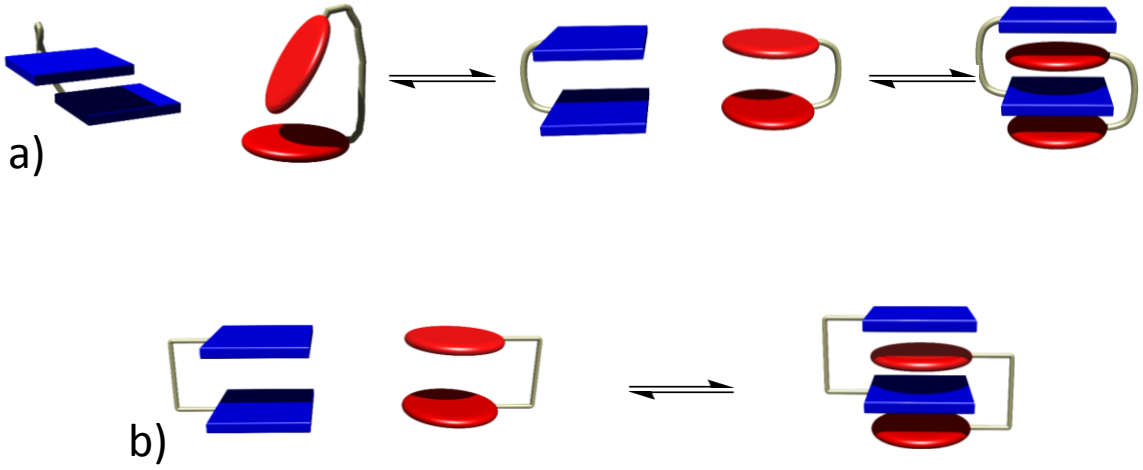

Figure 2.7 a) Cartoon illustrating the self stacking of the donor and acceptor monomers and rearrangement in to the conformation necessary for complexation. b) The rigidified linker backbone circumvents self stacking prior to duplex formation

Computer modeling was chosen as the starting point for the redesign of the water-soluble aedamer complexes. Although far from rigorous, modeling proved to be highly constructive in the exploration of potential linker molecules since it afforded a reasonable approximation of the structure and orientation of the oligomer complexes. Using the

orientation of the complexed aromatic units as evidenced in the crystal structure data, a variety of molecules were investigated for use as potential linkers. It soon became apparent that despite the importance of rigidity within the linker, it was still necessary to maintain some degree of flexibility. This provided the donor and acceptor units the ability to adjust themselves after complexation in order to maximize their face-to-face interaction. Molecules were also chosen on the basis of ease of derivitization since any potential linker required a functional handle which would allow the facile integration of the linker with both donor and acceptor molecules respectively.

Structures that looked promising after this initial simulation were then subjected to a secondary round of calculations in which the electron rich and electron poor dimers underwent molecular dynamics simulations in which the dimers were interrogated in orientations away in separate space, having no interaction whatsoever, as well as in the locked configuration of the hetero-duplex. The difference in energies between the model dimers in the complexed and uncomplexed conformation served as a guide for the affinity of the molecules for each other. It should be noted that these molecular calculations were all conducted *in vacuo* wherein the predominant driving force for the dimer geometry is based on electrostatic interactions. The desolvation effect observed in the formation of the hetero-duplex assemblies in aqueous media was not considered in the course of these calculations since the ultimate goal of this study was only to gain some insight into the orientation of the dimer linkers in the assembled complex.

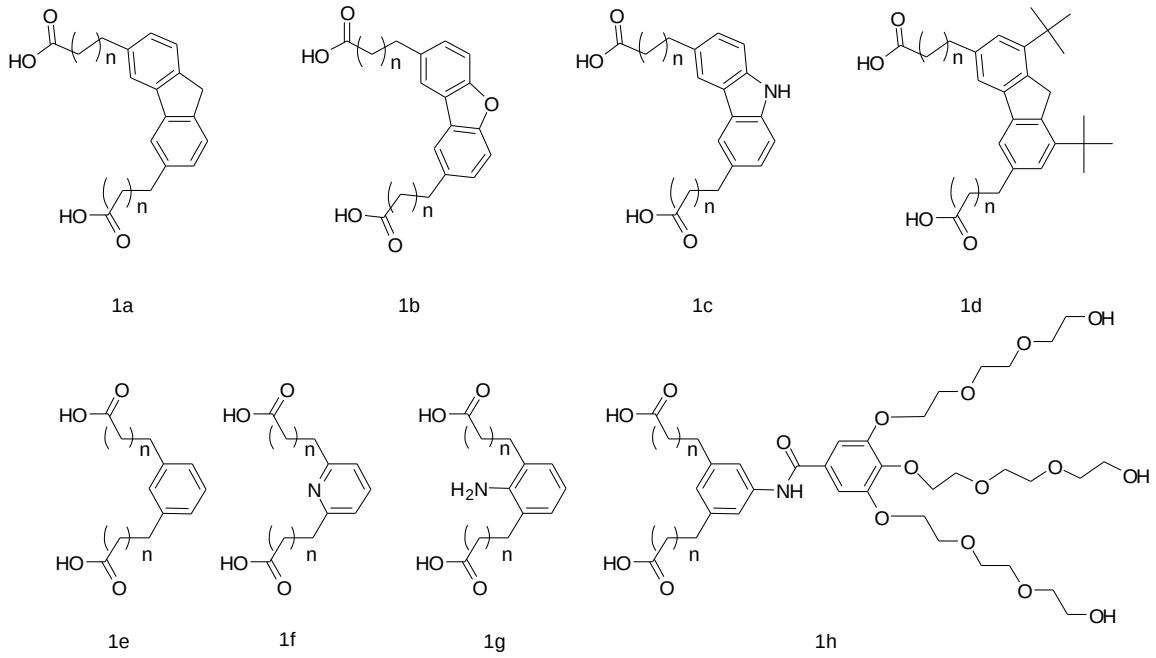

Figure 2.8 Various linker backbones modeled (n = 0,1,2)

Preliminary studies were based on the smallest unit of the oligomer strand, consisting of a dimer of similar donor or acceptor units using the linkers shown Figure 2.8. The rationale was that the interaction of a single dimer of electron rich units with a dimer of the electron poor units would be the most basic level of association in the formation of a larger hetero-duplex. Elucidation of the behavior of the oligomer backbone at this fundamental level would serve as the ideal stepping stone in the design of larger trimeric and tetrameric sytems. Computational investigation into the models chosen was conducted in two phases. The first step consisted of the attachment of the proposed linker to successive donor or acceptor subunits that were locked at the 7Å distance required for aromatic interaction upon complexation. Geometry optimization of the chosen linker was then conducted via molecular dynamics simulations using the MM+ force field. The structures obtained from these calculations were then closely inspected for the presence of any significant strain as evidenced by significantly distorted

bond angles or adverse steric interactions with the donor and acceptor molecules, indicating an unfavorable conformation of the linker upon complex formation.

Since structural rigidity was essential to the design of a successful linker, a number of molecules containing conjugated backbones were explored. The rationale for this design choice was that a fused ring system would prevent flexibility by restricting the degrees of freedom within the backbone. Additionally a number of these compounds were readily synthesized from commercially available starting materials allowing the incorporation of carboxylic acid moieties to be utilized in the attachment of the donor and acceptor molecules via amide bond formation. Preliminary modeling studies indicated that while the rigidity was indeed imparted to the linker through the fused aromatic frameworks of the furan and carbazole based derivatives, a significant amount of stacking was observed between the donor and acceptor molecules and the aromatic backbone. As a potential solution, bulky *t*-butyl substituents were introduced to the 4 and 6 positions of the dibenzofuran based linker with the hope that the increased steric bulk along the linker backbone would prevent the unwanted association of the individual dimers. This did in fact turn out to be the case, however, the fused ring systems were plagued by two other equally problematic issues. The first drawback to the furan and carbazole based derivatives was that the distances between the carbonyl centers of the two pendant carboxylic acid groups ranged from 10Å-11Å, orienting the molecules outside of the optimal 7Å window. Secondly, the issue of the water solubility properties of the large non-polar aromatic linkers became a cause for concern. In order to maximize the binding affinity of the donor and acceptor molecules the advantageous desolvation effect had to be preserved and for this to remain at all feasible the solubility of the linker had to be taken into consideration.

With these concerns in mind the focus on linker design shifted to the investigation of benzene based derivatives. These units while not as structurally rigid as the larger polycyclic molecules studied previously did allow some restriction of freedom within the linker. Additionally the smaller size of the aromatic surfaces within the linker allowed for the possibility of this class of molecules having increased water solubility properties over their predecessors. Reduction in the distance separating the carbonyl centers of the dicarboxylic acid functionalized linkers was also seen as being potentially beneficial in achieving a 7Å distance between dimers. Functionalized aromatic molecules such as pyridine and isophthalic acids were probed for their utility in rigidifying the linker within the dimer-based complex. Especially encouraging data was attained after computational analysis of the pyridine based linker 1f and the aminoisophthalic derivative 1g. The isophthalic acid linker was of significant interest since the amino substituent allowed the incorporation of other solubilizing groups onto the linker backbone potentially increasing the ability of the molecule to be solvated by water. This design element led to the construction of compound 1h where the ethyl gallate moiety could improve the overall solubility of the linker[67].

During the course of the synthesis of 1f and 1h the synthesis of a novel proline-based molecular scaffold was reported where the rigid assembly was maintained through the incorporation of intramolecular diketopiperazine ring formation[68]. The construction of this molecule, achieved via solid phase peptide synthesis (SPPS) immediately caught our attention since this approach was originally utilized in the fabrication of the DAN and NDI intra-molecularly associating oligomers. This meant that the incorporation of this molecule into the design scheme of the revised and aedamers would allow the retention of the facile yet modular approach to linker design, granting access to larger trimeric and tetrameric oligomers. Additionally, the absence of non-polar aromatic molecules within

this framework contributed to the remarkable solubility in aqueous environments of up to more than 5mg/ml. Modeling of a similar scaffold designed utilizing this approach indicated that the optimal 7Å distance between monomer units was easily accommodated by this proline-based linker. The versatility and the solubility properties of the linker designed using this methodology was influential in the decision to aggressively pursue the incorporation of this molecule into donor and acceptor oligomers in attempting to increase association constants of the hetero- duplex.

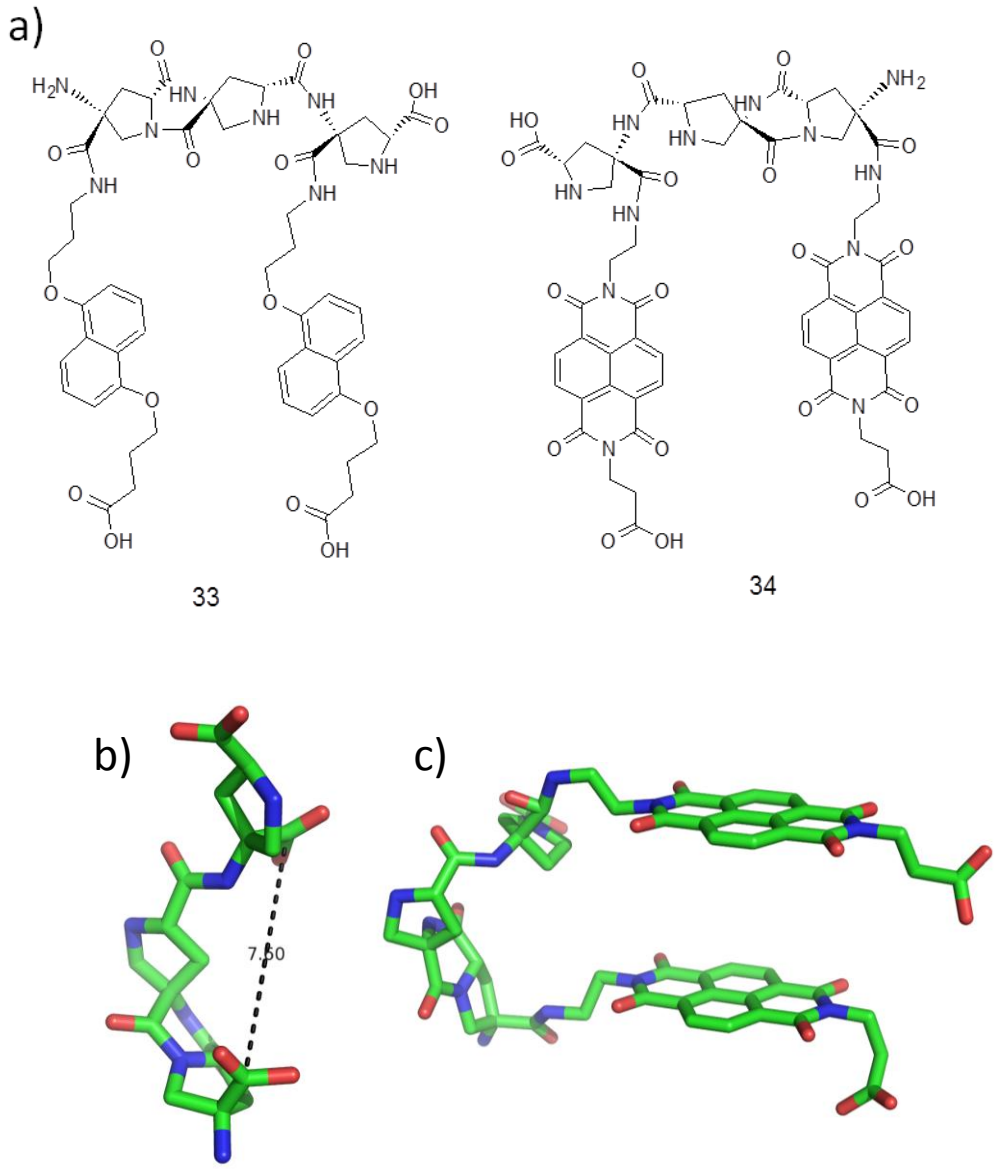

Figure 2.9 a) Target donor and acceptor dimers. b) Model of rigidified proline based linker. c) Model of NDI dimer functionalized with proline linker

2.3.2 Synthesis of proline based scaffold

The core unit of the linker chosen **8** is shown in Scheme 1. Starting with the *trans*-4-hydroxy-L-proline **1**, the amine functionality was protected using benzyl chloroformate to yield **2**. The hydroxyl group of the ring was then oxidized using Jones

reagent to give the corresponding ketone, followed by protection of the pendant carboxylic acid as the *t*-butyl ester **4**. Installation of the quaternary stereocenter on the linker was achieved via the Bucherer-Berg reaction, with good diastereoselectivity. The resultant hydantoin **5a** was protected using di-*tert*-butyl dicarbonate, subsequent alkaline hydrolysis of the intermediate **6**, led to the isolation of the unnatural amino acid **7**. Orthogonal protection of the free amine with fluorenylmethyl chloroformate led to the orthogonally protected linker core **8**.

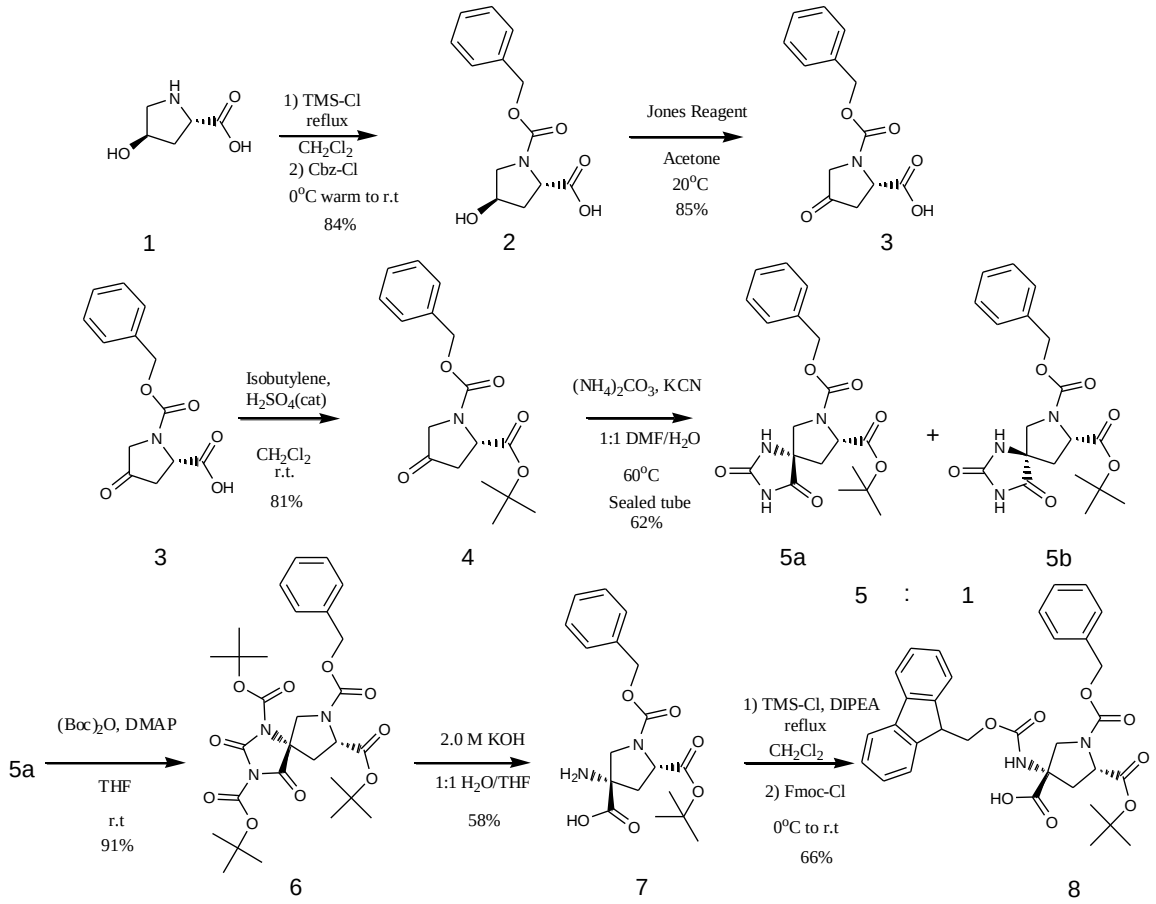

Scheme 2.1 Synthesis of proline based linker

The protected donor molecule **21** was achieved in four steps starting with the Boc-protection of 3–bromopropylamine hydrobromide **15** followed by monoalkylation of

the naphthalene core **29**, yielding compound **20**. 4-bromobutyric acid was protected as the benzyl ester yielding **18** which was then utilized in the alkylation of the intermediate **20** affording the orthogonally protected donor **21**. The protected acceptor was synthesized following procedures previously published.[40]

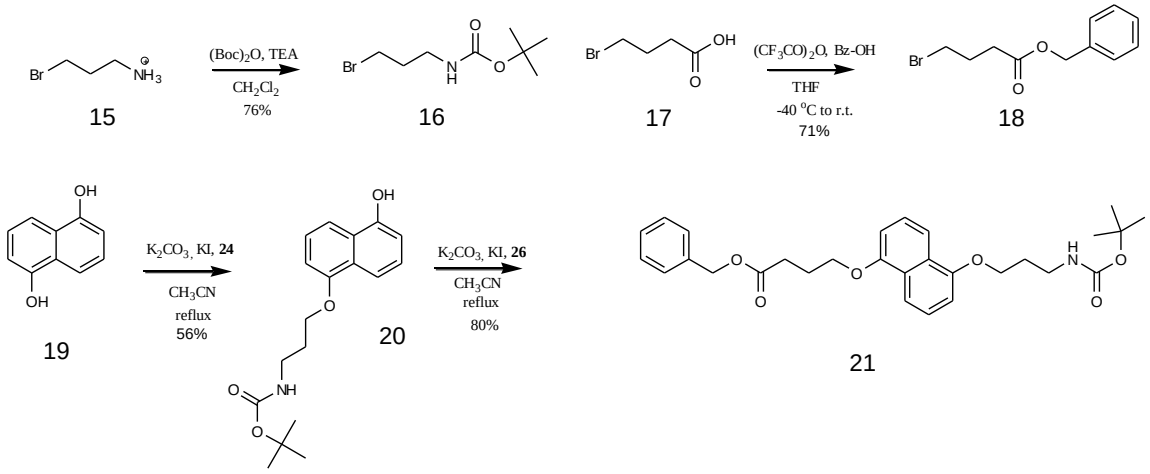

Scheme 2.2 Synthesis of donor molecule

Attachment of the linker **8** to the donor and acceptor molecules was achieved via amide bond formation between the free amine of compounds **11** and **22**. This coupling proved to be especially challenging in the synthesis of both key intermediates **12** and **23**. A number of different reaction conditions were employed in attempts to complete this coupling, ranging from exploration of different coupling partners (DCC, HOBt, HATU, Pfp), to the implementation of microwave methodologies. Promising results were obtained through the use of microwave irradiation in conjunction with HATU as the activating partner resulting in the synthesis of the desired molecules albeit in very modest yields.

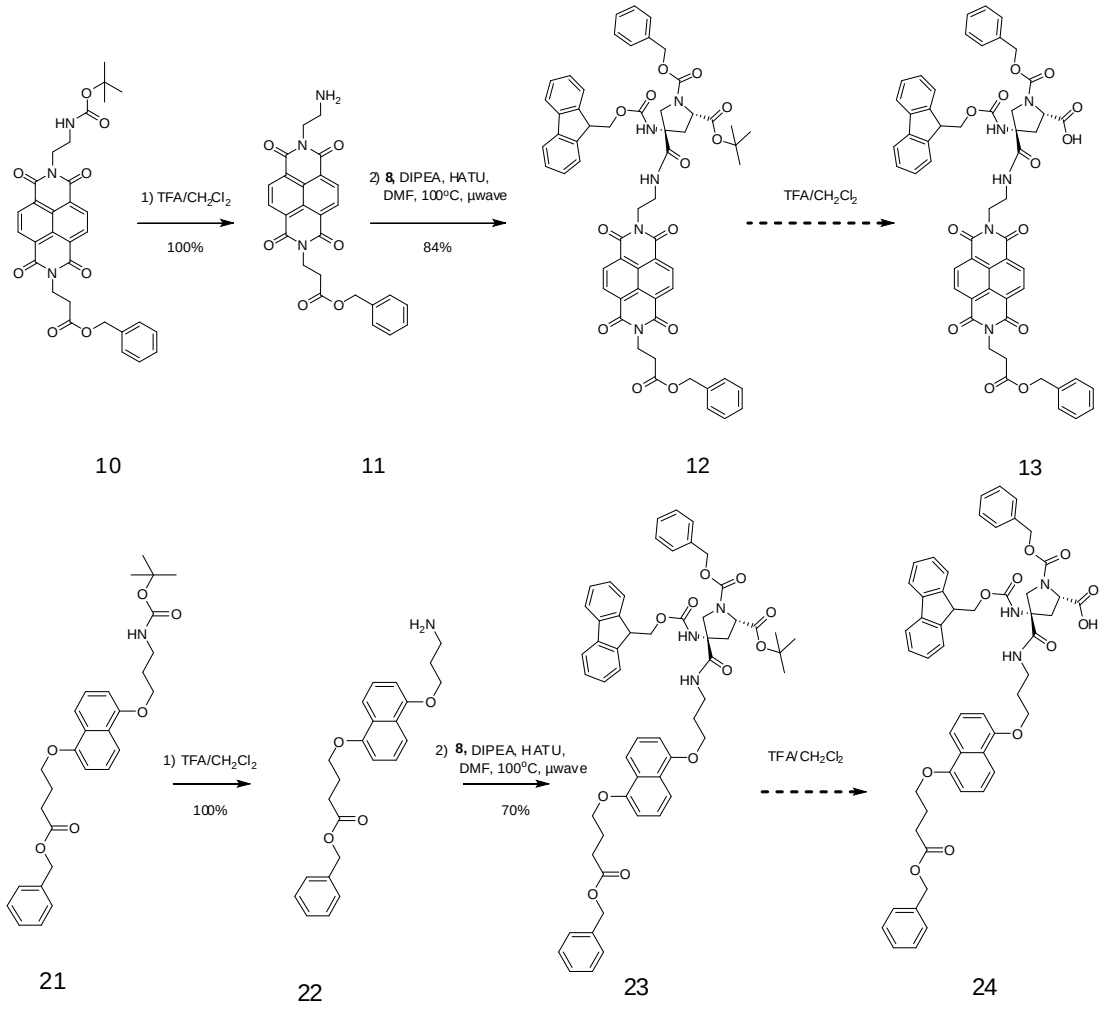

Scheme 2.3 Synthesis of donor and acceptor precursors to SPPS.

At this point in the synthesis of this proline based linker it became apparent that the design of the donor and acceptor monomers needed to be revised. Primarily due to the fact that with the donor and acceptor monomers **12** and **23** in hand, there were still an additional 12 steps before we would gain access to the individual dimers. More importantly, due to the relatively modest coupling efficiencies of large, extremely hindered molecules via standard solid phase coupling protocols, the donor and acceptor molecules would be required on a multigram scale. Given the modest yields throughout

the first 13 steps of this synthesis, coupled with the difficulty associated with the tethering of the proline monomer with the acceptor starting material it became quickly apparent that such an approach was synthetically demanding and ultimately unfeasible.

2.4 CHAPTER CONCLUSIONS

The approach to solving the problem of the acceptor units self-stacking and forming the unwanted homo-duplex prior to complexation with acceptor oliogomer is still worthy of some merit. Redesign of the linker backbone is critical to addressing the entropic penalty seen as the oligomeric complexes become larger. The new "comb-like" architecture proposed still has the potential to prevent the self stacking of adjacent acceptor units since the flexibility of the aspartic acid residues utilized in the previous "head-to-tail" design is now absent. More careful consideration must be paid however, to the ease of incorporation of the new rigidified linker into the existing hetero-duplex framework.

In spite of the seemingly disappointing end to this project there are few very important points that were learned. Firstly, the linkers need an optimal distance of 7 Angstroms between successive donor or acceptor units, secondly they also need to incorporate synthetic handles which not only allow facile integration of Dan and subunits, but also facilitate extension of the linker backbone so that the larger oligomers are readily accessible such as tetramers and hexamers.

2.5 EXPERIMENTAL METHODS

General Procedures

THF, CH_2Cl_2 and methanol were dried by distillation over CaH_2 under argon. Other reagents were used as received. All other reagents were purchased from the Sigma-Aldrich chemical company and were used as received with the exception of TMS-

Cl and DIPEA, which were both distilled prior to use. All microwave experiments were conducted in a C.E.M. Explorer 48 microwave reactor at a power of 300W. All modeling experiments were conducted using Hyperchem release 7 software. Reactions were carried out under argon using oven dried glassware. NMR experiments were conducted on a Varian 400MHz instrument in the solvent indicated in parentheses ($CDCl_3$, DMSO-*d*6)

2.5.1 Modeling

Molecular modeling was conducted using HyperChem 7 using the MM+ force field. Geometry optimization of the linker molecules investigated was conducted in two successive steps. The linker was first optimized while locked in the 7Å conformation of the co-crystal structure. Molecular dynamics calculations were then run on the molecule where the molecule underwent a simulation as it was computationally "heated" from 100K to 1000K and then cooled to a final temperature of 200K. The lowest energy structures obtained in this round of modeling were then subjected to molecular dynamics calculations utilizing the aforementioned parameters, where the donor and acceptor dimers modeled away from each other as well as locked in the 7Å conformation of the co-crystal. The difference in energies between the lowest energy conformations of the dimers together and the dimers apart were calculated for each of the molecules modeled.

4-Hydroxypyrrolidine-1,2-dicarboxylic acid 1-benzyl ester (2)

To a 500 mL three neck flask fitted with a reflux condenser, rubber septum, nitrogen adapter and magnetic stir bar was added *trans*-4-hydroxy-L-proline (**1**, 10.0 g, 76.2 mmol). The solid was suspended in 160 mL of CH_2Cl_2. Diisopropylethylamine (46.5 mL, 266 mmol) was added with stirring. Chlorotrimethylsilane (28.3 mL, 326.7 mmol)

was then added slowly, and the solution was heated a reflux gently for 2 hours. The flask was transferred to an ice bath, and benzyl chloroformate (Cbz-Cl, 10.2 mL, 72.3 mmol) was added in one portion via syringe. The stirred solution was allowed to warm to room temperature overnight. The reaction mixture was concentrated to a dark red oil, which was dissolved in 1 L of 2.5% aqueous $NaHCO_3$ and transferred to a separatory funnel. The solution was washed with ether (3 x 200 mL). The ether washes were combined and extracted into water (2 x 200 mL). The aqueous layers were combined and acidified to pH 2 with 2M aqueous HCl. This solution was extracted with EtOAc (4 x 250 mL). The EtOAc layers were washed with brine (3 x 250 mL), dried over Na_2SO_4, and filtered. The solvent was evaporated *in vacuo*, yielding the desired product **2** (17.12 g, 64.5 mmol, 84.7%) as a pink oil, used without further purification: ^{1}H NMR (DMSO-*d*6) δ 12.2-12.4 (br s, 1H), 7.31-7.35 (m, 5H), 5.08 (s, 2H), 4.30-4.35 (m, 2H), 3.51 (dd, *J* = 11.0, 4.7 Hz, 1H), 3.41 (ddd, *J* = 11.0, 2.8, 1.4 Hz, 1H), 2.19 (dddd, *J* = 12.0, 8.3, 4.1, 1.2 Hz, 1H), 2.02 (ddd,*J* = 12.0, 6.7, 5.2 Hz, 1H); ^{13}C NMR (DMSO-*d*6) δ 172.8, 153.7, 136.5, 127.7(2C), 127.0, 126.7 (2C), 67.79, 65.58, 57.38, 54.22, 38.03. HRMS CI found 265.959 calculated 265.0950

4-Oxopyrrolidine-1,2-dicarboxylic acid 1-benzyl ester (3)

An 8 molar solution of Jones reagent was prepared as described earlier (Hudlicky, M. *Oxidations in Organic Chemistry*; American Chemical Society, 1990). To a 2 L round-bottomed flask equipped with a magnetic stir bar were added (4*R*,2*S*)-4-hydroxypyrrolidine-1,2-dicarboxylic acid 1- benzyl ester (**2**, 17.1 g, 64.5 mmol) and acetone (1000 mL). To this solution was added the Jones reagent (65.3 mL, 523.1 mmol) dropwise over a period of approximately 15 minutes with stirring. The reaction mixture was stirred for an additional 60 minutes. Over this time the solution color changed from a bright red to a dark brown. The excess oxidant was consumed by slow addition of

isopropyl alcohol (10 mL) causing the solution to change from dark brown to dark green. The solution was filtered through a fine frit sintered glass funnel to remove the precipitated chromium salts, concentrated to 300 mL, diluted with EtOAc (500 mL), and transferred to a separatory funnel. This solution was washed with brine (6 x 100 mL), dried over Na_2SO4, and filtered. The solvent was evaporated *in vacuo*, yielding the desired product **3** (14.5 g, 55.1 mmol, 85.3%) as yellow oil, used without further purification: ^{1}H NMR (DMSO-*d*6) δ 13.2-13.8 (br s, 1H), 7.56-7.51 (m, 5H), 5.35 (s, 2H), 4.95 (dd, *J* = 10.4, 2.8 Hz, 1H), 4.14 (d, *J* = 18.2 Hz, 1H), 3.98 (d, *J* = 18.2 Hz, 1H), 3.29 (ddd, *J* = 18.7, 10.4, 0.9 Hz, 1H), 2.72 (dd, *J* = 18.5, 2.8 Hz, 1H); 13C NMR (DMSO-*d*6) 207.5, 172.4, 153.9, 136.3, 128.0 (2C), 127.5, 127.1 (2C), 66.42, 55.96, 52.10, 41.20. MS CI found 263.077.

4-Oxopyrrolidine-1,2-dicarboxylic acid 1-benzyl ester 2-*tert*-butyl ester (4)

To a 500 mL flask containing a magnetic stir bar were added (2*S*)-4-oxopyrrolidine 1,2-dicarboxylic acid 1-benzyl ester (**3**, 14.5 g, 55 mmol), and CH_2Cl_2 (100 mL). The solution was cooled to 0 ^oC using an ice bath, and concentrated sulfuric acid (0.51 ml, 9mmol) was added while stirring. Isobutylene was bubbled into the solution until the volume of the mixture had increased by approximately 50%. The reaction mixture was stirred overnight while warming to room temperature. The solution was then transferred to a separatory funnel with an additional volume of CH_2Cl_2 (300 mL), and washed with a solution of saturated aqueous Na_2CO_3 (100 mL) and water (100 mL). The mixture was agitated gently to prevent the formation of a tenacious emulsion. The organic layer was isolated and washed with water (2 x 100 mL), dried over Na_2SO_4, and filtered. The solvent was evaporated *in vacuo*, yielding the product **4** (14.4 g, 81% crude yield) as a yellow oil, used in the next reaction without further purification. An analytical sample was prepared by silica column chromatography (3:7 EtOAc/hexanes, R_f

= 0.27): ^{1}H NMR (DMSO-d_6) 7.42-7.38 (m, 5H), 5.22 (s, 2H), 4.72 (dd, *J* = 10.3, 2.5 Hz, 1H), 3.99 (d, *J* = 18.1 Hz, 1H), 3.81 (d, *J* = 18.1 Hz, 1H), 3.17 (dd, *J* = 18.5, 10.3 Hz, 1H), 2.52 (dd, *J* = 18.5, 2.2 Hz, 1H), 1.44 (s, 9H); ^{13}C NMR (DMSO-d_6) 207.9, 171.0, 154.6, 137.1, 128.8 (2C), 128.3, 128.0 (2C), 82.28 (2C), 67.22, 57.54, 52.93, 28.02 (3C); HRMS CI calculated 319.1420, found 319.1412

2,4-Dioxo-1,3,7-triazaspiro[4.4]nonane-7,8-dicarboxylic acid 7-benzyl ester 8-*tert*butyl ester (5a) and (5*R*,8*S*)-2,4-Dioxo-1,3,7-triazaspiro[4.4]nonane-7,8-dicarboxylic acid 7-benzyl ester 8-*tert*-butyl ester (5a)

A 75 mL pressure vessel was charged with ammonium carbonate (6.7 g, 57.9 mmol), potassium cyanide (1.85 g, 23.4 mmol), deionized water (35 mL) and a magnetic stir bar. To this vessel was added a solution of (2*S*)-4-oxopyrrolidine-1,2-dicarboxylic acid 1-benzyl ester 2-*tert*-butyl ester (**4**, 6,10 g, 19 mmol) in DMF (35 mL). After sealing the vessel, the reaction mixture was heated to 60 ^{o}C for 4 hours with vigorous stirring. The pressure vessel was cooled to 0 ^{o}C, opened cautiously, and the solution transferred to a separatory funnel with an additional volume of water (600ml). The aqueous solution was extracted with EtOAc (4 x 150 mL). The combined organic layers were washed with brine (4 x 150 mL), dried over Na_2SO_4, and the solvent removed *in vacuo* yielding a crude mixture of products **5a** and **5b** in a ratio of 5:1 (determined by ^{1}H NMR). This crude product was further purified by silica column chromatography (99:2 CH_2Cl_2/methanol) yielding the less polar diastereomer as a white foamy solid (**5a**, 4.58 g, 56.9% recovered yield).

^{1}H NMR (DMSO-d_6) 10.82 (s, 1H), 7.89 (s, 1H), 7.34 – 7.29 (m, 5H), 5.09 –5.04 (m, 2H), 4.33 – 4.23 (m, 1H), 3.89 – 3.82 (m, 1H), 3.43 – 3.36 (m, 1H), 2.70 – 2.63 (m,1H), 2.06 – 1.97 (m, 1H), 1.39 and 1.30 (s, rotameric, 9H); ^{1}H NMR (300 MHz, 75

^{o}C, DMSOd_6) 7.32 (m, 5H), 5.10 (s, 2H), 4.36 (dd, *J* = 8.2, 7.4 Hz, 1H), 3.84 (d, *J* = 11.2 Hz, 1H), 3.50 (d, *J* = 11.9 Hz, 1H), 2.63 (dd, *J* = 13.3, 8.6 Hz, 1H), 2.11 (dd, *J* = 13.3, 7.2 Hz, 1H), 1.40 (s,9H); ^{13}C NMR (DMSO-d_6) 176.7, 170.8, 156.0, 153.6, 136.6, 127.6 (2C),127.1, 126.7 (2C), 81.35 (2C), 66.47, 58.73, 52.32, 27.35 (3C); HRMS CI calculated 333.0961, found 333.0963

2,4-Dioxo-1,3,7-triazaspiro[4.4]nonane-1,3,7,8-tetracarboxylic acid 7-benzyl ester1,3,8-tri-*tert*-butyl ester (6)

To a 250 mL round bottom flask with magnetic stir bar were added DMAP (76.2 mg, 0.6mmol), (5*S*,8*S*)-2,4-dioxo-1,3,7-triazaspiro[4.4]nonane-7,8-dicarboxylic acid 7-benzyl ester 8-*tert*-butyl ester (**5a**, 3.47 g, 8.9 mmol), and THF (150 mL). The flask was flushed with argon and di-*tert*-butyl dicarbonate (6.22 g, 28.5 mmol) was added with stirring. The reaction mixture was stirred for 2 hours, by which time **5a** had been totally consumed (by TLC). The solution was concentrated on the rotary evaporator and the solvent removed *in vacuo* yielding foamy yellow oil (**6,** 5.13 g, 97 %). The crude material was purified by column chromatography before being used in the next step. (1:1 EtOAc/hexanes, R_f = 0.32): ^{1}H NMR ($CDCl_3$) 7.51 – 7.50 (m, 5H), 5.44 – 5.24 (m, 2H), 4.85 – 4.78 (m, 1H), 4.31 – 4.23 (m,1H), 4.19 – 4.11 (m, 1H), 3.12 – 3.03 (m, 1H), 1.75 – 1.66 (m, 27H); $_{1}$H NMR (DMSO-d_6) 7.35 (m, 5H), 5.10 (s, 2H), 4.40 (t, *J* = 8.4 Hz, 1H), 3.99 (d, *J* = 12.3 Hz, 1H), 3.76 (d, *J* = 12.4 Hz, 1H), 2.73 (dd, *J* = 13.2, 8.1 Hz, 1H), 2.63 (dd, *J* = 13.2, 8.7 Hz, 1H), 1.51 (s,9H), 1.40 (s, 18 H); ^{13}C NMR ($CDCl_3$) 169.7, 153.9, 147.4, 146.6, 144.5,135.8, 128.2 (2C), 127.8, 127.6 (2C), 86.92, 85.70, 81.71, 67.28, 65.46, 58.37, 50.35, 35.82, 27.72 (3C), 27.54 (3C), 27.45 (3C). HRMS CI calculated 589.2634 found 590.3263

4-Aminopyrrolidine-1,2,4-tricarboxylic acid 1-benzyl ester 2-*tert*-butyl ester (7)

A 250 mL round bottom flask with magnetic stir bar was charged with a solution of crude (5*S*,8*S*)-2,4-dioxo-1,3,7-triazaspiro[4.4]nonane-1,3,7,8-tetracarboxylic acid 7-benzyl ester 1,3,8-tri-*tert*-butyl ester (**6**, ~ 5.52 g, 9.3 mmol) in THF (40 mL). To this solution was added a 2.0M aqueous solution of potassium hydroxide (40 mL). The reaction mixture was stirred vigorously for 90 minutes. The solution was transferred to a 250 mL separatory funnel with an additional volume of ether (50 mL) and agitated. The aqueous layer was removed, and the THF-ether was washed with a 1% aqueous solution of potassium chloride (2 x 50 mL). The aqueous layers were combined in a 500 mL beaker and cooled to 0 ^{o}C using an ice bath. With stirring, the aqueous solution was acidified to pH 6.5 by dropwise addition of 6.0 M aqueous HCl, causing the precipitation of a fine, white solid, then left to sit for 15 minutes in an ice-bath. The solution was filtered and the collected precipitate was washed with ~ 250 mL of cold water. The precipitate was dried at 50 ^{o}C in a vacuum oven overnight yielding the desired product **7** (2.14 g, 58%), used without further purification: ^{1}H NMR (CD_3OD) 7.22 – 7.18 (m, 5H), 5.01 – 4.95 (m, 2H), 4.37 – 4.32 (m, 1H), 3.89 (d, J =11.6 Hz, 1H), 3.63 (d, J = 11.7 Hz, 1H), 2.84 – 2.73 (m, 1H), 2.06 – 2.00 (m, 1H), 1.35 and 1.18(s, rotameric, 9H); ^{13}C NMR (CD_3OD) 174.8, 173.2, 155.8, 137.4, 129.5(3C), 129.1 (2C), 84.16, 68.78, 64.47, 60.56, 56.21, 39.76, 27.99 (3C), HRMS CI calculated 364.1616 found 365.2501

(9*H*-Fluoren-9-ylmethoxycarbonylamino)pyrrolidine-1,2,4-tricarboxylic acid 1-benzyl ester 2-*tert*-butyl ester (8)

To a 250 mL flask fitted equipped with a magnetic stir bar and rubber septum were added (2*S*,4*S*)-4-aminopyrrolidine-1,2,4-tricarboxylic acid 1-benzyl ester 2-*tert*-butyl ester (**7**, 399 mg, 1.09 mmol). The solid was suspended in 80 mL of CH_2Cl_2.

Diisopropylethylamine (0.97 mL, 5.58 mmol) was added with stirring. Chlorotrimethylsilane (0.16 mL, 1.9 mmol) was then added slowly, and the solution was stirred at room temperature under nitrogen for 8 hours. The flask was transferred to an ice bath, and 9-fluorenylmethylchloroformate (Fmoc-Cl, 228 mg, 0.8 mmol) was added in one portion. The stirred solution was allowed to warm to room temperature overnight. The reaction mixture was concentrated to a yellow oil which was dissolved in EtOAc (30 mL), transferred to a separatory funnel, and washed with dilute aqueous HCl, pH ~2 (2 x 25 ml). The aqueous layers were combined and extracted with EtOAc (2 x 25 ml). The EtOAc layers were combined, washed with brine (2 x 50 mL) and dried over Na_2SO_4. The solvent was evaporated *in vacuo* to give a foamy, slightly yellow solid. This was then purified via flash chromatography (1:9 CH_3OH/CH_2Cl_2) to yield product **8** (425 mg, 0.7 mmol, 64%) which was used without further purification. ^{1}H NMR (DMSO-*d*6) 12.12 (br s, 1H), 7.84 (d, *J* = 7.1 Hz, 2H), 7.74 (br s, 1H),7.69 (d, *J* = 7.2 Hz, 2H), 7.42 – 7.29 (m, 8H), 5.10 (s, 2H), 4.39 – 4.20 (br m, 4H), 4.06 (d, *J* =11.3 Hz, 1H), 23.68 (d, *J* = 11.3 Hz, 1H), 2.87 (br m, 1H), 2.36 (dd, *J* = 13.1, 5.14 Hz, 1H), 1.37(s, 9H); ^{13}C NMR (DMSO-*d*6) 172.5, 169.9, 155.3, 153.3, 143.4 (2C), 140.4(2C), 136.3, 127.8 (2C), 127.3, 127.1 (2C), 126.9 (2C), 126.6 (2C), 124.7 (2C), 119.5 (2C),80.50, 65.91, 65.51, 62.15, 58.48, 54.68, 46.50, 38.57, 27.18 (3C) HRMS CI calculated 586.6315 found 587.9230

(3-bromopropyl)carbamic acid *tert*-butyl-ester (16)

To a 250 ml round bottomed flask were added 3-bromopropylamine hydrobromide (15 g, 68.5 mmol) and di-*tert*-butyldicarbonate (15 g, 68.7 mmol) in 150 ml CH_2Cl_2. The reaction was cooled to 0^{o}C and triethylamine (10.8ml, 61.6mmol) was added and the reaction stirred under argon and allowed to warm to room temperature for 16 h. The reaction was stopped and the organic layer washed with $NaHCO_3$ (2 x 125ml)

and Brine (2 x 125ml) and then dried over Na_2SO_4. The filtrate was reduced *in vacuo* to a pale brown oil. The solution was then frozen in liquid nitrogen and placed in the freezer for 4h. The solid product was then dissolved in hexanes and allowed to recrystallize overnight in the freezer. Product **16** isolated (12.4 g, 52.2 mmol, 76.2%) ^{1}H NMR ($CDCl_3$) 3.62(t, 2H), 3.17(t, 2H), 2.14(m, 2H), 1.34(2s, 9H) ^{13}C NMR ($CDCl_3$) 156.2, 79.6, 39.2, 32.9, 31.0, 28.5 (3C) MS, CI found 260.06 (+Na)

4-Bromobutyric acid benzyl ester (18)

In a 50ml round bottomed flask were dissolved, 4-bromo-butyric acid **17** (2g, 11.9 mmol) in THF (17ml) under an inert argon atmosphere. The reaction was cooled to -40 ^{o}C and trifluoroacetic acid anhydride (TFAA) (5.35ml, 25.4mmol) was added dropwise via syringe. Benzyl alcohol (1.16ml, 11.4mmol) was dissolved in a minimal amount of THF (~ 1 ml) and slowly added to the reaction at -40 ^{o}C . The reaction was then left to stir and warm to room temperature overnight. The reaction was reduced in vacuo to a pale amber oil and then purified via flash chromatography (3:1 Hexane/ EtoAc) yielding the product **18** as a pale yellow oil. (2.19 g, 8.5 mmol, 71.1%) ^{1}H NMR ($CDCl_3$) 7.30-7.27(m, 5H), 5.27(s, 1H), 3.73(t, 2H), 2.47(t, 2H), 2.14-1.99(m, 2H); 13C NMR ($CDCl_3$) 173.6, 159.6, 128.9(2C), 128.6(2C), 128.2, 66.9, 32.2(2C), 30.4. MS CI found 257.12

[3-(5-hydroxynaphthalen-1-yloxy)propyl]carbamic acid *tert*-butyl ester (20)

In a 100 ml round bottomed flask were added, (3-bromopropyl)carbamic acid *tert*-butyl ester **16** (6.0 g, 25.1 mmol), 1,5-dihydroxynaphthalene **19** (4.03 g, 25.2 mmol) and KI (41 mg, 0.25 mmol) in CH_3CN (66 ml). The solution was then saturated with argon and for 15 minutes. K_2CO_3 (8.71 g, 63 mmol) was then added and the reaction heated to reflux and left to stir for 16h. The solvent was removed *in vacuo* and the crude product

dissolved in CH_2Cl_2 (100 ml). The black solution was filtered through a plug of Celite and the plug washed with an additional volume of CH_2Cl_2 (100ml). The solution was then reduced in volume to a black oil which was then dissolved in a 5% w/v solution of NaOH. The aqueous solution was then washed with $NaHCO_3$ (2 x 75 ml) and Brine (2 x 75 ml) and then dried over Na_2SO_4. The filtrate was reduced in volume to a dark purple solid product **20** (4.53 g, 14.2 mmol, 56.7%) ^1H NMR ($CDCl_3$) ^{13}C NMR ($CDCl_3$) 156.5, 154.5, 152.5, 127.1, 126.8, 126.0, 125.6, 114.7, 114.5, 113.9, 109.5, 79.6, 66.4, 38.7, 29.7, 28.6 (3C); MS CI found 318.52

4-[5-(3-tert-butoxycarbonylamino-propoxy)-naphthalen-1-yloxy]-butyric acid benzyl ester (21)

In a 25 ml round-bottomed flask, 4-bromo-butyric acid benzyl ester **18** (0.613 g, 2.38 mmol) was added to [3-(5-hydroxy-naphthalen-1-yloxy)-propyl]-carbamic acid *tert*-butyl ester **20** (0.795 g, 2.14 mmol) and KI (35.5 mg, 2.14 mmol) in CH_3CN (11.3 ml) and the reaction allowed to stir for 15 minutes. The solution was then saturated with argon for 30 minutes and K_2CO_3 (3.25 g, 2.38 mmol) was added and the reaction heated to reflux and stirred under an inert argon atmosphere for 18h. The solvent was removed from the reaction *in vacuo* and the crude solid dissolved in CH_2Cl_2 (50 ml) and filtered. The filtrate was collected and washed with $NaHCO_3$ (2 x 15 ml) and Brine (2 x 15 ml) and then dried over Na_2SO_4. The filtrate was reduced to the crude brown solid. The material was purified via flash chromatography (1:4 Acetone/CH_2Cl_2) yielding the product **21** as a dark red oil. (828 mg, 1.6 mmol, 78.4%) ^{13}C NMR ($CDCl_3$) 173.3, 156.3, 154.5(2C), 136.1, 128.8(2C), 128.7(2C), 128.5, 128.4(2C), 126.8(2C), 114.7, 114.4, 105.6(2C), 68.7, 67.7, 66.5, 66.4, 32.9, 32.7, 28.6(3C), 24.9; MS found 493.69

4-{2-[7-(2-Benzyloxycarbonylethyl)-1,3,6,8-tetraoxo-3,6,7,8-tetrahydro-1H-benzo[lmn][3,8]phenanthrolin-2-yl]-ethylcarbamoyl}-4-(9H-fluoren-9-ylmethoxycarbonylamino)pyrrolidine-1,2-dicarboxylic acid 1-benzyl ester 2-*tert*-butyl ester (12)

In a 10 ml round bottomed flask the Boc-protected acceptor molecule **10** (21.8 mg, 0.03 mmol) was deprotected by stirring in a 1:1 TFA/CH_2Cl_2 mixture at room temperature for 30 minutes. The solvent was then removed via azeotropic evaporation from hexanes (x3) giving product **11**. 9*H*-Fluoren-9-ylmethoxycarbonylamino)pyrrolidine-1,2,4-tricarboxylic acid 1-benzyl ester 2-*tert*-butyl ester **8** (23.7 mg, 0.04 mmol) was dissolved in DMF (1ml) and diisopropylethylamine (7μl, 0.04 mmol) and HATU (14mg, 0.038 mmol) were added and the reaction placed in a microwave and irradiated at 300W to 100^{o}C where it was heated for 6 minutes. The reaction was then allowed to cool to 45 ^{o}C and compound **11** (18 mg, 0.03 mmol) dissolved in minimal DMF was added and the reaction once more irradiated and heated to 100^{o}C for 6 minutes. The reaction was reduced to a brown oil and purified via flash chromatography (1:4 CH_3OH/CH_2Cl_2). The product **12** was isolated as yellow solid. (29.5 mg, 0.02 mmol, 70.2%) ^{1}H NMR (DMSO-*d*$_6$) 8.67-8.50(m, 4H), 7.94(t,1H), 7.83, 7.68, 7.61-7.59(t, 2H), 7.34-7.25(br t,2H), 5.55(d, 2H), 5.05(d, 2H), 4.29(t, 2H), 4.18-4.12(m, 3H), 4.02(t, 2H), 3.85(d,2H), 3.44-3.41(m, 2H), 2.74(t, 2H), 1.31-1.29(2s, 9H); HRMS CI calculated 1039.3645 found 1041.3504

4-{3-[5-(3-Benzyloxycarbonylpropoxy)naphthalen-1-yloxy]propylcarbamoyl}-4-(9H-fluoren-9-ylmethoxycarbonylamino)pyrrolidine-1,2-dicarboxylic acid 1-benzyl ester 2-tert-butyl ester (23)

In a 10 ml round bottomed flask the Boc-protected donor molecule 21 (22.9 mg, 0.046 mmol) was deprotected by stirring in a 1:1 TFA/CH2Cl2 mixture at room temperature for 30 minutes. The solvent was then removed via azeotropic evaporation from hexanes (x3) giving product 22. 9H-Fluoren-9-ylmethoxycarbonylamino)pyrrolidine-1,2,4-tricarboxylic acid 1-benzyl ester 2-*tert*-butyl ester 8 (23.7 mg, 0.04 mmol) was dissolved in DMF (1ml) and diisopropylethylamine (7µl, 0.04 mmol) and HATU (18.1mg, 0.047 mmol) were added and the reaction placed in a microwave and irradiated at 300W to 100^{o}C where it was heated for 6 minutes. The reaction was then allowed to cool to 45 ^{o}C and compound 22 (18 mg, 0.03 mmol) dissolved in minimal DMF was added and the reaction once more irradiated and heated to 100^{o}C for 6 minutes. The reaction was reduced to a brown oil and purified via flash chromatography (1:4 CH_3OH/CH_2Cl_2). The product 12 was isolated as yellow solid. (39.6 mg, 0.02 mmol, 84.2%) 1H NMR (CDCl3) 8.63-8.43(m, 4H), 7.66-7.54(m, 4H), 7.21-6.92(br m, 12H), 5.03(t, 4H), 4.46(t, 4H), 4.32(br m, 2H), 4.01-3.96(br m, 2H), 3.85-3.75(m, 2H), 3.69(t, 2H), 3.61(t, 2H), 3.54(t, 2H), 2.77(br m, 2H), 1.72-1.69(br m, 2H), 1.42-1.28(br m, 9H); 13C NMR (CDCl3) 171.1, 162.8, 135.7, 131.3, 128.7, 128.6, 128.5, 128.4, 126.7, 66.9, 36.8, 32.8, 31.1, 28.2, 19.2; MS ESI found 962. 27

Chapter 3

3 Construction of a novel non-natural DNA analog

3.1 Chapter Summary

Introduction

As was noted in the previous chapter, our initial attempts to introduce rigidity within the backbone of our donor-acceptor hetero-duplexes were met with significant difficulty in terms of synthesis and construction of the scaffold. With this in mind we shifted the focus of our attentions to water soluble architectures more amenable to the modular synthetic approach we had initially envisioned. There has been a considerable amount of research recently in the field of non-natural nucleic acid analogs where substitution of the natural base has led to the development of novel material with interesting properties.

Goals

The goal of this project is to design and synthesize a novel DNA based scaffold which incorporates both donor (DAN) and acceptor (NDI) functionalities. It is hoped that the inherent water solubility and rigidity of the phosphate diester backbone would prove beneficial in the formation of discrete hetero-duplexes upon complexation of the individual donor and acceptor nucleotide analogs.

Approach

The phosphate diester backbone of DNA was chosen as the scaffold utilized in the construction of the second generation donor-acceptor oligomers. The advantages of using this nucleotide based architecture were twofold; firstly the deoxyribose subunit afforded a synthetic handle for the incorporation of the donor and acceptor monomers via glycosylation chemistry protocols. Secondly, the use of this nucleotide building block

allowed for the modular construction of the donor and acceptor oligomers through phosphoramidite mediated DNA synthesis enabling access to a variety of different combinations of donor and acceptor sequences. Low level molecular calculations were performed in order to assess the ability of the phosphate backbone to accommodate substitution of the natural nucleobases with the individual donor and acceptor monomers as well as to determine the steric requirements necessary for optimal face centered stacking of the DAN and NDI subunits within the DNA framework.

Results

The work in this chapter describes progress made towards the design and synthesis of DAN and NDI oligomers functionalized with the sugar phosphate backbone of DNA. The precursors made were designed to be amenable to standard automated DNA phosphoramidite protocols. Construction of the DAN donor oligomer proceeded smoothly however access to the NDI acceptor oligomer was plagued by significant synthetic difficulty due to the instability of key intermediates along the pathway to the NDI functionalized phosphoramidite. A short three residue sequence of the DAN donor oligomer was constructed in order to prove the feasibility of automated DNA synthesis in construction of these novel donor-acceptor oligomers.

3.2 BACKGROUND

Within the last decade a significant amount of research has been devoted to the design and synthesis of both natural and modified nucleotides, so much so that today chemists have the ability to selectively incorporate modified nucleotides into sequences of DNA with remarkably high efficacy. Since the elucidation of the structure of double stranded DNA by Watson and Crick nearly half a century ago the DNA double helix has been extensively investigated for its role as part of the genetic machinery of life and more

recently its ability to form well defined three dimensional structures. The high selectivity of a single strand of DNA for its complementary sequence coupled with the efficiency of phosphoramidite mediated automated DNA synthesis has given rise to a variety of modified oligonucleotide sequences with unique and highly interesting properties. Modified DNA sequences have found use in the construction of novel three dimensional architectures ranging from surface immobilized lattices[69,70] to complex shapes such as cubes and molecular cages[71,72,73]. Artificially modified oligonucleotides have also provided access to a variety of functional molecules ranging in applications from photoactive chromophores for DNA based nanomaterials[74,75], to novel site specific labels for DNA[76,77] as well as molecular nanowires[78].

It is important to note that within this field of non natural nucleotides the manner in which the deoxyribose subunit is modified dictates the relative position of the modified oligonucleotide within the three-dimensional framework of the assembled DNA helix and by extension the structural, photophysical and material properties of the modified DNA. These modifications can take place on the ribose ring itself at either the 2' or 4' positions or more commonly at the terminal 3' or 5' positions, additionally either one of the four naturally occurring nucleobases may also provide a synthetic handle for the site specific modification of oligonucleotides. Within recent literature an increasingly popular method of oligonucleotide modification has been the complete substitution of the nucleobase with the molecule of interest via novel *C* and *O* glycosydic bond formation.

3.3 RESULTS AND DISCUSSION

3.3.1 Design and Synthesis of Donor – Acceptor oligomers

Our previous attempts at constructing a redesigned donor-acceptor scaffold were met with synthetic difficulties due to the poor solubility of the naphthalene diimide substrates throughout the course of the synthesis. Redesign of the original aedamers from a head to tail orientation to the "comb-like" architecture proposed in Chapter 2 was still seen as the overall goal of this project, albeit now on a more synthetically accessible backbone. With this in mind computer modeling was once again the starting point for the design of the nucleoside based aedamers. Molecular mechanics calculations on a series of complexed Dan and Ndi sugar variants demonstrated that the inherent flexibility of the phosphodiester backbone was sufficient to accommodate the large aromatic cores without substantial disruption of the helical shape of associated donor-acceptor oligomers. Two key considerations in the design of the sugar monomers were the length of the linkers used to attach the donor and acceptor subunits to the backbone, as well as the steric bulk associated with the terminal position on each unit. The flexibility of the former essential in allowing the optimal face-centered mode of association of the donor and acceptor subunits, the latter being critical in facilitating minimal distortion of the phosphate backbone upon complexation of the individual oligomers.

The target compounds chosen are shown in Figure 3.1 Retrosynthetic analysis revealed that the donor and acceptor dimers **1** and **2** consisted of two key subunits, the protected deoxyribose sugar functionalized with the DAN or NDI aromatic unit and a spacer nucleoside comprised of a deoxyribose analog in which the nucleobase was removed (Figure 3.2). This spacer was commercially available as the di-methoxy trityl protected phosphoramidite and was used as such.

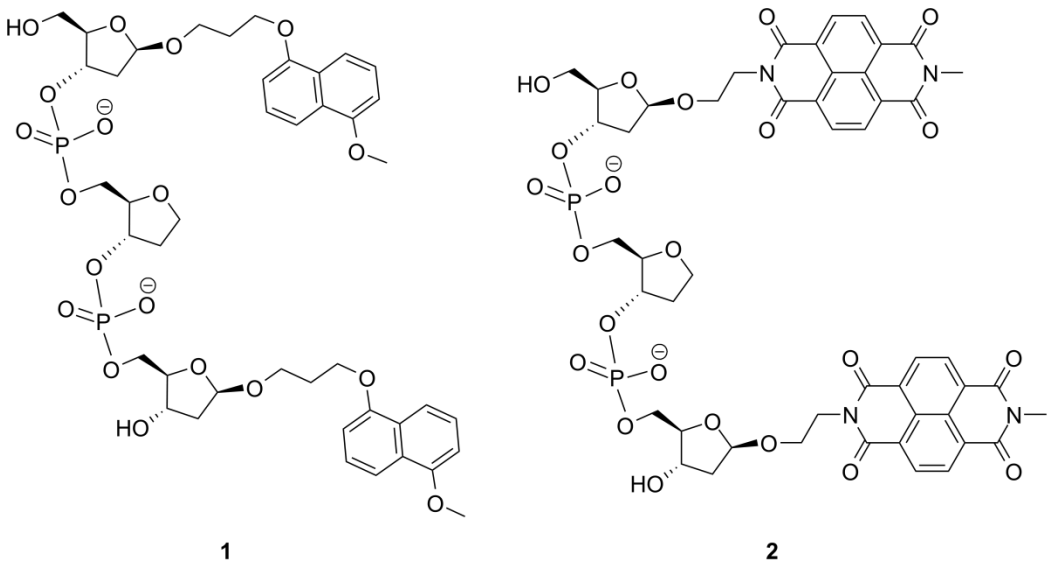

Figure 3.1 Target deoxyribose functionalized donor 3.1, and acceptor 3.2 dimers

In order to fully utilize the capability of automated DNA synthesis it was prudent to construct both donor and acceptor molecules amenable to phosphoramidite synthesis. With this in mind synthesis of donor monomer **3.9** began with formation of the bis-functionalized di-hydroxy naphthalene **3.2**. This was achieved starting with 1,5 di-hydroxy naphthalene which was selectively alkylated to yield the methyl ester protected alkoxy alcohol **3.1**. The toluyl protected chlororibose **3.5** was synthesized starting with 2-deoxyribose which was then selectively methlyated at the anomeric position, protection of the pendant C-3 and C-4 alcohols followed by subsequent cholorination yielded the target compound as outlined in Scheme 3.1

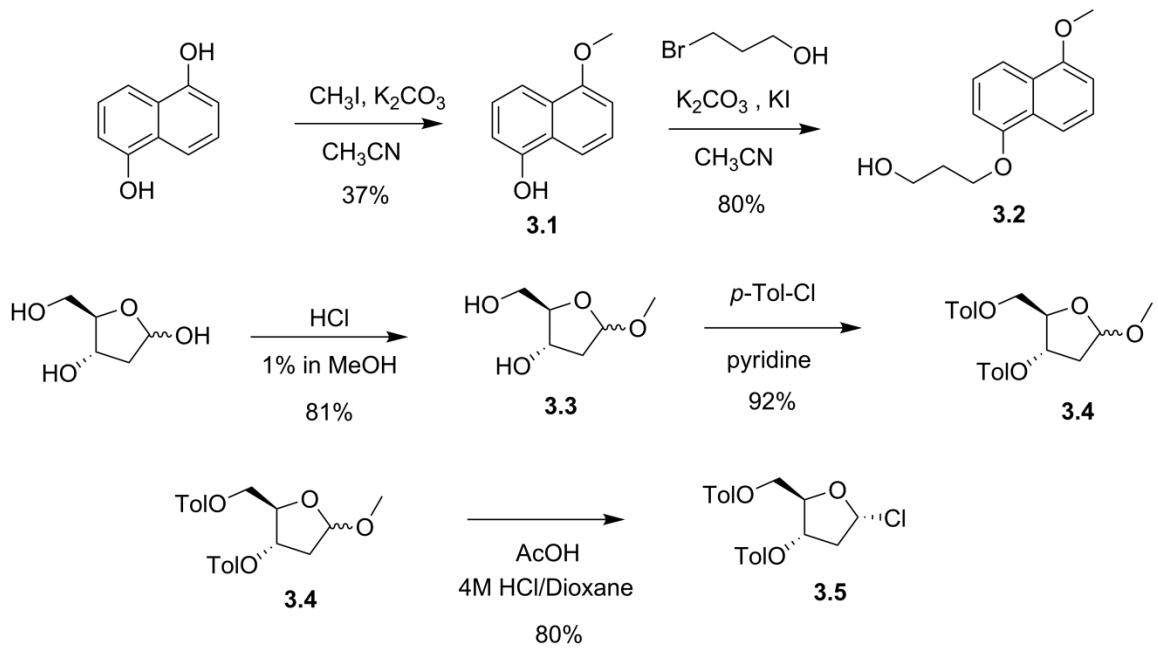

Scheme 3.1 Synthesis of Dan donor monomer

The donor monomer was appended to the protected sugar via silver promoted glycosylation to yield the functionalized deoxyribose monomer **3.6**. Removal of toluyl groups and selective protection of the terminal 5' alcohol as the di-methoxy trityl ether gave compound **3.8** in good yields as a 1.5 : 1 mixture of the α, β anomers respectively. Separation of the individual anomers followed by subsequent phosphoramidation provided the protected donor functionalized sugar monomer **3.9** in both α and β forms. See Scheme 3.2.

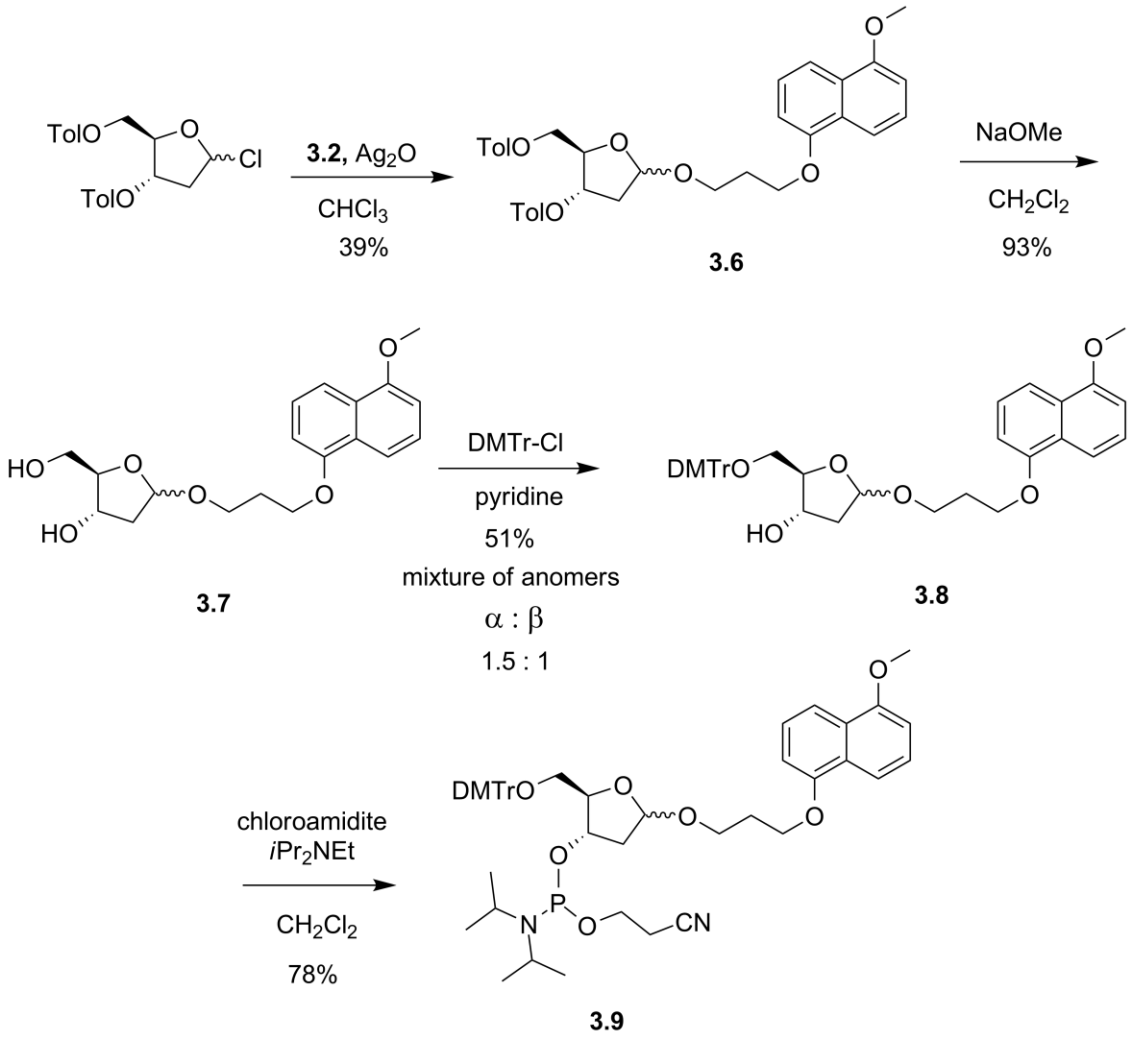

Scheme 3.2 Synthesis of donor phosphoramidite monomer

Synthesis of the acceptor functionalized sugar **3.2** was approached in a very similar fashion to that of the donor. Starting with the naphthalene tetracarboxylic dianhydride, successive condensations yielded the asymmetric alkoxy functionalized methyl imide **3.10**. This was then coupled to the protected chlorosugar **3.5** in an attempt to obtain the acceptor functionalized sugar. Unfortunately formation of the *O*-glycoside in this case did not proceed as smoothly as in the donor monomer synthesis. Limited

solubility of the diimide substrate in conjunction with its low coupling efficiency led target molecule **3.11** being obtained in very low yields.

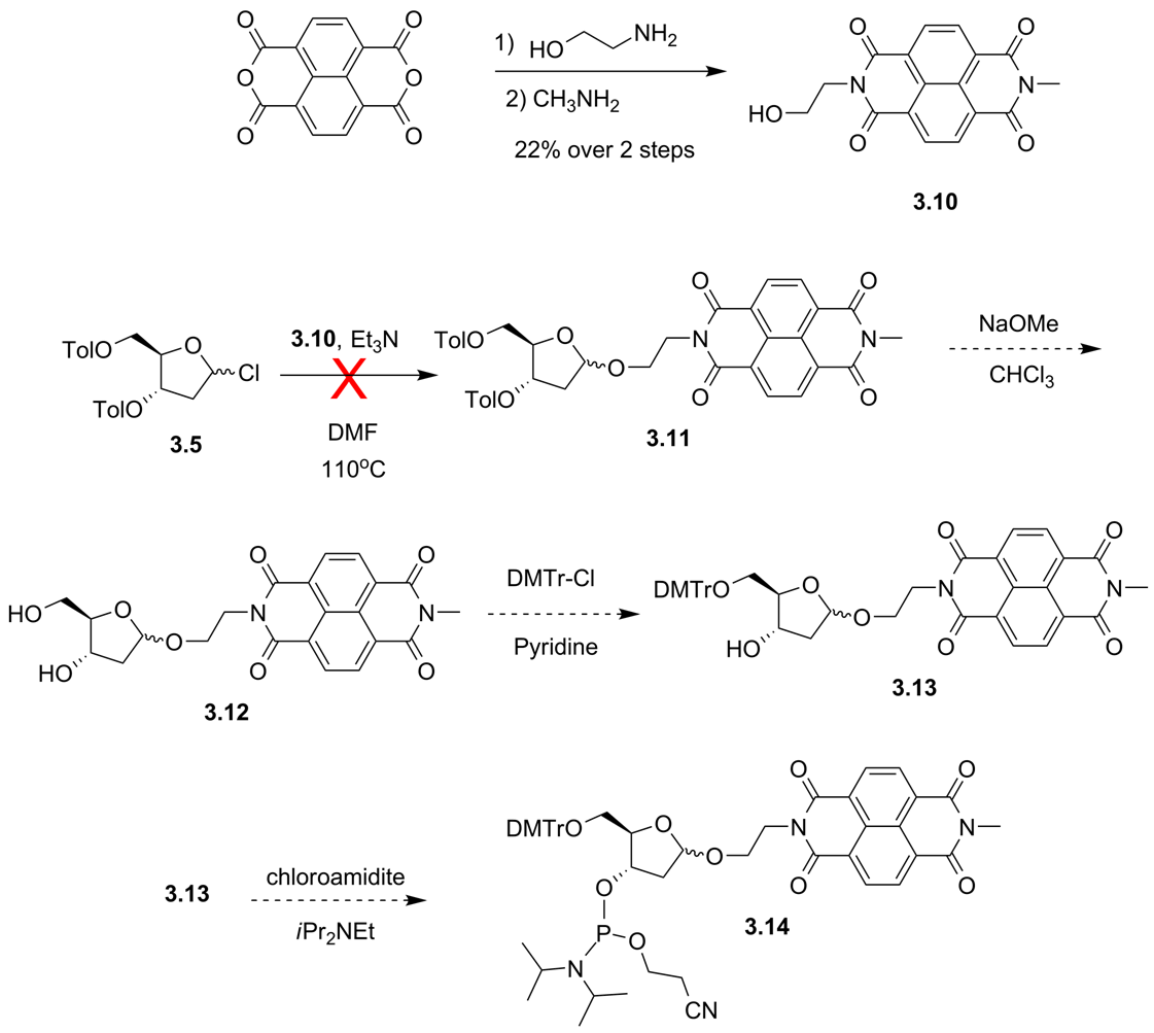

Scheme 3.3 Synthesis of the NDI acceptor phosphoramidite.

A variety of coupling conditions were investigated in an attempt to increase the yield on this glycosylation as seen in Table 3.1. Traditional nucleophilic coupling protocols under basic conditions proved unsuccessful with only very slight improvement

seen upon addition of NaH as the base. The highest coupling efficiencies were seen when the gylcosylation was carried out in THF in the presence of silver (I) oxide as a promoter, resulting in fair to moderate yields of compound **3.11**.

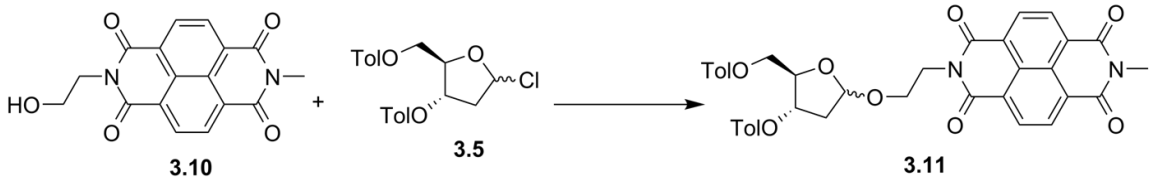

Entry	Ndi : Sugar	Conditions	Temperature (^{o}C)	Reaction Time (h)	% Yield
1	1 : 1	NaH / THF	22	12	14
2	1 : 1	DIEA / $CHCl_3$	22	12	-
3	1 : 0.95	Ag_2O / $CHCl_3$	60	15	7
4	1 : 0.95	Ag_2O / $CHCl_3$	80	15	10
5	1 : 0.95	Ag_2O / $CHCl_3$	75 [a]	1	5
6	1 : 0.95	Ag_2O / $CHCl_3$ [b]	75 [a]	1	12
7	1 : 0.95	Ag_2O / THF	65	12	24
8	1 : 0.95	Ag_2O / THF	65	24	34

Scheme 3.4 Glycosylation reaction conditions for formation of acceptor monomer 3.11. Heating done by microwave[a], tenfold excess of Ag2NO promoter used[b].

With the NDI functionalized *O*-glycoside monomer in hand our efforts turned towards removal of the toluyl protecting groups, selective protection of the pendant primary alcohol as the dimethoxytrityl ether and subsequent phosphoramidation to access compound **3.14**. Throughout the course of this synthesis construction of the naphthalene diimide functionalized molecules had always been significantly more problematic than that of the corresponding donor analogs, issues ranging from the poor solubility of the substrate to instability of the purified target intermediates. Once again this synthetic

intractability became apparent in the attempted removal of toluyl protecting groups of compound **3.11**. Standard base-mediated deprotection strategies proved extremely unsuccessful, resulting in a variety of side products inseparable by chromatography with no trace of the target compound or unreacted starting material.

After trying alternative deprotection schemes with the same results it became apparent that an unintended, more dominant reaction pathway was at work. Scanning the literature we came across very interesting research from the Saha group involving electron transfer due to anion-π interactions between anions and electron deficient naphthalene diimides[79,80]. Here the authors reported the consistent formation of naphthalene diimide radical anions due to electron transfer events arising out of the strong electronic interactions between the π^*-orbitals of the diimide and the lone pair electrons of the anions used. While it would be difficult to definitively say that the same reaction pathways were operative in the deprotection of compound **3.11**, the presence of the methoxide anion in conjunction with the formation of multiple unidentifiable side products with no recovery of the starting substrate, did not rule out an NDI radical pathway as a possibility.

Given the difficulty of accessing the acceptor functionalized sugar, it became clear that a re-evaluation of the synthetic approach to the desired phosphoramidite monomers was required. However before this was done, already having access to the donor phosphoramidite **3.9**, we decided to test the feasibility of automated DNA synthesis in building a short oligomer based on our donor monomer. With this in mind a short three residue sequence was designed and its synthesis attempted on the DNA synthesizer.

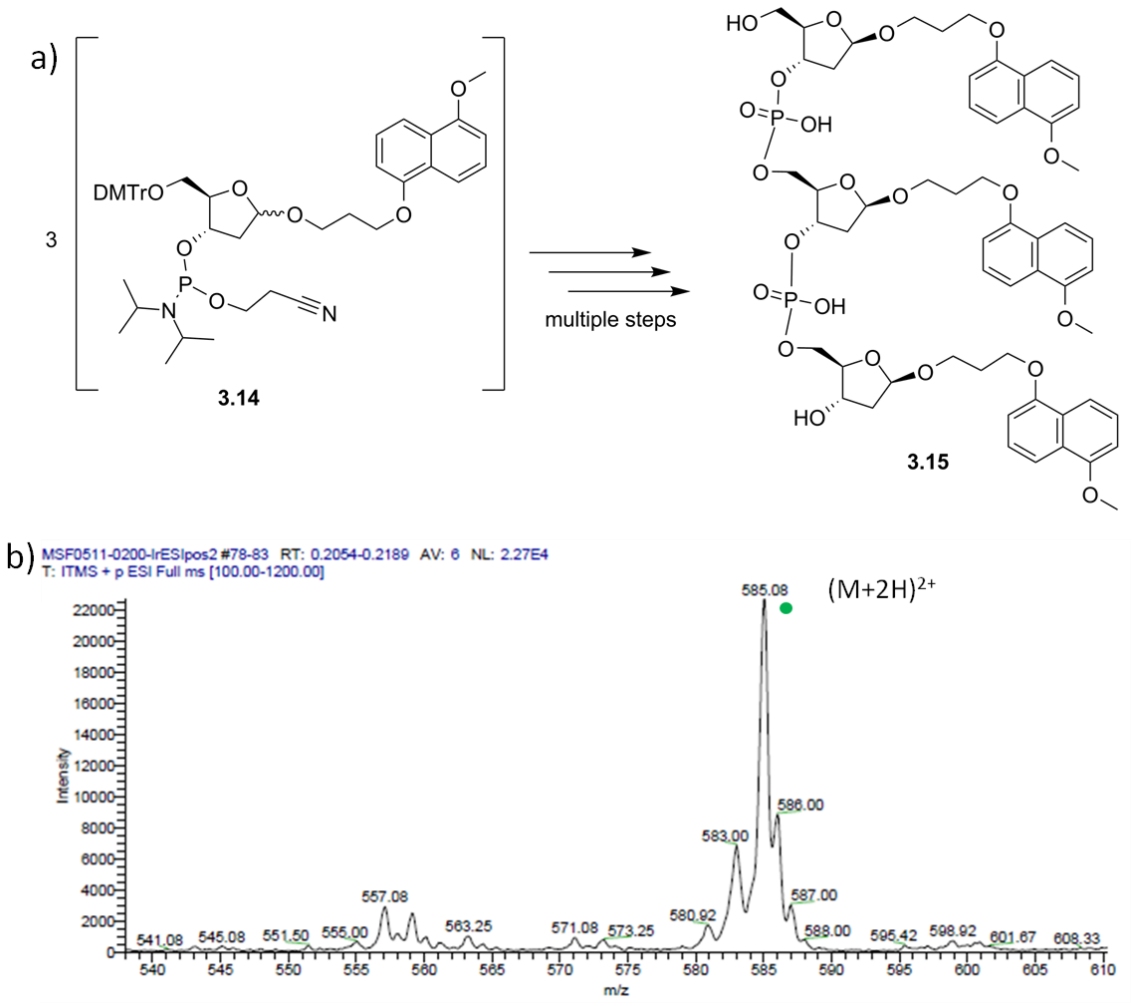

Figure 3.3 a) Chemical structure of the donor DAN trimer, synthesized via automated DNA synthesis. b) Mass spectrum of donor DAN trimer, observed as the $(M+2H)^{2+}$ ion.

The donor phosphoramidite **3.9** was loaded on to a Controlled Glass Pore universal support column and placed on the synthesizer where two successive couplings were carried out using standard phosphoramidite reaction conditions. UV monitoring of the removal of the trityl group indicated 98% coupling efficiency for each step in the constructing of the short trimer. Deprotection and cleavage of the oligomer from the

support was achieved by reaction with 30% NH_4OH for 8 hours. Mass spectrometry analysis of the mixture verified the presence of the trimer as the $(M+2H)^{2+}$ ion.

3.3.2 An alternative scaffold

After attempting the redesign and synthesis of the DNA based scaffold for our donor-acceptor oligomers, we did not achieve our initial target compounds but we did learn a few very important lessons. The successful synthesis of the DAN donor trimer via automated DNA protocols meant that at least with respect to the donor, larger oligomers could very easily by synthesized using the donor phosphoramidite. The apparent instability of the acceptor NDI sugar monomer and the poor coupling efficiencies seen mandated that an alternative approach be taken to ensure construction of these donor-acceptor oligomers.

With this in mind we went back to the literature in search a new backbone architecture that was relatively structurally rigid, water solube, easily functionalized with the donor and acceptor monomer and lastly, amenable to standard DNA phosphoramidite chemistry. We came across a novel acyclic phosphodiester backbone that was structurally very similar to that of DNA and consequently shared many of its characteristics. This scaffold was based on a glycol nucleic acid (GNA) framework and had already been incorporated into numerous sequences of DNA and DNA analogs by many different research groups[81-84]. The fact that this GNA scaffold contained the same phosphate diester linkages of regular DNA made it particularly attractive, since the diester afforded both water solubility as well as the structurally rigidified backbone we desired. More importantly the novel nucleoside monomers necessary for conversion to the corresponding phosphoramidite were easily accessible via the nucleophilic regioselective ring opening of either the (R)-(+) or (S)-(-) glycidol.

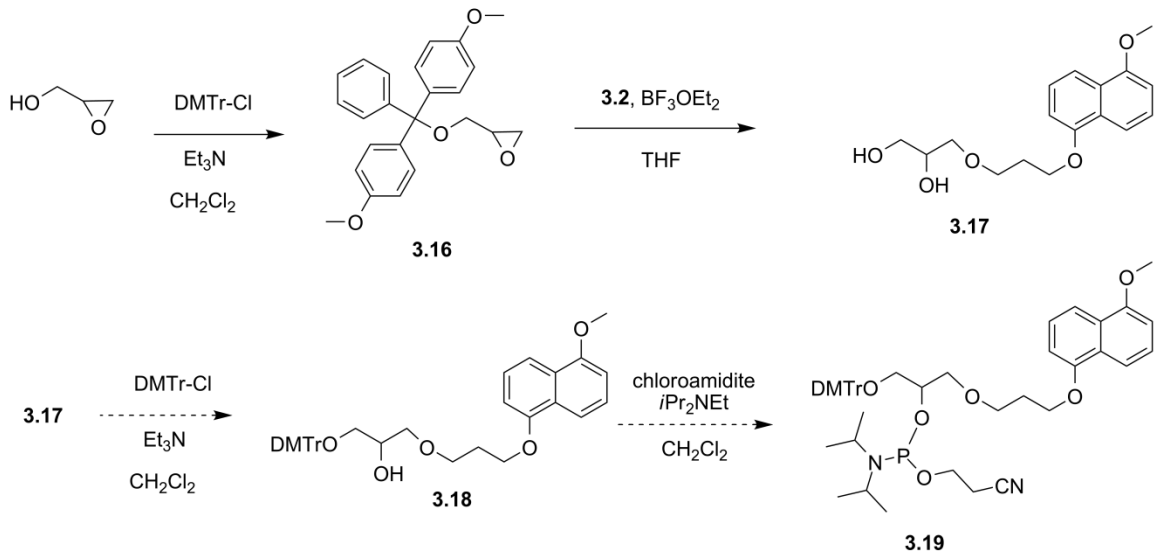

Scheme 3.5 Synthetic scheme of target donor phosphoramidite based on acyclic glycol nucleic acid backbone

In order to test the feasibility of this synthetic route, construction of the DAN donor monomer using this simplified GNA acyclic backbone was attempted. The outline of this scheme is seen in the figure below. Compound **3.16** was obtained via protection of the starting glycidol as the dimethoxytrityl ether. The regioselective ring opening was afforded through the use of boron trifluoride diethyl etherate as Lewis acid promoter, granting access to compound **3.17** in moderate yields. During the course of this reaction cleavage of the trityl ether was seen however this did not prove problematic since the pendant primary alcohol could easily be re-protected and the molecule moved forward toward the synthesis of the target compound **3.19**.

This alternative approach, towards both the donor and acceptor monomers, is an effort that is still currently underway in the Iverson lab, however the ease and utility of this methodology is evident in the reduction in the number of steps necessary towards the final phosphoramidite monomer required for automated DNA synthesis.

3.4 CHAPTER CONCLUSIONS

Our efforts toward the construction of a donor and acceptor oligomers based on a rigidified DNA scaffold were met with moderate degrees of success. The synthesis of the acceptor oligomer was defeated by the intractable nature of naphthalene diimide monomer as well as its poor solubility and the instability of key intermediates along the chosen synthetic route. The DAN phosphoramidite monomer was successfully synthesized and the efficacy of the automated DNA synthesis approach validated by the construction of a novel three residue oligomer based on a completely non-natural nucleic acid analog. Additionally progress has been made towards the design and synthesis of an alternative glycol nucleic acid based scaffold in the hope of circumventing the solubility and stability issues seen in the DNA based analogs.

3.5 EXPERIMENTAL METHODS

General Procedures

All solvents were freshly distilled prior to use. CH_2Cl_2, CH_3OH and pyridine were distilled over CaH_2 under Argon. All other reagents were purchased from the Sigma-Aldrich chemical company and were uses as received. All microwave experiments were conducted in a C.E.M. MARS microwave reactor at a power of 300W. All modeling experiments were conducted using Hyperchem release 7 software. Reactions were carried out under an Argon atmosphere using oven dried glassware. ^1H NMR experiments were conducted on a Varian 500 MHz instrument in the deuterated solvent indicated.

5-methoxynaphthalen-1-ol (3.1)

The starting naphthol (1g, 6.2mmol) was dissolved in acetonitrile (30ml) in a dry round bottomed flask and purged with Argon. Methyl iodide (0.338 ml, 6.25mmol) and

potassium carbonate (0.94g, 6.87mmol) were both added to the reaction mixture and the system sealed and allowed to stir while heated to reflux under Argon overnight. Upon completion of the reaction the mixture was filtered through a plug of Celite and the filtrate collected. The solvent was removed in vacuo and the residue dissolved in $CHCl_3$ (80 ml) and washed with sodium bicarbonate (2 x 75 ml), brine (2 x 75 ml) and dried over sodium sulfate. The crude product was purified by flash chromatography using 2% Acetone/$CHCl_3$ as the eluent. The target compound was isolated as a black solid (0.405 g, 35%). ^{1}H NMR ($CDCl_3$) δ: 7.87 (d, J = 8.4 Hz, 1H), 7.76 (d, J = 8.4 Hz, 1H), 7.40 (t, J = 11.2 Hz, 1H) 7.31 (t, J = 7.6 Hz, 1H), 5.20 (br s, 1H), 4.00 (s, 3H); ^{13}C NMR ($CDCl_3$) δ: 155.37, 151.15, 126.93, 125.29, 125.28, 125.14, 114.72, 113.62, 109.45, 104.44, 55.56; HRMS CI $C_{11}H_{11}O_2$ $(M+H)^{+1}$ m/z calculated 175.0759, found 175.0757.

3-(5-methoxynaphthalen-1-yloxy)propan-1-ol (3.2)

5-methoxynaphthalen-1-ol (1.38 g, 7.93mmol) was add to an oven dried round bottomed flask under an inert Argon atmosphere and dissolved in dry acetonitrile. 3-bromopropan-1-ol (1.04 ml, 8.73mmol), potassium iodide (0.013g, 0.079mmol) and potassium carbonate (1.20g, 8.73mmol) were all added to the reaction flask and the entire system sealed and heated to reflux and then left to stir under Argon overnight. Upon completion of the reaction the mixture was filtered through a plug of Celite and the filtrate collected. The solvent was removed in vacuo and the residue dissolved in $CHCl_3$ (80 ml) and washed with sodium bicarbonate (2 x 75 ml), brine (2 x 75 ml) and dried over sodium sulfate. The crude material was purified via flash chromatography using 1% Acetone/$CHCl_3$ as the eluting solvent system. The target compound was obtained as a dark brown solid (1.39g, 75%). ^{1}H NMR ($CDCl_3$) δ: 7.86 (d, J = 8.4 Hz, 1H), 7.78 (d, *J* = 8.4 Hz, 1H), 7.39 (t, *J* = 3.6 Hz, 1H), 7.37 (t, *J* = 3.6 Hz, 1H), 6.88 (d, *J* = 7.6 Hz, 1H),

6.86 (d, *J* = 8.8 Hz, 1H), 4.28 (t, *J* = 6 Hz, 2H), 3.99 (s, 3H), 3.96 (t, *J* = 6, 2H), 2.18 (quintet, *J* = 5.6 Hz, 2H), 1.79 (br s, 1H); ^{13}C NMR ($CDCl_3$) δ: 155.26, 154.30, 126.61, 126.57, 125.25, 125.16, 114.36, 114.01, 105.51, 104.50, 65.72, 60.57, 55.54, 32.12; HRMS CI $C_{14}H_{17}O_3$ $(M+H)^{+1}$: m/z calculated 233.1178, found 233.1179.

(2R,3S)-2-(hydroxymethyl)-5-methoxytetrahydrofuran-3-ol (3.3)

2 Deoxyribose (1g, 7.4mmol) was dissolved in dry methanol (18ml) and stirred under an inert Argon atmosphere for 5 minutes. A 1% HCl/ CH_3OH solution was prepared by adding 0.25ml (4.0M HCl in dioxane) to 4.3 ml of CH_3OH. 2ml of this solution was added to the reaction flask and the reaction allowed to stir at room temperature for 1 hour. The solvent was removed in vacuo and a minimal amount of pyridine (1ml) was added. This solution was then concentrated in vacuo to a brown oil. This procedure was then repeated twice. The crude mixture was purified via flash chromatography using a gradient of 2% CH_3OH/CH_2Cl_2 to 10% CH_3OH/CH_2Cl_2 to give a mixture of both α and β anomers as an off white solid (0.8857g, 6.05mmol, 81%). ^1H NMR ($CDCl_3$) : δ 5.10-5.07 (m, 1H), 4.13-4.08 (m 1H), 3.69-3.63 (m, 2H), 3.37 (d, *J* = 2.8Hz, 3H), 2.24-1.96, (m, 2H); ^{13}C NMR ($CDCl_3$) δ 106.8, 87.5, 70.7, 63.1, 56.3, 41.8. MS ESI 148.2754.

(2R,3S,5S)-5-methoxy-2-((4-methylbenzoyloxy)methyl)tetrahydrofuran-3-yl-4-methylbenzoate (3.4)

In an oven dried round bottomed flask the O-methlyated deoxyribose (0.885g, 5.9mmol) was dissolved in anhydrous pyridine (18ml) and cooled to 0^oC. The reaction vessel was purged with Argon for 10 minutes and the *p*-Toluyl chloride (1.6ml, 12.1mmol) was added slowly dropwise via addition funnel over the course of 20 minutes. Upon addition the reaction was allowed to warm up to room temperature and then left to

stir overnight under Argon. The reaction was stopped by removal of the solvent in vacuo and the crude residue dissolved in CH_2Cl_2 (30ml) which was then washed with water (2 x 20ml) and then saturated $NaHCO_3$ (2 x 20ml). The organic phase was then washed with brine (2 x 40ml) and dried over Na_2SO_4 and concentrated in vacuo. The crude mixture was then purified via flash chromatography using 15% EtoAC/Hexanes as the eluting solvent to give the product α, β anomers: 1-O-methyl-3, 5-di-(O-p-toluoyl-methyl)-2-deoxy-D-ribose. (2.11g, 5.42mmol, 92%). ^{1}H NMR ($CDCl_3$) α-OCH_3 δ : 7.93 (dd, *J* = 8, 4.8 Hz, 4H), 7.19-7.14 (m, 4H), 5.53-5.52 (m, 1H), 5.17 (dd, *J* = 2, 2 Hz, 1H), 4.5-4.39 (m, 3H), 3.29 (s, 3H, O-CH_3), 2.52 (qd, *J* = 7.2, 2 Hz, 1H), 2.36 (dd, *J* = 6.4 Hz, 6H, Ar-CH_3), 2.29 (dt, *J* = 14, 5.2 Hz); ^{13}C NMR ($CDCl_3$) 166.33, 166.11, 144.02, 143.68, 129.78 (2C), 129.70 (2C), 129.13 (2C), 129.07 (2C), 127.19, 126.87, 105.61, 81.89, 75.41, 65.14, 55.20, 39.29, 21.68, 21.66; β-O-CH_3 δ 7.96 (td, *J* = 8.4, 1.6 Hz, 4H), 7.25 (td, *J* = 7.2, 0.8 Hz, 4H), 5.43-5.39, (m, 3H), 5.19 (dd, *J* = 5.6, 0.8, Hz, 1H), 4.65-4.55 (m, 1H), 4.54-4.50 (m,2H), 3.42 (s,3H, O-CH_3), 2.58 (qd, *J* = 5.6, 2.8 Hz, 1H), 2.40 (d, *J* = 3.6, 6H, Ar-CH_3), 2.21 (dq, *J* = 14, 1.2 Hz, 1H); ^{13}C NMR ($CDCl_3$) 166.49, 166.27, 143.93, 143.77, 129.81 (2C), 129.68 (2C), 129.11 (2C), 129.09 (2C), 127.09, 127.02, 105.06, 80.98, 74.61, 64.31, 55.09, 39.27, 21.68, 21.66. MS CI+ 384.27

(2R,3S,5R)-5-chloro-2-((4-methylbenzoyloxy)methyl)tetrahydrofuran-3-yl-4-methylbenzoate (3.5)

The purified O-methyl deoxyribose (2.09g, 5.4mmol) was dissolved in glacial acetic acid (4.3ml) and cooled in an ice bath to 0^{o}C. The flask was then purged with Argon for 15 minutes after which a 4M solution of HCl in dioxane (6ml) was added and the system sealed under Argon and left to stir for 3 hours. The progress of the reaction was tracked via TLC for the disappearance of the starting material. Upon completion, the

reaction mixture was diluted with minimal glacial acetic acid (2ml) and placed in the freezer (-20^{o}C) overnight. The product precipitated as white solid that was filtered and washed with cold ether and then collected and dried under vacuum overnight. (1.673g, 80%). ^{1}H NMR ($CDCl_3$) α-Cl δ : 8.00 (d, *J* = 8 Hz, 2H), 7.90 (d, *J* = 8 Hz, 2H), 7.28 (d, *J* = 8 Hz, 2H), 7.25 (d, *J* = 8 Hz, 2H), 6.48 (d, J = 5.2, 1H), 5.58 (dq, *J* = 7.2, 1.2 Hz, 1H), 4.87 (quartet, *J* = 2.8, 1H), 4.70 (dd, *J* = 12, 3.2 Hz, 1H), 4.62 (dd, *J* = 12.4, 4.4 Hz, 1H), 2.91 (qd, *J* = 4, 2.4 Hz, 1H), 2.77 (dd, *J* = 15.2, 0.8 Hz, 1H), 2.42 (d, *J* = 4.8 Hz, 1H); ^{13}C NMR ($CDCl_3$) δ : 166.38, 166.06, 144.29, 144.06, 129.90 (2C), 129.66 (2C), 129.23 (2C), 129.21 (2C), 126.78, 126.65, 95.33, 84.70, 73.54, 63.49, 44.52, 21.74, 21.69; MS CI+ 389.23

(2R,3S,5R)-5-(3-(5-methoxynaphthalen-1-yloxy)propoxy)-2-((4-methylbenzoyloxy)methyl)tetrahydrofuran-3-yl 4-methylbenzoate (3.6)

To a dry three-necked flask was added **3.2** (0.328g, 1.43mmol) under an inert Argon atmosphere. Silver oxide (0.444g, 1.92mmol) was added to the flask after the addition of molecular sieves. A minimal amount of $CHCl_3$ was added to the flask and the α-chlorosugar (0.50g, 1.28mmol) was added in one portion and the flask sealed and covered with aluminum foil and left to stir under Argon at room temperature overnight. After 15 hours and additional 0.5 equivalence of the cholorosugar (0.25g 0.64mmol) was added and the reaction left to stir for an additional 12 hours. The crude reaction mixture was filtered over a plug of cotton which was washed with CH_2Cl_2 and the filtrate collected and washed with water (2 x 50 ml) and brine (2 x 50 ml) and dried over sodium sulfate. The solvent was removed under reduced pressure and the crude product purified using flash chromatography into the individual anomers using 1% Acetone/ CH_2Cl_2 as the eluting solvent. The target compound was isolated as a yellow oil (0.771g, 92%). ^{1}H

NMR ($CDCl_3$) α-anomer δ: 7.98 (d, *J* = 6.4 Hz, 2H), 7.93 (d, *J* = 6.4 Hz, 2H), 7.84 (d, *J* = 5.2 Hz, 1H), 7.35 (t, *J* = 8.8 Hz, 2H), 7.25 (d, *J* = 8.8 Hz, 2H), 7.19 (d, *J* = 8.8 Hz, 2H), 6.84 (d, *J* = 7.2 Hz, 1H), 6.82 (d, *J* = 6.8 Hz, 1H), 5.60 (m, 1H), 5.39 (dd, *J* = 6.8, 2.4 Hz, 1H), 4.58-4.47 (m, 3H), 4.19-4.14 (m, 2H), 4.10-3.99 (m, 1H), 3.99 (s, 3H), 3.75-3.72 (m, 1H), 2.57 (qd, *J* = 7.2, 2.4, 1H), 2.41 (s, 3H), 2.38-2.35 (m, 1H), 2.36 (s, 3H), 2.17-2.13 (m, 1H); β-anomer δ: 7.93-7.88 (m, 6H), 7.38 (t, *J* = 7.6 Hz, 1H), 7.29-7.16 (m, 5H), 6.85 (d, *J* = 7.2 Hz, 1H), 6.75 (d, *J* = 6.8 Hz, 1H), 5.43 (dt, *J* = 12, 1.6 Hz, 1H), 5.36 (d, *J* = 6 Hz, 1H), 4.55-4.43 (m, 3H), 4.25 (td, *J* = 6.4, 0.8 Hz, 2H), 4.13-4.09 (m, 1H), 3.97 (s, 3H), 3.77-3.71 (m, 1H), 2.50-2.46 (m, 1H), 2.40 (s, 3H), 2.38 (s, 3H), 2.27-2.22 (m, 1H)

(2R,3S,5R)-2-(hydroxymethyl)-5-(3-(5-methoxynaphthalen-1-yloxy)propoxy) tetrahydrofuran-3-ol (3.7)

The protected sugar (0.453g, 0.77mmol) **3.6** was added to a dried reaction vessel under an inert Argon atmosphere. The solid was then dissolved in dry CH_2Cl_2 and $NaOCH_3$ dissolved in CH_3OH (4.8 ml, 2.4mmol, 0.5M solution) was added and the reaction left to stir under Argon at room temperature overnight. The reaction was tracked via TLC for the disappearance of the starting material, after which the reaction was diluted with CH_2Cl_2 and then washed with $NaHCO_3$ (2 x 30ml) and brine (2 x 30ml) and dried over Na_2SO_4. The solvent was removed under reduced pressure and the crude product purified using flash chromatography using 3% Acetone/ $CHCl_3$ as the eluting solvent system. The product compound was isolated as the individual anomers as a pale white solid. (0.157g, 58%). ^{1}H NMR ($CDCl_3$) α anomer δ: 7.85 (dd, *J* = 4.4, 0.8 Hz, 2H), 7.39 (dd, *J* = 6.4, 5.2 Hz, 2H), 6.86 (d, *J* = 7.6 Hz, 2H), 5.24 (d, *J* = 4.4 Hz, 1H), 4.23 (quintet, *J* = 4.4 Hz, 2H), 4.10-4.04 (m, 3H), 3.99 (s, 3H), 3.74-3.56 (m, 3H), 2.28-1.99 (m, 2H); ^{13}C NMR ($CDCl_3$) δ: 155.23 (2C), 154.30, 154.29, 126.59 (2C), 125.19 (2C),

114.24 (2C), 114.09 (2C), 105.42, 104.51, 104.49, 87.45, 72.23, 64.88, 64.56, 63.55, 55.53, 42.59, 29.56; ^{1}H NMR ($CDCl_3$) β anomer δ: 7.84 (d, *J* = 8.4 Hz, 2H), 7.39 (dd, *J* = 6.8, 6.4 Hz, 2H), 6.85 (dd, *J* = 5.6, 1.6 Hz, 2H), 5.26 (dd, *J* = 3.6, 2 Hz, 1H), 4.51-4.47 (m, 1H), 4.19 (quintet, *J* = 6.4, 2 Hz, 2H), 4.05-3.99 (m, 5H), 3.74-3.59 (m, 3H), 2.30 (qd, *J* = 4.8, 2 Hz, 1H), 2.21-2.07 (m, 3H); ^{13}C NMR ($CDCl_3$) δ: 155.23 (2C), 154.36, 126.63, 126.61, 125.19, 125.14, 114.25, 114.14, 105.47, 104.49, 87.49, 72.87, 64.78, 64.34, 63.09, 55.53, 41.64, 29.63; HRMS ESI $C_{19}H_{24}O_6Na$ $(M+Na)^{+1}$: m/z calculated 371.1471, found 371.1468.

(2R,3S,5R)-2-((bis(4-methoxyphenyl)(phenyl)methoxy)methyl)-5-(3-(5-methoxynaphthalen-1-yloxy)propoxy)tetrahydrofuran-3-ol (3.8)

A mixture of the anomers of the deprotected sugar **3.7** (0.279 g, 0.8mmol) was dissolved in dry pyridine (5ml) under an inert Argon atmosphere. N,N-Diisopropylethylamine (0.419 ml, 2.4mmol) was added and the reaction was left to stir for 15 minutes. 4,4-Dimethoxytrityl chloride (0.406 g, 1.2mmol) was dissolved in pyridine (5ml) and added to the reaction in one portion. The mixture was then left to stir overnight at room temperature. The reaction was tracked for disappearance of the starting material, upon which the reaction was quenched by the addition of CH_3OH (2ml). The solvent was removed in vacuo and the residue dissolved in a minimal amount of CH_2Cl_2 (1ml) and the crude mixture purified via flash chromatography using a gradient of 4:1 EtoAc/Hexanes with 3% Triethylamine to 3:2 EtoAc/Hexanes with 3% Triethylamine. The target compound was isolated as the individual anomers as a pale white foam (0.219g, 42%). ^{1}H NMR ($CDCl_3$) α anomer δ: 7.84 (t, *J* = 8 Hz, 1H), 7.41 (d, *J* = 8.4 Hz, 2H), 7.37 (td, *J* = 8.4, 1.2 Hz, 2H), 7.29-7.25 (m, 8H), 7.19 (tt, *J* = 8, 1.5 Hz, 1H), 6.84-6.77 (m, 6H), 5.29 (d, *J* = 4.4 Hz, 1H), 4.22-4.18 (m, 3H), 4.16-4.14 (m, 1H), 4.05-4.00

(m, 1H), 3.97 (s, 3H), 3.76 (s, 6H), 3.74-3.69 (m, 1H), 3.12-3.05 (m, 2H), 2.21-2.03 (m, 3H), 2.02-1.99 (m, 1H); ^{13}C NMR ($CDCl_3$) δ: 158.45 (2C), 155.23, 154.41, 144.79, 136.01, 135.93, 130.03, 128.14 (2C), 127.79 (2C), 126.73, 126.64, 125.16, 125.10, 114.22, 113.09, 105.49, 104.57, 104.49, 86.79, 86.06, 73.51, 64.93, 64.36, 64.02, 55.51, 55.19 (2C), 41.03, 29.73; ; ^{1}H NMR ($CDCl_3$) β anomer δ: 7.82 (t, *J* = 6.8 Hz, 2H), 7.46 (dd, *J* = 8.4, 1.2 Hz, 2H), 7.33-7.25 (m, 9H), 7.21 (tt, *J* = 8.4, 1.2 Hz, 1H), 6.84 (d, *J* = 7.6 Hz, 1H), 6.80 (d, *J* = 7.2 Hz, 4H), 6.74 (d, *J* = 7.2, 1H), 5.19 (dd, *J* = 5.2, 2 Hz, 1H), 4.44 (quartet, *J* = 2.8 Hz, 1H), 4.13-4.07 (m, 3H), 4.05-3.95 (m, 4H), 3.86-3.82 (m, 1H), 3.84 (s, 6H), 3.63-3.59 (m, 1H), 3.34 (qd, *J* = 5.2, 4 Hz, 1H), 3.18 (dd, *J* = 6.8, 2.4 Hz, 1H), 2.23 (qd, *J* = 6.8, 2.4, 1H), 2.07-2.00 (m, 1H); ^{13}C NMR ($CDCl_3$) δ: 158.48, 158.47, 155.19, 154.41, 144.85, 136.05, 136.02, 130.03, 130.01, 128.13 (2C), 127.82 (2C), 126.78 (2C), 126.69, 126.60, 125.16, 125.04, 114.28, 114.06, 113.11 (4C), 105.39, 104.47, 104.06, 84.65, 73.54, 65.16, 65.01, 64.52, 55.52, 55.16 (2C), 41.18, 29.64; HRMS ESI $C_{40}H_{42}O_8Na$ $(M+Na)^{+1}$: m/z calculated 673.2777, found 673.2767.

(2R,3S)-2-((bis(4-methoxyphenyl)(phenyl)methoxy)methyl)-5-(3-(5-methoxynaphthalen-1-ylox)propoxy)tetrahyrofuran-3-yl-2-cyanoethyl diisopropylphosphoramidite (3.9)

The β-anomer of compound **3.8** (0.086g, 0.132mmol) **was** placed in an oven dried three necked flask and dissolved in dry CH_2Cl_2 under an inert Argon atmosphere. Diisopropylethylamine (0.092ml, 0.528 mmol) was added to the flask and the reaction left to stir for 5 minutes. The commercially available chlorophosphoramidite (0.073ml, 0.33 mmol) was added in one portion and the reaction left to stir at room temperature for 6 hours. The progress of the reaction was tracked by TLC for the disappearance of the starting material. The crude reaction mixture was purified via flash chromatography using

1:4 ethyl acetate/hexanes as the eluting solvent. The target compound was isolated as an off-white foam after drying under vacuum overnight. (0.087g, 78%)

2-(2-hydroxyethyl)-7-methylbenzo[lmn][3,8]phenanthroline-1,3,6,8(2H,7H)-tetraone (3.10)

Napthalene-1,4,5,8-tetracarboxylic dianhydride (6.0 g, 22.3mmol) was dissolved in dry DMF (200 ml) in an oven dried flask under an inert Argon atmosphere. 2-aminoethanol (0.034 ml, 5.5mmol) was then added to the flask in one portion and the flask sealed and heated to reflux overnight under Argon. The crude reaction mixture (65 ml, 1.8mmol) was then transferred to a pressure tube and a solution of 2.0M CH_3NH_2 in THF (9 ml, 18mmol) was added. The vessel was then sealed and heated to 120^oC for 14 hours. Upon completion of the reaction the solvent was removed in vacuo and the residue dissolved in $CHCl_3$ (100 ml) and the organic phase washed with $NaHCO_3$ (2 x 75ml), then brine (2 x 75 ml) and dried over Na_2SO_4. The target compound was obtained as a pale red solid following purification by flash chromatography using 1% $CH_3OH/CHCl_3$ as the eluting solvent (1.39 g, 21% over 2 steps). ^1H NMR ($CDCl_3$) δ: 8.73 (s, 4H), 4.24 (t, J = 5.2 Hz), 3.95 (quart, J = 5.6 Hz), 3.55 (s, 3H); ^{13}C NMR ($CDCl_3$) δ: 163.02 (2C), 163.61 (2C), 131.25 (4C), 130.99 (4C), 126.76, 126.45, 61.27, 43.01, 27.44; HRMS CI $C_{17}H_{13}N_2O_5$ $(M)^{+1}$: m/z calculated 325.0824, found 325.0822.

(2R,3S,5R)-5-(2-(7-methyl-1,3,6,8-tetraoxo-7,8-dihydrobenzo[lmn][3,8]phenanthrolin-2(1H,3H,6H)-yl)ethoxy)-2-((4-methylbenzoyloxy)methyl)tetrahydrofuran-3-yl 4-methylbenzoate (3.11)

To a dry three-necked flask was added **3.10** (0.291g, 0.89mmol) under an inert Argon atmosphere. Silver oxide (0.312g, 1.34mmol) was added to the flask after the

addition of molecular sieves. A minimal amount of THF was added to the flask and the α-chlorosugar (0.331g, 0.85mmol) was added in one portion and the flask sealed and covered with aluminum foil and left to stir under Argon at room temperature overnight. After 15 hours and additional 0.5 equivalence of the cholorosugar (0.166g 0.42mmol) was added and the reaction left to stir for an additional 12 hours. The crude reaction mixture was filtered over a plug of cotton which was washed with CH_2Cl_2 and the filtrate collected and the solvent removed in vacuo. The crude residue was dissolved in CH_2Cl_2 and washed with water (2 x 50 ml) and brine (2 x 50 ml) and dried over Na_2SO_4. The crude product was purified by flash chromatography using a gradient of 1:4 EtoAc/Hexanes to 1:1 EtoAc/Hexanes as the eluting solvent. The target compound was isolated as a mixture of anomers a pale red solid. ^{1}H NMR ($CDCl_3$) δ: 8.67 (s, 2H), 8.63 (dd, J = 10.8, 7.6 Hz, 2H), 7.85-7.31 (m, 4H), 7.18-7.12 (m, 4H), 5.44-5.37 (m. 1H), 5.38 (d, J = 4.8 Hz, 1H), 5.32-5.28 (m, 1H), 4.55-4.24 (m, 5H), 4.13-4.05 (m, 2H), 3.98-3.96 (m, 1H), 3.91-3.84 (m, 1H), 3.56 (s, 3H), 2.47-2.45 (m, 1H), 2.37-2.35 (m, 6H); ^{13}C NMR ($CDCl_3$) δ: 166.33, 166.10, 162.98 (2C), 162.79 (2C), 144.02, 143.86, 130.86 (4C), 129.77 (4C), 129.21 (2C), 129.07 (2C), 128.97 (2C), 128.96 (2C), 126.95 (2C), 126.40 (2C),104.35, 81.41 75.43, 64.65, 60.39, 39.79, 39.15; HRMS CI $C_{40}H_{37}N_2O_{10}$ (M + $C_2H_5)^+$: m/z calculated 705.2443, found 705.2439.

Bibliography

(1) Watson, J. D.; Crick, F. H. C. Molecular Structure of Nucleic Acids: A Structure for Deoxyribose Nucleic Acid. *Nature* **1953**, *171*, 737-738.

(2) Prins, L. J. Reinhoudt, D. N.; Timmerman, P. Noncovalent Synthesis Using Hydrogen Bonding. *Angewandte Chemie International Edition* **2001**, *40*, 2382-2426.

(3) Coulocheri, S. A. Pigis, D. G. Papavassiliou, K. A.; Papavassiliou, A. G. Hydrogen bonds in protein–DNA complexes: Where geometry meets plasticity. *Biochimie* **2007**, *89*, 1291-1303.

(4) Hubbard, R. E. Hydrogen Bonds in Proteins: Role and Strength. **2011**.

(5) Beijer, F. H. Kooijman, H. Spek, A. L. Sijbesma, R. P.; Meijer, E. W. Self-Complementarity Achieved through Quadruple Hydrogen Bonding. *Angewandte Chemie International Edition* **1998**, *37*, 75-78.

(6) Sherrington, D. C.; Taskinen, K. A. Self-assembly in synthetic macromolecular systems via multiple hydrogen bonding interactions. *Chem. Soc. Rev.* **2001**, *30*, 83-93.

(7) Sijbesma, R. P. Beijer, F. H. Brunsveld, L. Folmer, B. J. B. Hirschberg, J. H. K. K. Lange, R. F. M. Lowe, J. K. L.; Meijer, E. W. Reversible Polymers Formed from Self-Complementary Monomers Using Quadruple Hydrogen Bonding. *Science* **1997**, *278*, 1601 -1604.

(8) Zeng, H. Ickes, H. Flowers, R. A.; Gong, B. Sequence Specificity of Hydrogen-Bonded Molecular Duplexes. *J. Org. Chem.* **2001**, *66*, 3574-3583.

(9) Mayer, M. F. Nakashima, S.; Zimmerman, S. C. Synthesis of a Soluble Ureido-Naphthyridine Oligomer that Self-Associates via Eight Contiguous Hydrogen Bonds. *Org. Lett.* **2005**, *7*, 3005-3008.

(10) Gong, H.; Krische, M. J. Duplex Molecular Strands Based on the 3,6-Diaminopyridazine Hydrogen Bonding Motif: Amplifying Small-Molecule Self-Assembly Preferences through Preorganization and Iterative Arrangement of Binding Residues. *J. Am. Chem. Soc.* **2005**, *127*, 1719-1725.

(11) Pedersen, C. J. Cyclic polyethers and their complexes with metal salts. *J. Am. Chem. Soc.* **1967**, *89*, 7017-7036.

(12) Cheney, J. Lehn, J. M. Sauvage, J. P.; Stubbs, M. E. [3]-Cryptates: metal cation inclusion complexes with a macrotricyclic ligand. *J. Chem. Soc., Chem. Commun.* **1972**, 1100.

(13) Helgeson, R. C. Timko, J. M.; Cram, D. J. Structural requirements for cyclic ethers to complex and lipophilize metal cations or .alpha.-amino acids. *J. Am. Chem. Soc.* **2011**, *95*, 3023-3025.

(14) Kruppa, M.; König, B. Reversible Coordinative Bonds in Molecular Recognition. *Chem. Rev.* **2006**, *106*, 3520-3560.

(15) Fujita, M. Yazaki, J.; Ogura, K. Preparation of a macrocyclic polynuclear complex, [(en)Pd(4,4'-bpy)]4(NO3)8 (en = ethylenediamine, bpy = bipyridine), which recognizes an organic molecule in aqueous media. *J. Am. Chem. Soc.* **1990**, *112*, 5645-5647.

(16) Leininger, S. Olenyuk, B.; Stang, P. J. Self- Assembly of Discrete Cyclic Nanostructures Mediated by Transition Metals. *ChemInform* **2000**, *31*, no-no.

(17) Fiedler, D. Bergman, R. G.; Raymond, K. N. Stabilization of Reactive Organometallic Intermediates Inside a Self- Assembled Nanoscale Host. *Angewandte Chemie International Edition* **2006**, *45*, 745-748.

(18) Dobrawa, R. Lysetska, M. Ballester, P. Grüne, M.; Würthner, F. Fluorescent Supramolecular Polymers: Metal Directed Self-Assembly of Perylene Bisimide Building Blocks. *Macromolecules* **2005**, *38*, 1315-1325.

(19) Hunter, C. A.; Sanders, J. K. M. The nature of .pi.-.pi. interactions. *J. Am. Chem. Soc.* **1990**, *112*, 5525-5534.

(20) Hunter, C. A. Lawson, K. R. Perkins, J.; Urch, C. J. Aromatic interactions. *Journal of the Chemical Society, Perkin Transactions 2* **2001**, 651-669.

(21) Nelson, J. C. Saven, J. G. Moore, J. S.; Wolynes, P. G. Solvophobically Driven Folding of Nonbiological Oligomers. *Science* **1997**, *277*, 1793 -1796.

(22) Lahiri, S. Thompson, J. L.; Moore, J. S. Solvophobically Driven π-Stacking of Phenylene Ethynylene Macrocycles and Oligomers. *Journal of the American Chemical Society* **2000**, *122*, 11315-11319.

(23) Stone, M. T.; Moore, J. S. A Water-Soluble m-Phenylene Ethynylene Foldamer. *Org. Lett.* **2004**, *6*, 469-472.

(24) Berl, V. Huc, I. Khoury, R. G.; Lehn, J. M. Helical Molecular Programming: Supramolecular Double Helices by Dimerization of Helical Oligopyridine-dicarboxamide Strands. *Chemistry-A European Journal* **2001**, *7*, 2810–2820.

(25) Berl, V. Huc, I. Khoury, R. G. Krische, M. J.; Lehn, J.-M. Interconversion of single and double helices formed from synthetic molecular strands. *Nature* **2000**, *407*, 720-723.

(26) Jiang, H. Maurizot, V.; Huc, I. Double versus single helical structures of oligopyridine-dicarboxamide strands. Part 1: Effect of oligomer length. *Tetrahedron* **2004**, *60*, 10029-10038.

(27) Bisson, A. P. Carver, F. J. Eggleston, D. S. Haltiwanger, R. C. Hunter, C. A. Livingstone, D. L. McCabe, J. F. Rotger, C.; Rowan, A. E. Synthesis and Recognition Properties of Aromatic Amide Oligomers: Molecular Zippers. *J. Am. Chem. Soc.* **2000**, *122*, 8856-8868.

(28) Allwood, B. L. Spencer, N. Shahriari-Zavareh, H. Stoddart, J. F.; Williams, D. J. Complexation of Diquat by a bisparaphenylene-34-crown-10 derivative. *J. Chem. Soc., Chem. Commun.* **1987**, 1061-1064.

(29) Ashton, P. R. Bissell, R. A. Górski, R. Philp, D. Spencer, N. Stoddart, J. F.; Tolley, M. S. Towards Controllable Molecular Shuttles - 2. *Synlett* **1992**, *1992*, 919,922.

(30) Ashton, P. R. Bissell, R. A. Spencer, N. Stoddart, J. F.; Tolley, M. S. Towards Controllable Molecular Shuttles - 3. *Synlett* **1992**, *1992*, 923,926.

(31) Coskun, A. Spruell, J. M. Barin, G. Fahrenbach, A. C. Forgan, R. S. Colvin, M. T. Carmieli, R. Benítez, D. Tkatchouk, E. Friedman, D. C. Sarjeant, A. A. Wasielewski, M. R. Goddard, W. A.; Stoddart, J. F. Mechanically Stabilized Tetrathiafulvalene Radical Dimers. *J. Am. Chem. Soc.* **2011**, *133*, 4538-4547.

(32) Archer, E. A. Sochia, A. E.; Krische, M. J. The Covalent Casting of One- Dimensional Hydrogen Bonding Motifs: Toward Oligomers and Polymers of Predefined Topography. *Chemistry - A European Journal* **2001**, *7*, 2059-2066.

(33) Ashton, P. R. Goodnow, T. T. Kaifer, A. E. Reddington, M. V. Slawin, A. M. Z. Spencer, N. Stoddart, J. F. Vicent, C.; Williams, D. J. A [2] Catenane Made to Order. *Angewandte Chemie International Edition in English* **1989**, *28*, 1396-1399.

(34) Ashton, P. R. Johnston, M. R. Stoddart, J. F. Tolley, M. S.; Wheeler, J. W. The template-directed synthesis of porphyrin-stoppered [2]rotaxanes. *J. Chem. Soc., Chem. Commun.* **1992**, 1128.

(35) Scott Lokey, R.; Iverson, B. L. Synthetic molecules that fold into a pleated secondary structure in solution. *Nature* **1995**, *375*, 303-305.

(36) Bradford, V. J.; Iverson, B. L. Amyloid-like Behavior in Abiotic, Amphiphilic Foldamers. *Journal of the American Chemical Society* **2008**, *130*, 1517-1524.

(37) Zych, A. J.; Iverson, B. L. Synthesis and Conformational Characterization of Tethered, Self-Complexing 1,5-Dialkoxynaphthalene/1,4,5,8-Naphthalenetetracarboxylic Diimide Systems. *Journal of the American Chemical Society* **2000**, *122*, 8898-8909.

(38) Zych, A. J.; Iverson, B. L. Conformational Modularity of an Abiotic Secondary- Structure Motif in Aqueous Solution. *Helvetica Chimica Acta* **2002**, *85*, 3294-3300.

(39) Cubberley, M. S.; Iverson, B. L. 1H NMR Investigation of Solvent Effects in Aromatic Stacking Interactions. *Journal of the American Chemical Society* **2001**, *123*, 7560-7563.

(40) Cubberley, M. Investigation of solvent effects in aromatic electron donor-acceptor interactions, The University of Texas at Austin, 2000.

(41) Zhao, X. Jia, M.-X. Jiang, X.-K. Wu, L.-Z. Li, Z.-T.; Chen, G.-J. Zipper-Featured δ-Peptide Foldamers Driven by Donor−Acceptor Interaction. Design, Synthesis, and Characterization. *J. Org. Chem.* **2003**, *69*, 270-279.

(42) Ghosh, S.; Ramakrishnan, S. Structural Fine-Tuning of (−Donor−spacer−acceptor−spacer−)n Type Foldamers. Effect of Spacer Segment Length, Temperature, and Metal-Ion Complexation on the Folding Process. *Macromolecules* **2005**, *38*, 676-686.

(43) Ghosh, S.; Ramakrishnan, S. Aromatic Donor–Acceptor Charge- Transfer and Metal- Ion- Complexation- Assisted Folding of a Synthetic Polymer. *Angewandte Chemie International Edition* **2004**, *43*, 3264-3268.

(44) Ghosh, S.; Ramakrishnan, S. Small- Molecule- Induced Folding of a Synthetic Polymer. *Angewandte Chemie* **2005**, *117*, 5577-5583.

(45) Gabriel, G. J.; Iverson, B. L. Aromatic Oligomers that Form Hetero Duplexes in Aqueous Solution. *Journal of the American Chemical Society* **2002**, *124*, 15174-15175.

(46) Reczek, J. J.; Iverson, B. L. Using Aromatic Donor Acceptor Interactions to Affect Macromolecular Assembly. *Macromolecules* **2006**, *39*, 5601-5603.

(47) Reczek, J. J. Aromatic Electron Donor-Acceptor Interactions in NovelSupramolecular Assemblies, The University of Texas at Austin, 2006.

(48) Alvey, P. M. Reczek, J. J. Lynch, V.; Iverson, B. L. A Systematic Study of Thermochromic Aromatic Donor−Acceptor Materials. *The Journal of Organic Chemistry* **2010**, *75*, 7682-7690.

(49) Ma, D. Brandon, N. R. Cui, T. Bondarenko, V. Canlas, C. Johansson, J. S. Tang, P.; Xu, Y. Four-[alpha]-Helix Bundle with Designed Anesthetic Binding Pockets. Part I: Structural and Dynamical Analyses. *Biophysical Journal* **2008**, *94*, 4454-4463.

(50) Cui, T. Bondarenko, V. Ma, D. Canlas, C. Brandon, N. R. Johansson, J. S. Xu, Y.; Tang, P. Four-[alpha]-Helix Bundle with Designed Anesthetic Binding Pockets. Part II: Halothane Effects on Structure and Dynamics. *Biophysical Journal* **2008**, *94*, 4464-4472.

(51) Ottesen, J. J.; Imperiali, B. Design of a discretely folded mini-protein motif with predominantly [beta]-structure. *Nat Struct Mol Biol* **2001**, *8*, 535-539.

(52) Mizuno, M. Tonozuka, T. Suzuki, S. Uotsu-Tomita, R. Kamitori, S. Nishikawa, A.; Sakano, Y. Structural Insights into Substrate Specificity and Function of Glucodextranase. *Journal of Biological Chemistry* **2004**, *279*, 10575 -10583.

(53) Ghadiri, M. R. Granja, J. R. Milligan, R. A. McRee, D. E.; Khazanovich, N. Self-assembling organic nanotubes based on a cyclic peptide architecture. *Nature* **1993**, *366*, 324-327.

(54) Padilla, J. E. Colovos, C.; Yeates, T. O. Nanohedra: Using symmetry to design self assembling protein cages, layers, crystals, and filaments. *Proceedings of the National Academy of Sciences of the United States of America* **2001**, *98*, 2217.

(55) Zhang, S. Marini, D. M. Hwang, W.; Santoso, S. Design of nanostructured biological materials through self-assembly of peptides and proteins. *Current opinion in chemical biology* **2002**, *6*, 865–871.

(56) Miller, M. Shuman, J. D. Sebastian, T. Dauter, Z.; Johnson, P. F. Structural Basis for DNA Recognition by the Basic Region Leucine Zipper Transcription Factor CCAAT/Enhancer-binding Protein α. *Journal of Biological Chemistry* **2003**, *278*, 15178 - 15184.

(57) Ellenberger, T. Getting a grip on DNA recognition: structures of the basic region leucine zipper, and the basic region helix-loop-helix DNA-binding domains. *Current Opinion in Structural Biology* **1994**, *4*, 12-21.

(58) Mayer, M. F. Nakashima, S.; Zimmerman, S. C. Synthesis of a Soluble Ureido-Naphthyridine Oligomer that Self-Associates via Eight Contiguous Hydrogen Bonds. *Organic Letters* **2005**, *7*, 3005-3008.

(59) Zeng, H. Miller, R. S. Flowers, R. A.; Gong, B. A Highly Stable, Six-Hydrogen-Bonded Molecular Duplex. *Journal of the American Chemical Society* **2000**, *122*, 2635-2644.

(60) Archer, E. A.; Krische, M. J. Duplex Oligomers Defined via Covalent Casting of a One-Dimensional Hydrogen-Bonding Motif. *Journal of the American Chemical Society* **2002**, *124*, 5074-5083.

(61) Petitjean, A. Cuccia, L. A. Lehn, J. M. Nierengarten, H.; Schmutz, M. Cation-Promoted Hierarchical Formation of Supramolecular Assemblies of Self-Organized Helical Molecular Components. *Angewandte Chemie International Edition* **2002**, *41*, 1195–1198.

(62) Oleksi, A. Blanco, A. G. Boer, R. Usón, I. Aymamí, J. Rodger, A. Hannon, M. J.; Coll, M. Molecular Recognition of a Three-Way DNA Junction by a Metallosupramolecular Helicate. *Angew. Chem. Int. Ed.* **2006**, *45*, 1227-1231.

(63) Ikeda, M. Tanaka, Y. Hasegawa, T. Furusho, Y.; Yashima, E. Construction of Double-Stranded Metallosupramolecular Polymers with a Controlled Helicity by Combination of Salt Bridges and Metal Coordination. *Journal of the American Chemical Society* **2006**, *128*, 6806-6807.

(64) Iida, H. Shimoyama, M. Furusho, Y.; Yashima, E. Double-Stranded Supramolecular Assembly through Salt Bridge Formation between Rigid and Flexible Amidine and Carboxylic Acid Strands. *The Journal of Organic Chemistry* **2010**, *75*, 417-423.

(65) Bisson, A. P. Carver, F. J. Hunter, C. A.; Waltho, J. P. Molecular zippers. *Journal of the American Chemical Society* **1994**, *116*, 10292–10293.

(66) Zhou, Q.-Z. Jiang, X.-K. Shao, X.-B. Chen, G.-J. Jia, M.-X.; Li, Z.-T. First Zipper-Featured Molecular Duplexes Driven by Cooperative Donor−Acceptor Interaction. *Org. Lett.* **2003**, *5*, 1955-1958.

(67) Brunsveld, L. Zhang, H. Glasbeek, M. Vekemans, J. A. J. M.; Meijer, E. W. Hierarchical Growth of Chiral Self-Assembled Structures in Protic Media†. *Journal of the American Chemical Society* **2000**, *122*, 6175-6182.

(68) Levins, C. G.; Schafmeister, C. E. The Synthesis of Functionalized Nanoscale Molecular Rods of Defined Length. *Journal of the American Chemical Society* **2003**, *125*, 4702-4703.

(69) Park, S. H. Pistol, C. Ahn, S. J. Reif, J. H. Lebeck, A. R. Dwyer, C.; LaBean, T. H. Finite-Size, Fully Addressable DNA Tile Lattices Formed by Hierarchical Assembly Procedures. *Angewandte Chemie International Edition* **2006**, *45*, 735-739.

(70) Yan, H. Park, S. H. Finkelstein, G. Reif, J. H.; LaBean, T. H. DNA-Templated Self-Assembly of Protein Arrays and Highly Conductive Nanowires. *Science* **2003**, *301*, 1882-1884.

(71) Seeman, N. C. DNA in a material world. *Nature* **2003**, *421*, 427-431.

(72) Gu, H. Chao, J. Xiao, S.-J.; Seeman, N. C. A proximity-based programmable DNA nanoscale assembly line. *Nature* **2010**, *465*, 202-205.

(73) Batalia, M. A. Protozanova, E. Macgregor; Erie, D. A. Self-Assembly of Frayed Wires and Frayed-Wire Networks: Nanoconstruction with Multistranded DNA. *Nano Lett.* **2011**, *2*, 269-274.

(74) Chworos, A. Severcan, I. Koyfman, A. Y. Weinkam, P. Oroudjev, E. Hansma, H. G.; Jaeger, L. Building Programmable Jigsaw Puzzles with RNA. *Science* **2004**, *306*, 2068 - 2072.

(75) Zhang, R. S. McCullum, E. O.; Chaput, J. C. Synthesis of Two Mirror Image 4-Helix Junctions Derived from Glycerol Nucleic Acid. *J. Am. Chem. Soc.* **2011**, *130*, 5846-5847.

(76) Weisbrod, S. H.; Marx, A. A nucleoside triphosphate for site-specific labelling of DNA by the Staudinger ligation. *Chem. Commun.* **2007**, 1828.

(77) Varghese, R.; Wagenknecht, H.-A. DNA as a supramolecular framework for the helical arrangements of chromophores: towards photoactive DNA-based nanomaterials. *Chem. Commun.* **2009**, 2615.

(78) Li, G. Liu, H. Chen, X. Zhang, L.; Bu, Y. Multi-Copper-Mediated DNA Base Pairs Acting as Suitable Building Blocks for the DNA-Based Nanowires. *J. Phys. Chem. C* **2011**, *115*, 2855-2864.

(79) Guha, S.; Saha, S. Fluoride Ion Sensing by an Anion−π Interaction. *J. Am. Chem. Soc.* **2011**, *132*, 17674-17677.

(80) Guha, S. Goodson, F. S. Roy, S. Corson, L. J. Gravenmier, C. A.; Saha, S. Electronically Regulated Thermally and Light-Gated Electron Transfer from Anions to Naphthalenediimides. *J. Am. Chem. Soc.* **2011**, *133*, 15256-15259.

(81) Schlegel, M. K. Peritz, A. E. Kittigowittana, K. Zhang, L.; Meggers, E. Duplex formation of the simplified nucleic acid GNA. *Chembiochem* **2007**, *8*, 927-932.

(82) Johnson, A. T. Schlegel, M. K. Meggers, E. Essen, L.-O.; Wiest, O. On the Structure and Dynamics of Duplex GNA. *J. Org. Chem.* **2011**, *76*, 7964-7974.

(83) Meggers, E.; Zhang, L. Synthesis and Properties of the Simplified Nucleic Acid Glycol Nucleic Acid. *Acc. Chem. Res.* **2010**, *43*, 1092-1102.

(84) Zhang, L. Peritz, A. E. Carroll, P. J.; Meggers, E. Synthesis of Glycol Nucleic Acids. *Synthesis* **2006**, *2006*, 645-653.

Vita

Stevan A. Samuel was born to Evan and Stella Samuel in Port-of-Spain, Trinidad on December 24th 1981. He graduated from Fatima College in 2000 and attended Benedict College in Columbia, South Carolina in the fall of 2001. He began his research as an undergraduate in labs of Linda S. Shimizu at the University of South Carolina in the summer of 2003 where he worked until the spring of 2005. He received his Bachelor of Science Degree with Distinction from Benedict College in 2005 and immediately entered the graduate program at the University of Texas at Austin where he joined the labs of Professor Brent L. Iverson.

Permanent email : stevsamuel@utexas.edu

This dissertation was typed by the author